RAIN ATTENUATION AT 74 GHz

by

JOHN DUNCAN McNICOL

B.Eng., Carleton University, 1975

A THESIS SUBMITTED IN PARTIAL FULFIMENT OF

THE REQUIREMENTS FOR THE DEGREE OF

MASTER OF APPLIED SCIENCE

in the Department of Electrical Engineering

We accept this thesis as conforming to the
required standard

THE UNIVERSITY OF BRITISH COLUMBIA

March 1977

In presenting this thesis in partial fulfilment of the requirements for an advanced degree at the University of British Columbia, I agree that the Library shall make it freely available for reference and study. I further agree that permission for extensive copying of this thesis for scholarly purposes may be granted by the Head of my Department or by his representatives. It is understood that copying or publication of this thesis for financial gain shall not be allowed without my written permission.

Department of Electrical Engineering

The University of British Columbia
2075 Wesbrook Place
Vancouver, Canada
V6T 1W5

Date March 28, 1977

ABSTRACT

A millimetric wave transmission link of the radar type has been established at the University of British Columbia campus. It operates at 74 GHz and has a 1.8 km total transmission length. The RF source is an unmodulated klystron and a phase-locked receiver is used to detect the received signal.

The main objective is to measure the excess path attenuation due to precipitation. For this purpose a weather station has been constructed. It consists of 5 tipping-bucket rain gauges distributed along the path and apparatus for the measurement of temperature and wind velocity.

The level of the microwave signal and the outputs of the weather sensors are transmitted to a central station. There, initial processing and data recording on magnetic tape are performed on a continuous basis by a Nova 840 minicomputer. Subsequently, data is further processed on an IBM 370.

Of the 1400 hours of data recorded during a four month period, approximately 25 hours included simultaneous rain and microwave data and were sufficiently "reliable" to analyse. The processed experimental data are compared with the theory of Ryde and Ryde over the range of rain rates observed (0 to 10 mm/hour).

TABLE OF CONTENTS

LIST OF ILLUSTRATIONS

FIGURE

FIGURE

LIST OF TABLES

TABLE

ACKNOWLEDGEMENT

I would like to express my appreciation to Dr. M.M.Z. Kharadly for his invaluable supervision and keen interest throughout the course of this research.

Grateful acknowledgement is made to the Communications Research Centre for their support of this work under contract numbers OSU5-0030 and OSU76-00097.

I wish to express my appreciation to the following people at the Department of Electrical Engineering for their contributions: Mr. D. Holmes for the design of much of the meteorological equipment and his assistance in constructing the computer interface; Mr. J. Stuber for the design and installation of the reflector, antenna mounts and tipping bucket rain gauges and his help in path alignment, and Mr. G. Austin for his advice and assistance on minicomputer matters.

Thanks are also due to Ms. M.E. Flanagan for typing the manuscript, Mr. T.K. Chu for the photography and Mr. T. Enegren for proofreading.

I would also like to thank all my friends and colleagues, particularly Mr. Roger Wood and Mr. Bruce Hanson, for creating an enjoyable and stimulating working environment.

Finally, the financial support received from the National Research Council in the form of a 1967 Science Scholarship is gratefully acknowledged.

CHAPTER I

INTRODUCTION

1.1 An Overview of the Atmospheric Propagation of Microwaves

Microwave radio currently provides the backbone of long-haul communications both in Canada and globally [1]. In spite of recent advances in coaxial, waveguide and optic fibre transmission systems [2,3,4], radio is expected to enjoy continued importance. It has special advantages over long routes and is particularly applicable over difficult terrain where it would be impractical to install guided systems [1].

Microwave transmission systems find application in several areas:

1. Common carrier (terrestrial)
   (a) telephone, broadcast TV networks
   (b) CATV networking
2. Satellite

At present, common carrier systems operate mostly in the 4 GHz and 6 GHz bands with substantial use of 8 GHz and 11 GHz imminent [5,6]. These systems are characterized by 40 to 50 km hop lengths and 40 dB fade margins [7]. Fading in such links is primarily due to multipath propagation (selective) and excessive refraction effects (non-selective). By the use of frequency diversity and space diversity in tandem systems, propagation outages are typically reduced to the 10^{-5} level (5 minutes/year). The CATV application is less demanding: routes are shorter and outages of up to 500 minutes/year are often acceptable [1]. A further increase in the utilization of the spectrum is obtained by the use of orthogonal polarizations in the above systems.

The situation for satellite applications is somewhat different. Most communication satellites are placed in geostationary orbits. Because

of the relatively large distances involved and limited power output of satellite transmitters, fade margins in these systems are typically much lower than on terrestrial links. At elevation angles above 5°, multipath and refractive effects are not large; the principal cause of both attenuation and interference is scattering by hydrometeors [8,9].

With an ever-increasing demand for channel capacity the use of higher and higher frequencies becomes inevitable [7,9]. For example, in the U.S. there are over 4000 relays in the 4 GHz band; further expansion is being limited by interference at network junctions [6,7,10] and the number of available satellite bands below 10 GHz is small. It is contemplated that frequencies above 10 GHz will soon be in widespread use [10-13]. The availability of medium power microwave sources at the higher frequencies, efficient downconverters [14,15] and microwave integrated circuits [16] make the 10 to 150 GHz range look increasingly attractive. Field trials have shown that, at least from the technological (as opposed to propagation) aspect, mm-wave radio systems are practical [12,17].

Characteristics of Propagation above 10 GHz:

Fig. 1.1 shows the attenuation by a "standard atmosphere" [18]. In the 10 to 150 GHz range, several features are of interest: the H_2O resonance at 22.2 GHz and the O_2 resonances at 60 GHz and 118 GHz. The increase in attenuation in the H_2O resonance band is small enough that use of this band would not be affected. In the O_2 resonance band, however, attenuation is so large that operation in this band would not be contemplated for long-haul transmission. The band may however find use in applications where limited range is required or desirable. In short, for most uses, two ranges are considered: 10-50 GHz and 70-110 GHz.

Above 10 GHz, fading by rain is the dominant cause of propagation

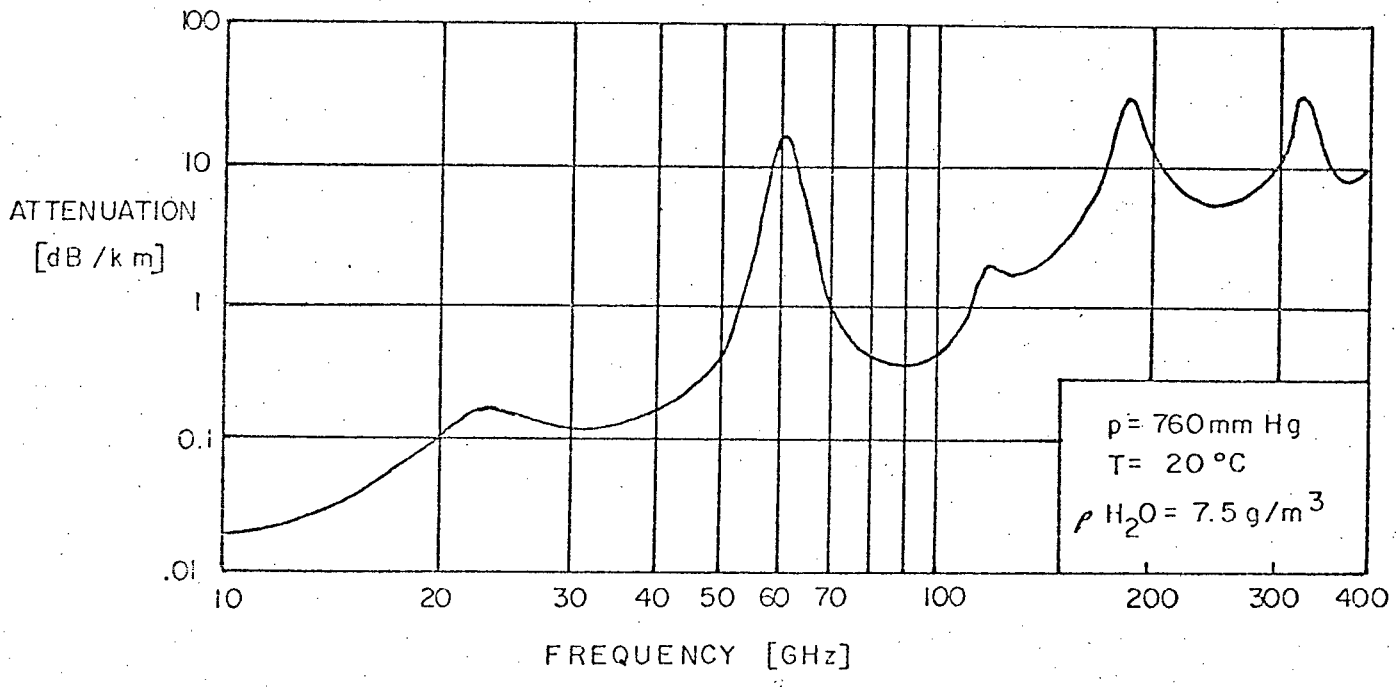

Fig. 1.1 Atmospheric attenuation in the 10 - 400 GHz range (from [18]).

outages [10,12]. The typical variation of specific attenuation with frequency and rain rate is given by Fig. 1.4 for the 1-1000 GHz range [19]. Fading due to rain is non-selective, thus frequency or space diversity cannot be used to maintain availability as is the case below 10 GHz. At these frequencies, shorter hops and possibly path diversity must be used instead [20]. The allowable repeater spacing would greatly depend on the location and would "appear to be prohibitively short in some areas" [7] but acceptable in other areas.

In the short mm-wave region, antennas of reasonable size (<1 m diameter) may be constructed with sharp beams and low side lobe radiation [21] making intra-city microwave links appear attractive. Other possibilities for high capacity distribution in cities involve the use of Gaussian beams on so-called "Hertzian cables" [22].

1.2 Atmospheric Effects

1.2.1 Attenuation

Ryde [23] predicted the attenuation of centimetre waves due to rain. This was based on single scattering by a dielectric sphere as given by Mie and later, by Stratton. Medhurst [24] extended the calculations to the millimetric wave region and corrected some of Ryde's numerical results. More recently the effects of multiple scattering and of considering a beam as opposed to a plane wave were studied by Lin and Ishimaru [25]. They showed, in general, that a beam wave suffers somewhat higher attenuation than a plane wave and that at 3 and 5 mm wavelengths multiple scattering results in attenuations 10% to 30% below Medhurst's results. Current work by Rogers and Olsen (1976) [19] suggests, however, that the so-called "single scattering" treatment actually includes all forward multiple scattering processes and that the effect of "backward

multiple scattering" is negligible. Using Twersky's multiple scattering formulation they obtained results virtually identical to those given by Ryde's method. In the following simplified review only single scattering will be considered.

"Single Scattering" by Spherical Drops

The attenuation of a plane wave in a uniform distribution of spherical drops (all the same size) is given by [23]

$$\alpha = 0.4343 \cdot N \cdot \frac{\pi D^2}{4} f_a\left(\frac{D}{\lambda}, m\right) \text{ dB/km} \qquad (1)$$

where N is the density of drops (m^{-3})

D is the drop diameter (cm)

$m = n - jn\chi$ is the complex refractive index of water

f_a is the ratio of energy absorbed and scattered to that incident upon the projected area of a drop.

Table 1.1 [24] gives the complex refractive index of water, m, as a function of wavelength and temperature. Knowing m, the parameter f_a may be calculated for a particular λ. A typical graph of f_a vs. D/λ [23] is included here as Fig. 1.2. It shows that attenuation by rain is most pronounced in the mm-wave range.

To relate the attenuation in (1) to rain rate, R, a relationship between N and R is required. This is given, in terms of the terminal velocity of a falling drop, by

$$R = 1.885 \cdot v \cdot N \cdot D^3 \text{ (mm/hr)} \qquad (2)$$

The terminal velocity in (2) is dependent on drop diameter. The dependence, as measured by Gunn and Kinzer [24], is shown in Fig. 1.3. The coefficient of attenuation for uniform rain of a single drop size may now be calculated for a range of drop sizes and wavelengths. These results [24] are given in Table 1.2. It is observed that at $\lambda = 4$ mm a rainfall of relatively small drops can cause ten times the attenuation of a rainfall of large drops at the same rain rate. This happens because

λ[mm]	η	ηχ
3	3.51	2.01
4	3.94	2.27
5	4.37	2.52
10	8.25	1.83

Table 1.1 Refractive and absorptive indices of water at 20°C (from [24]).

Wavelength	Drop Diameter [mm]												
[mm]	0.5	1.0	1.5	2.0	2.5	3.0	3.5	4.0	4.5	5.0	5.5	6.0	6.5
3	1.85	1.49	0.66	0.41	0.28	0.21	0.17	0.14	0.12	0.10	0.092	0.083	0.076
4	1.15	1.15	0.67	0.41	0.28	0.21	0.17	0.14	0.12	0.11	0.094	0.085	0.077
5	0.46	0.74	0.68	0.42	0.28	0.21	0.17	0.14	0.12	0.11	0.096	0.087	0.079
10	0.097	0.14	0.20	0.22	0.22	0.21	0.18	0.15	0.12	0.11	0.099	0.091	0.083

Table 1.2 Normalized specific attenuation [(dB/km)/(mm/hr)] by monodisperse rain (from [24]).

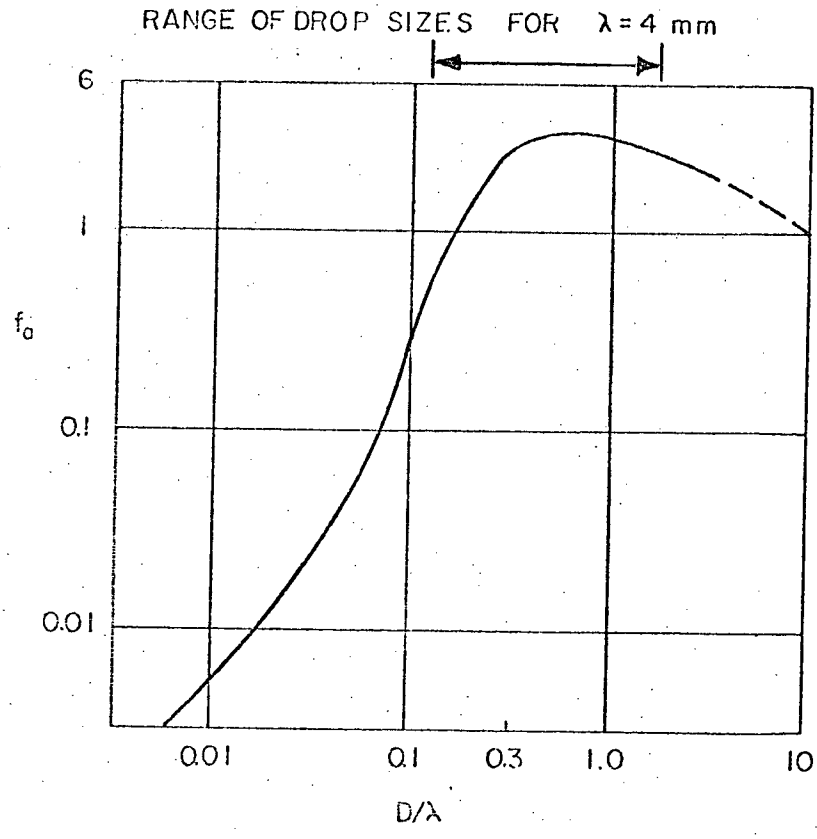

Fig. 1.2 Ratio of effective scattering and absorption cross section to physical cross section for a sphere of water (calculated using the refractive index of water for λ = 1 cm)(from [23]).

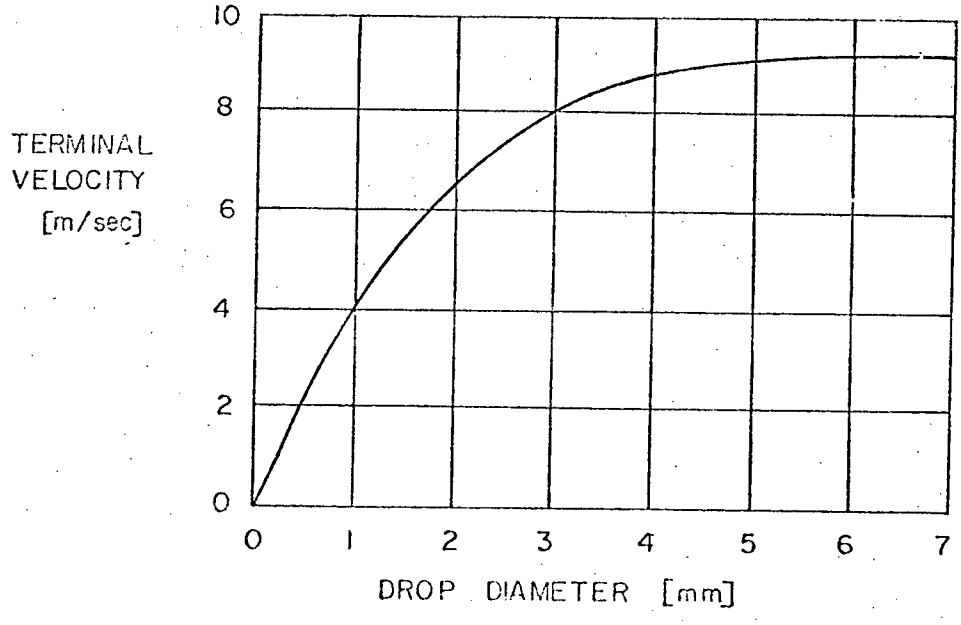

Fig. 1.3 Terminal velocity of rain drops vs. drop diameter (from [24]).

at short wavelengths, f_a is similar for all drop sizes so that by distributing rain into smaller drops, which increases the projected area of the rain, the attenuation increases. (At longer wavelengths f_a decreases more rapidly than $\frac{\pi D^2}{4} \cdot N$ with decreasing D so here, the larger drops cause highest attenuations.)

Actual rain is composed of drops with a continuous range of diameters from 0.5 mm to 7mm. The drop size distribution varies with rain rate; an average relation is given by Table 1.3 (Laws and Parsons [56]). Combining this with attenuation by rain of a single drop size, attenuation by actual rain vs. rain rate, as shown in Table 1.4 has been calculated [24]. A graph of specific attenuation vs. frequency at various rain rates [19] is given by Fig. 1.4.

The above prediction of attenuation is based on a one-to-one correspondence of drop size distribution and rain rate. Zavody and Harden [26] have shown that substantial deviations from the Laws and Parsons distribution do, however, occur. This may account for some of the observed scatter [8,24,27] in experimental attenuation vs. rain rate data.

Attenuation in Non-Uniform Rain:

It is known that rain generally occurs in cells of limited extent [28,29]. In practice the full spatial variation of rain rate is not measured but, rather, point rain rates are sampled at various locations along the path. That is, the path is broken into segments each with a rain gauge and for each segment the attenuation is calculated. The total excess path attenuation is thus the sum of all partial attenutaions.

$$A = \sum_{i=1}^{n} A_i = \sum_{i=1}^{n} \alpha_\lambda(R_i) \cdot l_i \qquad (3)$$

where R_i is the rain rate as measured by the i^{th} rain gauge

Drop size (cm) (mean in interval)	Precipitation rate (mm/hour)	Percent of total volume							
	0.25	1.25	2.5	5	12.5	25	50	100	150
0.05	28.0	10.9	7.3	4.7	2.6	1.7	1.2	1.0	1.0
0.1	50.1	37.1	27.8	20.3	11.5	7.6	5.4	4.6	4.1
0.15	18.2	31.3	32.8	31.0	24.5	18.4	12.5	8.8	7.6
0.2	3.0	13.5	19.0	22.2	25.4	23.9	19.9	13.9	11.7
0.25	0.7	4.9	7.9	11.8	17.3	19.9	20.9	17.1	13.9
0.3		1.5	3.3	5.7	10.1	12.8	15.6	18.4	17.7
0.35		0.6	1.1	2.5	4.3	8.2	10.9	15.0	16.1
0.4		0.2	0.6	1.0	2.3	3.5	6.7	9.0	11.9
0.45			0.2	0.5	1.2	2.1	3.3	5.8	7.7
0.5				0.3	0.6	1.1	1.8	3.0	3.6
0.55					0.2	0.5	1.1	1.7	2.2
0.6						0.3	0.5	1.0	1.2
0.65							0.2	0.7	1.0
0.7									0.3

Table 1.3 Drop size distribution for various rain rates (Laws and Parsons) (from [24]).

λ	Rain Rate [mm/hr]								
[mm]	0.25	1.25	2.5	5	12.5	25	50	100	150
3	.250	1.29	2.19	3.68	7.08	11.7	19.6	33.7	46.8
4	.204	1.03	1.81	3.15	6.27	10.8	18.3	31.5	43.8
5	.159	.764	1.43	2.63	5.46	9.86	17.0	29.4	40.9
10	.035	.210	.447	.933	2.43	4.87	9.59	18.4	26.5

Table 1.4 Specific attenuation for various rain rates assuming the Laws and Parsons drop size distribution (from [24]).

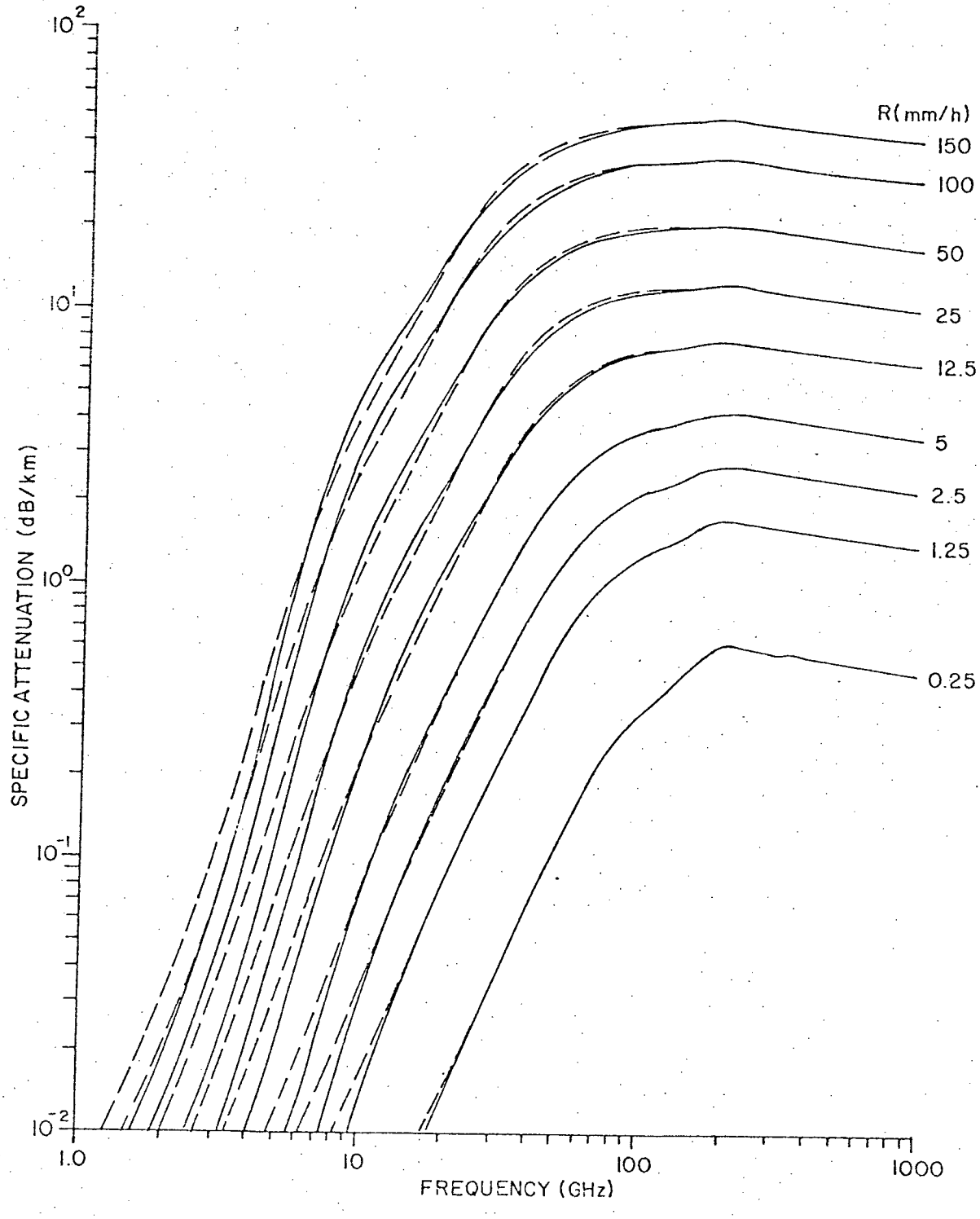

Fig. 1.4 Specific attenuation as a function of frequency for coherent wave propagation through uniform rain. The curves are based on Laws and Parsons dropsize distribution and the terminal velocities of Gunn and Kinzer. _____ Rain temperature of 20°C. ----- Rain temperature of 0°C. (from [19])

l_i is the length of the i^{th} segment ($\sum_i l_i = L$, path length)

α_i (R_i) is attenuation in dB/km at rain rate, R_i

If the rain rates at each gauge are similar or if specific attenuation and rain rate are linearly related:

$$A \tilde{-} \alpha_\lambda \left(\sum_{i=1}^{n} \frac{R_i l_i}{L} \right) \cdot L \qquad (4)$$

where $\sum_{i=1}^{n} \frac{R_i l_i}{L}$ is the so-called path-average rain rate.

Most published experimental work compares excess path attenuation directly with path-average rain rate although this is not strictly correct.

Differential Attenuation

It has been shown that large rain drops tend to be flattened at the bottom [30]. This would suggest that attenuation by rain is polarization dependent. Measurements have shown that attenuation is larger for horizontal polarization than vertical polarization [31]. The differential attenuation, however, is less than 15% of the average attenuation.

Effects of Updrafts

Vertical wind modifies the terminal velocity of rain drops such that the drop density in air would be different than indicated by the surface rain rate. Small drops are particularly affected because of their low terminal velocity. As these cause a large portion of the attenuation at 4 mm wavelengths, the effect of updrafts (or downdrafts) could be substantial.

Effect of Temperature

Temperature affects attenuation by rain insomuch as the complex refractive index of water is temperature dependent. While Medhurst [24] reports that, at λ = 5 mm, the change in attenuation for temperatures between 0° and 40°C is as large as 17%, more recent calculations by

Rogers and Olsen [19] have shown that the change is only 4%.

Attenuation by Water Vapour, Oxygen and Fog

Water vapour itself, as measured by humidity, causes attenuation. At 100% relative humidity, at 10°C, attenuation of 4 mm waves is about 0.5 dB/km (extrapolated from Bussey [32]). Of the other gases in the atmosphere only oxygen causes significant losses, 0.3 dB/km at sea level [18]. Fog attenuates microwave radiation by the same mechanism as rain. The parameter f_a is small even for short mm-waves so that attenuation is not large; measured attenuations of 1 dB/km at 90 GHz have been reported by Weibel and Dressel [33].

1.2.2 Cross Polarization

The shape of a falling drop may be approximated by an oblate spheroid, the minor axis of which is generally aligned in the direction of fall. Measurements, however, have shown that an average canting of axes away from the vertical does occur [30]. (This could possibly be due to gradients in wind velocity or atmospheric turbulence.) The drops which are subject to canting couple power between vertical and horizontal polarizations as shown theoretically by Ogouchi and Hogg [34,35,36]. Such cross polarization may seriously limit the simultaneous use of orthogonal polarizations. Above 60 GHz, however, depolarization may be lower because attenuation by the smaller (almost spherical) drops predominates [31].

1.3 Considerations in an Experimental Transmission Link at 75 GHz

1.3.1 Background

An examination of propagation studies intent on observing fading due to rain shows frequencies ranging from 8 GHz to 110 GHz and total transmission lengths of 100 m to 45 km. Refer to Table 1.5 for a partial but representative list of experiments. In an attempt to compare studies

Ref. No.	Authors	If radar link ✓	Freq. [GH_3]	Path Length [m]	"75 GH_3 Transmission Length"
37	Blevis, Dohoo, McCormick		8.0	15,800	650
38	Robertson, King		9.4	274	20
39	Skerjanec, Samson		10.0	4,700	370
24	Hathaway, Evans		11.4	45,000	4,800
40	Vorst, Gandissart	✓	11.7	1,000	230
39	Skerjanec, Samson		14.4	4,700	790
37	Blevis, Dohoo, McCormick		15.0	15,800	2,800
41	Straiton		15.3	20,000	3,700
42, 43	Semplak, Turrin		18.5	6,400	1,600
44	Anderson et al.		24.0	1,950	740
24	Rado		24.0	3,970	1,500
38	Robertson, King		27.5	383	180
43	Semplak		30.9	1,900	1,020
24	Adam et al.		31.3	2,000	1,080
45	Harrold	✓	34.8	6,900	8,100
24	Okamura et al.	✓	34.9	400	480
24	Okamura et al.	✓	34.9	3,550	4,200
24	Funakawa, Kato		34.9	24,000	14,000
40	Vorst, Gaudissart	✓	35.0	1,000	1,200
46	Roche et al.		35.0	8,000	4,700
46	Roche et al.		35.0	32,000	19,000
47	Norbury, White	✓	35.8	224	270
26	Zavody, Harden		36.0	220	130
24	Usikov et al.	✓	36.8	50	60
24	Usikov et al.	✓	44.1	50	70
48	Mueller		48.4	365	280
24	Usikov et al.	✓	69.7	50	96
33	Weibel		90.5	2,000	2,200
49	Hoffman et al.		94.0	19,000	20,000
50	Lane, Gordon-Smith, et al.	✓	101.0	150	320
26	Zavody & Harden		110.0	220	240
51, 52	Llewellyn-Jones, Zavody		110.0	2,650	2,900

Table 1.5 A comparison of path lengths used in various propagation studies.

done at different frequencies, path lengths were normalized to ones that would give the same attenuation at 75 GHz using the relative coefficients of attenuation for rain at 50 mm/hr. Figure 1.4 gives a plot of these coefficients versus frequency. Table 1.6 shows the number of these studies in various classes of normalized path length; the spread in path lengths is almost three orders of magnitude.

1.3.2 Expected Rain Rates in Vancouver

The climate in Vancouver is moderately wet (1070 mm/year) and subject to little thundershower activity. Rain rate distributions are not yet available for Vancouver but estimates may be obtained by examining published values [29,32,53,54] for other locations; refer to Table 1.7. It is felt that of the information available, perhaps Portland, Oregon is most representative of conditions in Vancouver. This would indicate rain rates exceeding 50 mm/hr (subject to a 1 minute averaging time) might occur 10 minutes/year. Rain rates exceeding 100 mm/hr would occur less than 1 minute/year. The results of Bussey [32] are not used here because they include only the occurence of long bursts of intense rain.

It is noted that such estimates (as above) are very sensitive to local conditions; a variability of two orders of magnitude in rain rate distributions exists within the continental U.S. alone [53]. It is apparent, then, that an accurate measurement of the local rain rate distribution, per se, is important. Indeed, in calculating the reliability of a given path, more uncertainty appears to exist in the rain rate distribution than in the relation between attenuation and rain rate.

1.3.3 Estimated Reliability of Two Paths in Vancouver

Because past work provides little guidance for choosing the

Normalized Path Lengths [m]	Number
< 100	4
100 to 1,000	12
1,000 to 10,000	13
> 10,000	3

Table 1.6 Propagation studies classed by normalized path length.

Location	Averaging Time [min]	Time in min/year Rain Rate Exceeded 50 mm/hr	100 mm/hr	Reference No.
Salt Lake City, Utah	1	5	< ½	[53]
Portland, Ore.	1	9	½	[53]
Miami, Fla.	1	400	80	[53]
Bedfordshire, England	2	6	< 1	[29]
Crawford Hill, N.J.	0.15	80	20	[54]
Corvallis, Ore.	-	< ½	< ½	[54]
Vancouver, B.C.	5	2.5	-	[32]

Table 1.7 Probability of selected point rain rates in various locations.

proper path length of a propagation study it is instructive to examine the reliability (with respect to propagation) of particular microwave links. Two links will be analyzed here, one of length 2 km and the other of 10 km. It will be assumed that each has the same fade margin (in free space) of 40 dB. Outages could result from both precipitation and multipath effects and for this analysis, both events will be regarded as disjoint so that the total outage will be the sum of the respective outages.

a) Length = 2 km

At 75 GHz no multipath fading would be expected to occur for path lengths below 3.5 km [55]. Gaseous absorption of 0.7 dB/km [32] will reduce the fade margin to 38.6 dB. An attenuation of greater than 19.3 dB/km would then cause an outage. Referring to Fig. 1.4, this would result from a path-average rain rate of 55 mm/hr. It has been shown that the statistics of path-average rain rate are similar to those of point rain rate subject to a unique averaging time related to the path length [53]. The appropriate averaging time for this path is 16 seconds. However, for rates below 60 mm/hr the point rain rate distribution is independent of averaging times between 1.5 sec and 120 sec [53] so that the 1 minute averages of Section 1.3.2 will suffice to describe path-average rain rate. This gives an outage time of 8 minutes/year.

b) Length = 10 km

On this link, multipath fading would be expected to occur [55] but experimental values of this fading are not available for the 4 mm band. One may estimate the outage time, however. It has been shown [55] that the attenuation distribution is independent of path length, L, and wave-length, λ, as long as the ratio L^3/λ remains constant. Thus the attenuation distribution of this path should be the same as, for example,

paths of:

f = 15 GHz L = 16.9 km

f = 8 GHz L = 20.9 km

Published results [1] indicate an outage time of 50 minutes/year for those frequencies and lengths.

Accounting for oxygen and water vapour absorption the fade margin of this path is reduced to 33 dB [32]. Referring to Fig. 1.4 an outage would occur for a path-average rain rate of 6 mm/hr. The statistics of rain rate on this 10 km path should be the same as those of point rain rate subject to a 39 second averaging time [53]. By normalizing a typical rain rate distribution to the figure of 10 min/year at 50 mm/hr, a rain rate of 6 mm/hr would be exceeded 300 minutes/year. The total outage time of this 10 km link is expected to be 350 minutes/year.

The availabilities of the two links indicate that, in Vancouver, a 2 km link would be of a reliability suitable for telephony and that a 10 km link would be better suited to CATV applications [1].

1.3.4 Considerations in Path Selection

A long path has easily-measured values of attenuation but is faded out quite often so that no knowledge of events below a given probability is obtained. It is also difficult to adequately measure the rain rate profile on such a path. A short link, on the other hand, generally has small values of excess path attenuation which may be difficult to measure but is rarely faded out so that events of very low probability will be measured. The rain rate measurement on the short path is also more tractable.

A comprehensive study would require that all but the rarest of rain induced fades be observed and thus a short path would be desirable in an initial study. From the results on a short path and by ascertaining

the spatial variation of rain over the long path, it should be possible to predict the performance of the latter. A subsequent study of the long path with its more complex characteristics would then become appropriate.

1.4 Scope of the Thesis

1.4.1 Thesis Objective

The ultimate objectives of this research program could be stated as follows:

1) To establish a millimetric wave link with appropriate weather monitoring apparatus and a suitable data gathering system. To operate the system for a sufficiently long period of time in order to acquire a large data base of atmospheric propagation-related events.
2) To establish the relation between mm-wave propagation characteristics in the atmosphere and the various physical phenomena that affect these characteristics.
3) To be able to predict the propagation statistics of a path in this location. It is desirable to predict this from the knowledge of (2) and the statisitcs of the "causes".

The work described in this thesis provides the basic features of an experimental system designed to achieve the above ultimate objectives. Specifically, the points covered are:

1) Identification of the parameters affecting mm-wave propagation in the atmosphere and of problems associated with propagation studies.
2) Establishment of a millimetric wave link capable of automatically measuring excess path attenuation.
3) Installation of weather monitoring apparatus for the automatic measurement of parameters related to excess path attenuation.

4) Implementation of a system to record, in a form suitable for later analysis, data from the microwave link and the weather sensors.
5) Development of techniques for editing data so as to allow accumulation of a data base of propagation-related events.

This thesis is basically concerned with the design and implementation of a system. The work done involves the installation of equipment to measure a diverse range of phenomena and the chanelling of large volumes of data through several stages of processing. This was accomplished by making effective use of available resources and within certain budgetary constraints.

The thesis covers a diverse range of topics. Of necessity, more detail is included in each section than experts in a particular field might deem warranted.

1.4.2 Thesis Outline

A millimetric wave link which allows continuous measurement of excess path attenuation at 74 GHz (and optionally 35 GHz) is the subject of Chapter II. Included are descriptions of the various sub-systems in the link as well as the calculated and measured system performance.

Chapter III deals with the meteorological sensors by which parameters affecting excess path attenuation are measured. The sensors implemented are a network of tipping bucket rain gauges and units to measure temperature and wind velocity.

Chapter IV is concerned with the recording of data from the microwave and weather sensors and their eventual transfer into a permanent data base. The topics covered are a minicomputer interface, real time data logging with a minicomputer and post processing of data on an IBM 370 computer.

Results of operation at 74 GHz with the real time data acquisition system from November, 1976 to March, 1977 are given in Chapter V. They represent a limited set of data and are included to convey the character the data measured and the viability of the techniques used in this thesis.

Suggestions for further developments on the systems described in this thesis and the conclusions are contained in Chapter VI.

CHAPTER II

MILLIMETRIC WAVE LINK AND MEASUREMENT SYSTEMS

2.1 Introduction

This chapter describes the design of a millimetric wave propagation link used in the measurement of excess path attenuation (mainly) due to precipitation. It is a radar-type path of total transmission length 1.8 km operating at a frequency of about 74 GHz with a 40 dB fade margin. The link can also be operated at 35 GHz with few modifications. Much of the design is predicated upon the facilities available with little choice in the following areas:

1. Antennas
2. Receiver
3. Transmission path

The scope of discussions in this section is necessarily restricted by these considerations.

A general description of the propagation link is given in Section 2.2 together with a prediction of its fade margin. This calculation is largely based on measurements and/or analysis of the link's constituent sub-systems as detailed in Section 2.3. The measured fade margin of the system and a comparison with the predicted value is given in Section 2.4. Finally, a summary of the millimetric wave link characteristics is presented in Section 2.5.

2.2. System Description

A millimetric-wave link of the radar type is used here, that is, the signal traverses the path twice via a passive reflector. Separate transmitting and receiving antennas, each 1 meter diameter parabaloid dishes are used. These are positioned 20 metres apart on the roof of the MacLeod Building. The direct coupling between the antennas is below the receiver

noise level. The antennas are mounted at an elevation of 148 metres above sea level. A plane reflector, 1 m^2, is located about 900 m away at an elevation of 178 m, giving a total transmission length of 1.8 km. The path is over flat ground and several buildings with a minimum clearance of 4 m. Details of the path are given by Fig. 2.1.

A 74 GHz source (located one floor beneath the antennas) supplies a continuous wave signal to the transmitting antenna via a waveguide system. A mixer, located at the receiving antenna, down-converts the signal received to an intermediate frequency which is transmitted through coaxial cable to a receiver located near the source. Refer to Fig. 2.2 for a block diagram of this system. Photographs of various components are given in Figs. 2.3, 2.4 and 2.5.

Calculated Fade Margin:

Using the results developed in Section 2.3, the fade margin of this system may be calculated.

L_f	Free-space loss (20 Log_{10} $(\frac{2\pi d}{\lambda})$):	128.5 dB
L_g	Gaseous Absorption (0.7 dB/km)	1.2 dB
L_r	Reflector "Loss"	5.2 dB
$L_{w/g}$	Waveguide Losses (total)	8.6 dB
G_T, G_R:	Antenna Gains	49.5 and 48 dB respectively
P_o;	Klystron Power Output, P_o	+27. dBm

$P_{recv} = p_o - L_f - L_g - L_r - L_{w/g} + G_r + G_R = -19$ dBm

With the current mixer sensitivity of -81 dBm, this is a fade margin of 62 dB.

2.3 Sub-Systems

2.3.1 Antennas

The antennas used in this experiment are both center-fed para-

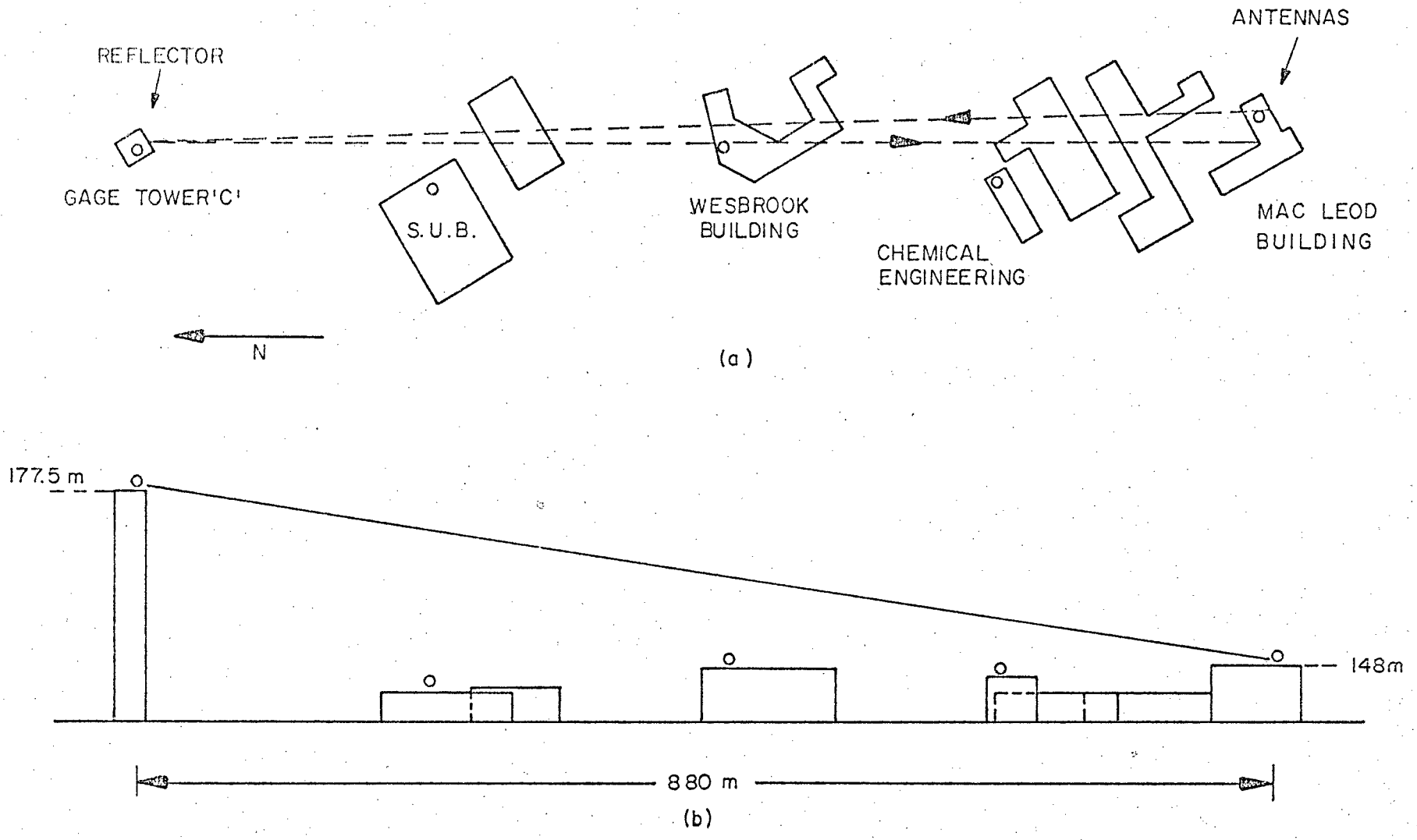

Fig. 2.1 Transmission path (a) Aerial view (b) Side view.
Circles mark the 5 rain gauges.

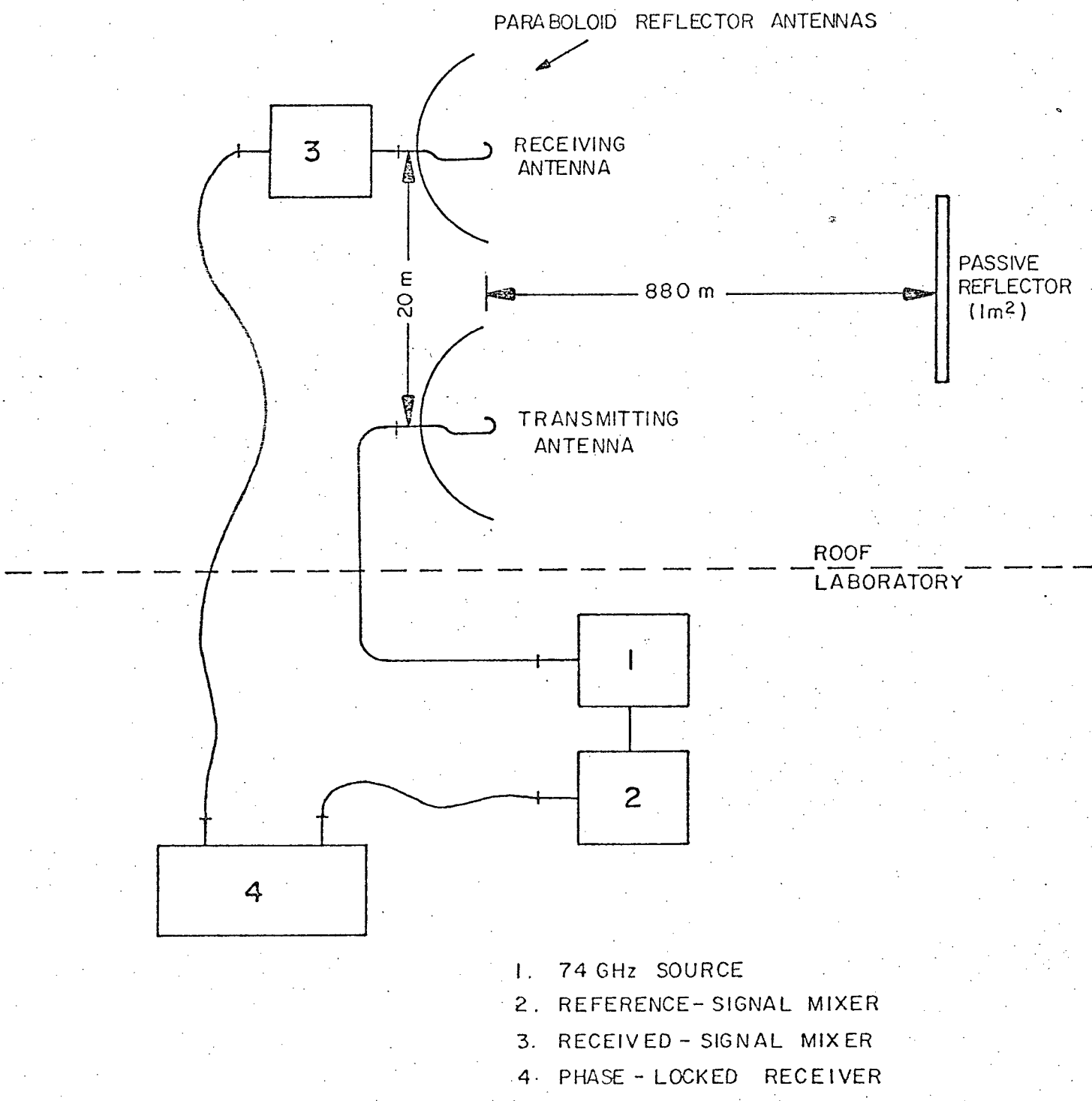

Fig. 2.2 Microwave system: block diagram

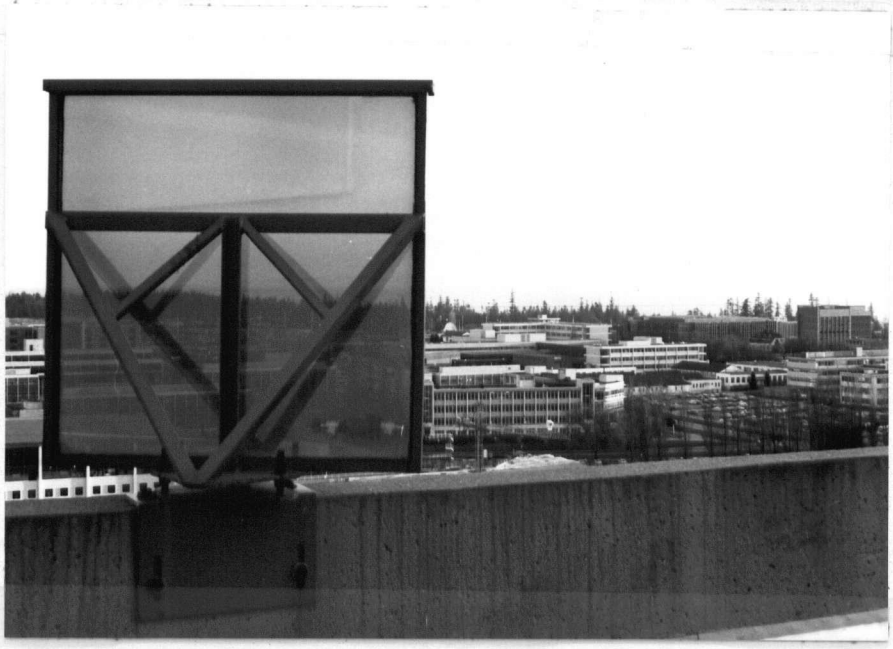

Fig. 2.3 The reflector at Gage Tower 'C'. Past it and to the right is the MacLeod Building where the antennas are installed.

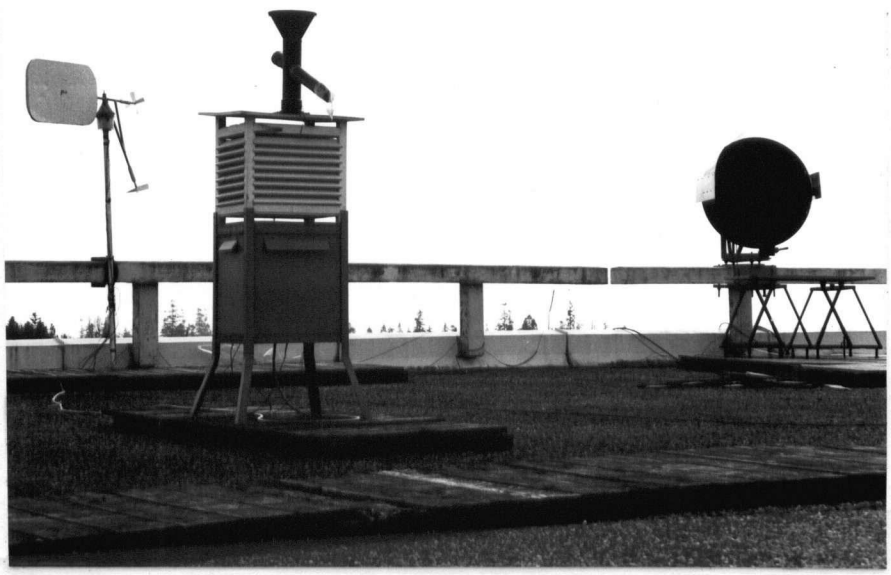

Fig. 2.4 The transmitting antenna, the anemometer, a Stevenson's screen and a prototype capacitative rain gauge.

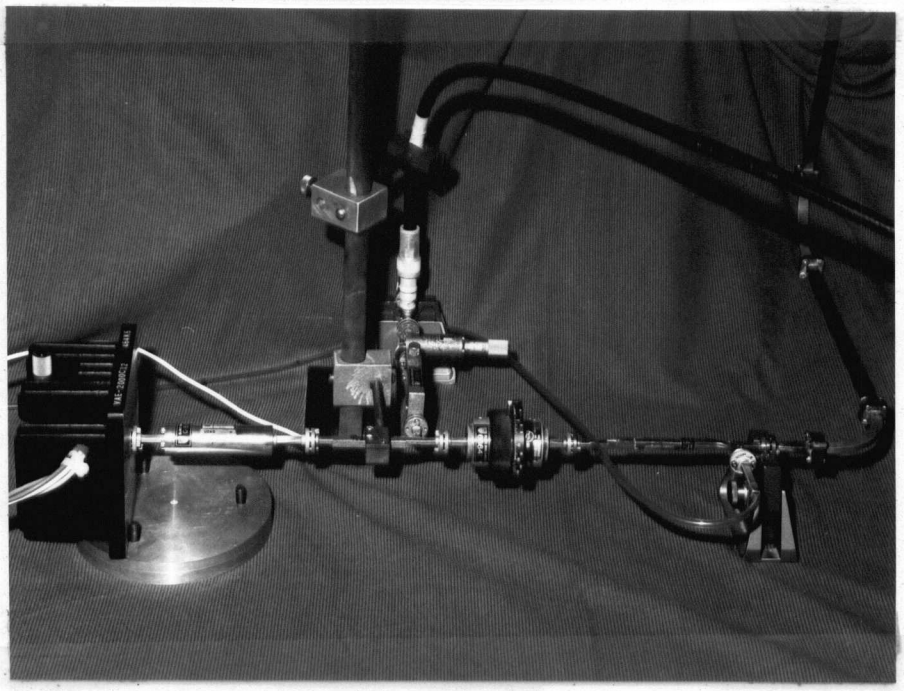

Fig. 2.5 The '74 GHz klystron and associated waveguide components.

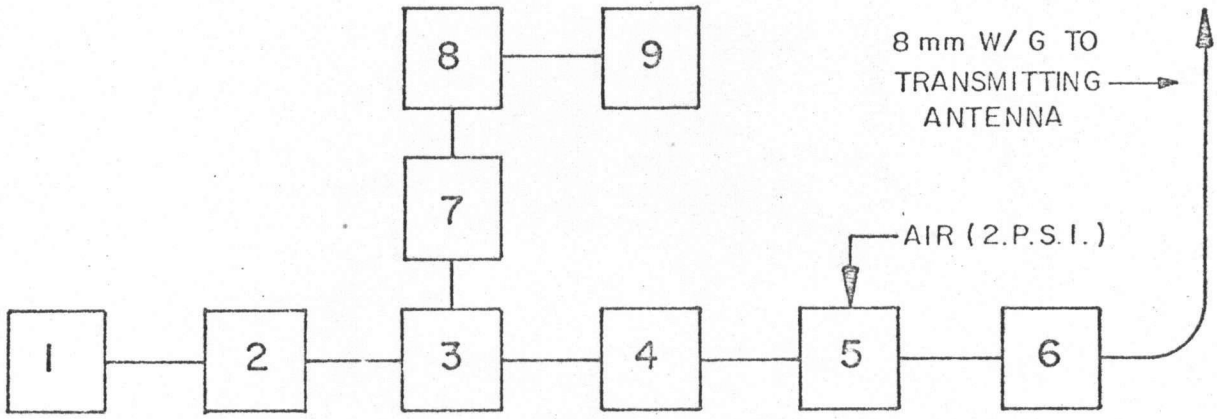

1 74 GHz KLYSTRON
2 ISOLATOR
3 DIRECTIONAL COUPLER (6dB)
4 CALIBRATED ATTENUATOR
5 DIRECTIONAL COUPLER (20 dB)
6 4mm W/G TO 8mm W/G TAPER
7 ATTENUATOR
8 FREQUENCY METER
9 REFERENCE MIXER

Fig. 2.6 Block diagram of transmitter apparatus.

boloids, one of aluminum, the other of fiberglass with a conductive coating. Originally manufactured for operation at 35 GHz, modifications to the feed were made to allow use at twice this frequency. The original waveguide (7.11 x 3.56 mm) was left intact except for the last 2 cm. which was replaced by a taper to 3.8 mm x 1.9 mm waveguide thus permitting only the TE_{10} mode to excite the aperture. Polarization was horizontal.

It was desirable to operate the antennas at both 35 GHz and 75 GHz. This would allow antenna alignment at 35 GHz where higher sensitivity is available as well as system operation during rain at 35 GHz. For this purpose, tapered teflon plugs, machined to fit the aperture and about 2 cm long, were inserted in the feed to expand its electrical size and allow radiation. These inserts were broadband and well matched to the waveguide. It was also observed that operation at 75 GHz was not impaired by the plugs (though it was usual to operate without them).

Measurements on the Antennas:

(a) Mechanical:

Measurements were carried out on the surface of the aluminum dish. Curve fitting of the points obtained to a parabola showed the focal length to be 305 mm. The diameter was 1.05 m giving it a ratio of focal length to diameter, f/D, of 0.29 and a subtended angle of 160°.

(b) Aperture Illumination:

With a tapered aperture illumination, the maximum value of gain is usually achieved with an edge illumination of -12 dB relative to the center [58]. The primary source was an open ended waveguide (3.8 x 1.9 mm). Its radiation pattern was investigated to determine the actual illumination. At a frequency of 73 GHz ($2a = 1.83\ \lambda_o$), both theory and experiment indicated the 3 dB beamwidth to be 74° in the E-plane and 59° in

the H-plane. Accounting for space attenuation, the illuminated area (i.e. with illumination > - 12 dB) was calculated to be about 50% of the actual area [58].

(c) Radiation Pattern:

Near field measurements on the antennas revealed some assymetry of the aperture fields. It was not convenient (because of the large extent of the Fresnel zone) to measure the far field pattern on a conventional antenna pattern range. Instead, the antennas were installed on the path with the reflector and were aligned for optimum reception. Then one antenna was rotated past the reflector while the other remained fixed. The results of these measurements at 74 GHz are given in Table 2.1. They indicate [58] that the gains of the transmitting and receiving antennas are, respectively, 49.5 and 48 dB.

Calculated Gain:

The best possible gain that could be obtained from such an antenna is

$$G = 10 \log_{10} \{0.65 \frac{4\pi A}{\lambda^2}\} = 53 \text{ dB}$$

where: A = illuminated area (> -12 dB) = 0.38 m^2

λ = 4.1 mm

2.3.2 Reflector

The passive reflector used in this microwave link is made of a 1 m x 1 m sheet of 3/8" (0.95 cm) thick plate glass covered with "Scotch Tint", an adhesive plastic sheet loaded with fine conducting particles. The reflection coefficient of a surface thus constructed was found indistinguishable from that of a solid metallic structure at 35 and 75 GHz. This arrangement provides a large, smooth and relatively flat reflecting surface at reasonable cost. The reflector is supported by a structure

Antenna	3-dB beamwidth [degrees]	
	E-plane	H-plane
Transmitting	0.55	0.55
Receiving	0.67	0.62

Table 2.1 Measured 3-dB beamwidths of transmitting and receiving antennas.

Waveguide Type	Nominal Inner Dimensions [mm]		Attenuation [dB/m]	
	a	b	theoretical	measured
X-band	22.86	10.16	0.162	0.4
8 mm	7.11	3.56	0.546	1.0
4 mm	3.76	1.88	1.34	1.8

Table 2.2 Theoretical and measured attenuation at 75 GHz of 3 sizes of rectangular waveguide.

designed to stand winds of 100 km/hr with only small angular deflections.

Reflector Loss:

The component of path loss due to the reflector is given by [58]:

$$\text{Loss}_R = 20 \log \frac{\lambda d}{2A} = 5.2 \text{ dB}$$

where: $d = 880$ m separation between antennas and reflector

$\lambda = 4.1$ mm signal wavelength

$A_r = 1 \text{ m}^2$ reflector area

subject to the following conditions

(a) reflector and antennas are in each other's Fraunhofer region

$$d > \frac{2a^2}{\lambda} = 490 \text{ m}$$

(b) surface must be flat within $\pm\lambda/16$ (± 0.25 mm).

Although steps were taken to ensure flatness, some distortion outside these limits may have occurred due to mounting stresses and thermal expansion. The extent of such distortion and its effect are not easily measured.

2.3.3 Waveguide

Because of the relatively high attenuation of the single moded rectangular waveguide in the 70 to 75 GHz range, the use of larger, over-moded guides was investigated. Two sizes, 8 mm and 3 cm (X-band) waveguide sections, were considered. Power is coupled to and from these sections with gradual tapers to ensure the transmission is mainly by TE_{10} mode with little conversion to higher order modes. Characteristics of the various waveguides and the tapers are given in Tables 2.2 and 2.3.

The attenuations of the above waveguides suggested that the X-band type should be used where significant lengths of guide are required. However, measurements on X-band waveguide systems indicated that they had a highly oscillatory frequency response. Typical varia-

Taper Designation	Reflection Coefficient
4 mm to 8 mm	- 25 dB
8 mm to X-band	- 25 dB

Table 2.3 Measured reflection coefficients of waveguide tapers.

Location of Waveguide Section	Type	Length [m]	Loss [dB]
Klystron to 4 - 8 mm taper	4 mm	0.4	0.7
to transmitting antenna	8 mm	6.5	6.5
in transmitting antenna	8 mm	0.7	0.7
in receiving antenna	8 mm	0.7	0.7
	Total Waveguide Loss		8.6

Table 2.4 Calculation of system waveguiding losses

tions in transmission coefficient were 6 dB for a change in frequency of 1 in 10^5. As the frequency drifts encountered in long periods were much more than that, such a system was unacceptable. Further measurements indicated that bends were mainly responsible for this performance.

A similar investigation using 8 mm waveguide revealed much more acceptable characteristics: frequency response flat to within measurement uncertainties (±0.4 dB) over a wide range of frequencies. Based on this overmoded 8 mm waveguide was extensively used. The waveguide losses of the various sections in this system are given in Table 2.4.

All waveguides were pressurized to continually remove moisture which might leak in through joints or form by condensation. The continuous flow of air also ensured that, during rain, drops of water would not accumulate on the antenna feeds.

2.3.4 Receiver and Associated Measurement Units

The receiver used in this propagation experiment is a phase-locked, superheterodyne Scientific Atlanta Model 1751. This design is intended primarily for antenna work but functions well in a diverse range of applications. In this work two of its three channels are used:

1. reference channel - phase-locked to the source oscillator
2. signal channel - monitors the received signal

Associated with each channel is an external harmonic mixer pumped by a common S-band (2 to 4 GHz) local oscillator (LO) in the receiver. The same cable that carries the local oscillator to each mixer serves to return the intermediate frequency (IF) to receiver. With the reference channel phase-locked to the transmitted frequency (RF), the LO frequency automatically adjusts to maintain the IF at 45 MHz. Inside the receiver this 45 MHz IF is donwconverted again to give a standard

1 KHz output whose amplitude and phase relative to the reference channel may be easily measured.

The receiver has a dynamic range of 60 dB and ±0.25 dB linearity. The sensitivity to IF is -125 dBm or better (the sensitivity to RF is considerably less, depending on the conversion loss in the mixer used). Available local oscillator drive is rated at +24 dBm per channel (but is actually only +17 dBm).

Three additional units were used to convert received amplitude, phase and frequency to a machine-readable form. These units are listed below:

Amplitude:

The amplitude of the received signal, in the 1 KHz IF form, was measured by a Scientific Atlanta Model 1832. An averaging time of 1 second and a resolution of 0.1 dB were selected for this system. Accuracy is better than 0.2 dB over a 60 dB range. Use over extended periods indicated that this measurement unit had excellent stability.

Phase:

It is anticipated that future work will be concerned with measuring the relative phase angle of the received and transmitted signals. When operating with the S/A 1751 Receiver this would usually be measured by a S/A model 1822 Digital Phase Display. It accepts a digital analog of phase from the receiver and displays a result averaged over a selected number of cycles. For laboratory tests this works well but the path length and residual FM inhibit the instrument's operation. It should, however, be a simple task to build an adequate phase measurement unit with lower resolution.

Frequency:

The frequency of the transmitted signal is measured indirectly by monitoring the local oscillator frequency. Since the harmonic number, the IF frequency and whether mixing is upper or lower single-sideband are known, the RF signal frequency may be calculated. Measurement is made with a 0 to 18 GHz EIP Autohet Counter Model 351C with a selected resolution of 1 KHz.

2.3.5 Mixers

Harmonic mixers pumped by a 2 to 4 GHz local oscillator down-convert the 74 GHz signals to 45 MHz IF signals. In this application two mixers are required, one at the receiving antenna and the other at the source. Mixers must operate under the constraint of available local oscillator power, the best mixer being the one with the lowest conversion loss (from RF to IF). Three mixers, compatible with the current system, were evaluated; they were:

1) Standard Laboratory Detector (μLAB M206C or equivalent): A single 1N53 crystal in a pressure mounting on the waveguide with a BNC connector through which LO and IF are coupled.
2) S/A Model 13A/50: Rigid crystal mount of 1N53C diode. IF and LO are coupled through a type-N connector with matching of IF to the cable provided by a S/A Model 1767-45.
3) S/A Model 17-50-45: Cross-waveguide mixer with a rigid mount for a 1N53C diode. It is used with the S/A Model 1772 Local-Oscillator Frequency Multiplier which triples the local oscillator. This X-band signal is used to pump the cross-waveguide mixer.

All of the mixers are provided with stub tuners for matching.

The first mixer type was found unsuitable for use at the re-

ceiving antenna due to its poor sensitivity and mechanical instability. It is adequate, however, to monitor the source because high levels of oscillator and RF power are available.

The second type of mixer is used with a 1N53C diode which provides improved sensitivity over 1N53 diodes. By diode selection, careful tuning and optimum local oscillator drive a sensitivity of -81 dBm or better has been obtained repeatedly. This corresponds to a conversion loss of 45 dB and may be partly accounted for the high harmonic numbers employed in the downconversion [21 or 22]. (Current at the nth harmonic flowing in a diode decreases as $1/n^2$ if parasitics are neglected [57]).

By reduction of the harmonic mixing number substantial improvement may be achieved. The third mixer type does just this. It triples the local oscillator in a balanced frequency multiplier and mixes this X-band signal with the RF (a harmonic number of 7). With a 50 mwatt (+17 dBm) local oscillator drive, it gives a sensitivity of -98 dB, 17 dB improvement over the Model 13 mixer.

In this application, there are 42 m of RG - 8 coaxial cable (spiral dielectric, semi-rigid) with an attenuation of 11.8 dB at 4.0 GHz connecting the receiver to the receiving antenna mixer. Under this condition of limited local oscillator power, the second mixer type is superior to the third. Detailed measurements showing this are given in Appendix A. At present, then, the S/A Model 13A-50 mixer is used at the receiving antenna. (The third mixer could be used if the local oscillator power at the receiving antenna were boosted. This may be done with commercially available 2-4 GHz power amplifier with a gain of 18 dB and a saturated power output of +25 dBm,)

2.3.6 Millimetric Wave Source

A reflex klystron (VRE-2101B5 Varian Associates of Canada) is used as the mm - wave source. It has a power output of 500 mwatts and a 1.5 % tuning range about its center frequency of 73.5 GHz. FM noise levels are low so, consequently, receiver phase-lock is usually stable. The disadvantages of this source are the high operating voltages required (2500 volts DC) and the relatively short tube lifetime (guaranteed operation is 500 hours).

To overcome some of these problems an attempt was made to use a solid state mm-wave source. A Hughes Model 44051 H IMPATT diode oscillator was available with a rated power output of 50 mwatts at 70.25 GHz. Its low power requirement makes it feasible to mount the source directly to the transmitting antenna with considerable savings in waveguide losses. However, the FM noise levels in the mm-wave output were high enough that receiver lock was unattainable making this source useless in the present system.

2.4 Discussion

The received signal in the mm-wave link was measured to be -41 dBm, 40 dB above the receiver noise level. This is 22 dB below the calculated received signal level. The difference between the calculated and measured system performance has been only partially accounted for:

1) Phase Modulation:

Because the receiver is phase locked to the RF source, frequency changes of the source appear as phase changes in the receiving channel IF signal. The magnitude of these phase changes is proportional to the frequency change and the path length. Measurements have shown that the phase modulation results mostly from 60 Hz FM modulation of the klystron (caused by power supply ripple and by interference). Because of the narrow band filters used in the amplitude measurement, phase modulation reduces the apparent received signal level. This is thought to be about 3 dB with the present equipment.

2) Reflector:

The reflector "loss" of 5.2 dB was calculated assuming a perfectly flat reflecting surface. If it was distorted, the loss would, in general, be higher. For example, consider the surface distorted spherically such that the center of the reflector protrudes 2 mm from its former position. This would reduce its equivalent area to 0.125 m^2 [58] and increase reflector loss by 18 dB. The actual extent of reflector distortion is unknown but it is apparent that losses due to distortion could be high.

2.5 Summary

A short radar-type mm-wave link has been established. It is summarized below:

Frequency (GHz)		74.
Path length (km)		1.8
Free space loss (dB)		128.5
Gaseous Absorption (dB)		1.2
Reflector loss (dB)		5.2
Waveguide losses (dB)		8.6
Antenna gains (dB):	transmitting	49.5
	receiving	48.
Other losses (dB)*		22.
Source power output (dBm)		+27.
Receiver sensitivity (dBm)		-81.
Fade Margin (dB)		40.

* See Section 2.4

CHAPTER III

METEOROLOGICAL MEASUREMENT SYSTEM

3.1 Measurement of Rain Rate

3.1.1 Description of Rain Gauges

The rain gauges used in this thesis are intended to measure point rain rates up to 100 mm/hr. Accurate operation above this rate is not considered important because of the low probability of such events in this area. Rain gauges of the tipping bucket variety were specially designed for this purpose.

These rain gauges have a collecting area of 920 cm^2 and a nominal tip size of 4.6 grams so that a tip occurs after each 1/20 mm of rain. To allow electrical sensing of which way the bucket is tipped, a permanent magnet is fastened to the bucket in close proximity to a glass-encapsulated dry reed switch which is mounted on the rain gauge chassis. In the construction of these rain gauges, corrosion resistant materials were used as necessary to achieve low maintenance requirements and stable long-term operation. Further details are shown in Figs. 3.1, and 3.2.

3.1.2 Rain Gauge Network

Five rain gauges of the type described in Section 3.2.1 were installed on rooftops along the path at roughly equal spacings of 220 m. The detailed positions are given in Figs. 2.1 and 2.2. It is noted that the rain gauges are located at various heights between 1 and 35 meters below the microwave beam.

Connection of each rain gauge is made to the central measurement station (at the transmitter) by dedicated half-duplex telephone lines, one line per rain gauge. There, custom hardware biases each telephone line, detects the presence or absence of loop current, displays the state of the

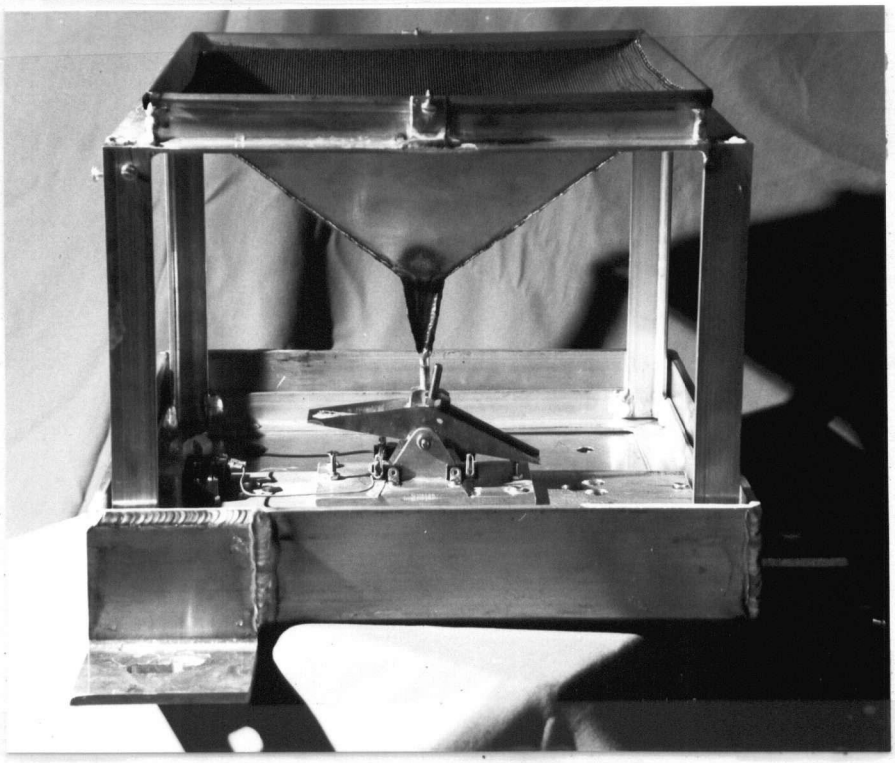

Fig. 3.1 A tipping bucket rain gauge with the side panels removed.

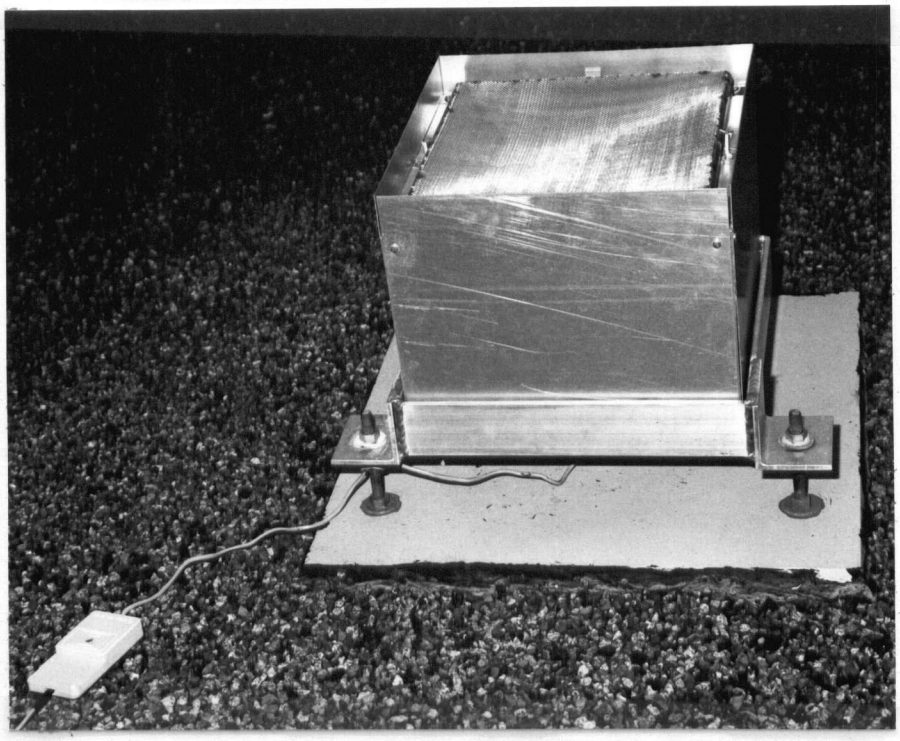

Fig. 3.2 A tipping bucket rain gauge as installed on a roof.

rain gauges and provides a machine-readable output. Details of this unit are given in Appendix B.

3.2 Other Measurement Units

Although the excess path attenuation on a short, millimetric-wave link is thought to be principally due to instantaneous rain rate along the path, other meteorological variables such as wind, temperature, humidity, drop-size distribution and gradient of refractive index may have some effect. Instrumentation has been installed to allow measurement of temperature and wind velocity.

(a) Temperature:

Two temperature transducers, placed out-of-doors in a Stenvenson's screen near the antennas, serve to measure ambient temperature. Their design is based on the National Semiconductor LX500 integrated circuit which gives an analog output of 0.1 volt/°C.

(b) Wind Velocity:

A propeller-type anemometer has been assembled. The transducers used are dc generators with linear voltage-speed characteristics. Two transducers are mounted on a platform free to face into the wind, one horizontally and the other at 45° from the vertical. A synchronous motor with its rotor geared to the platform is used to sense wind direction. Further details are given in Appendix C. The anemometer developed here allowed measurement of horizontal and vertical wind speeds and wind direction. At present, however, the unit is positioned too close to the roof and outside wall of the building for the measurements to be considered accurate.

3.3 Discussion

Point rain rate, as measured by a tipping-bucket rain gauge, is

subject to a variable integration time directly proportional to tip size and inversely proportional to rain rate. The often-used 0.25 mm/tip rain gauge [37,39] has an integration time of 18 sec. at 50 mm/hr. This is thought to be rather long, motivating the selection of a 0.05 mm tip size in the rain gauge described in Section 3.2.1, which has an integration time of 3.6 sec. at 50 mm/hr.

It is noted that virtually all studies in the last ten years used capacitative rather than tipping-bucket rain gauges. Capacitative rain gauges potentially offer an averaging time independent of rain rate and as small as 1 second. In practice, however, they suffer from calibration drifts and give erratic results at low rain rates [28]. Two capacitative gauges were developed here and later abandoned because of their poor performance at low rates. This behavior was particularly unsuitable for the present work since most rainfall is light, meaning that accurate results would be available only a small part of the time it was raining. In contrast, the tipping bucket rain gauge used in this work is reliable and accurate (within 5%) for all rain rates between 0 and 100 mm/hr.

The spacing of 220 meters between rain gauges may be compared with spacings in previous studies: 3300 m [37,46], 1300 m [28], 240 m [39] and about 40 m [47,26]. Certainly, high rain gauge densities are desirable since this allows for accurate measurement of the spatial variation of rain rate. It is thought that the spacing used in this work provides a reasonable compromise between accuracy and efficiency.

The drop size distribution of rainfall could also be an important parameter. It is usually reported as a histogram of distribution by volume of rain into various drop size classes. The measurement of drop size spectrum has not so far been implemented in the system, however.

CHAPTER IV

DATA ACQUISITION AND DATA BASE FORMATION

4.1 Introduction

To be able to carry out comprehensive statistical analyses of accumulated weather and propagation data, it is desirable to have the data in a form compatible with a general purpose computer. This chapter is concerned with the collection and transfer of observations from the sensors of Chapters 2 and 3 into a machine readable data base.

The techniques required to do the above must, at some stage, record the data and digitize it. The sequence of these two operations is different for different systems. Four data-logging systems in common usage were considered:

1) Recording on strip chart followed by manual digitization
2) Analog recording on magnetic tape and later digitization under software control
3) Recording on paper tape by a hardwired controller
4) Real time digitization and recording on an intermediate medium under software control.

For this work, the last method was selected. It is an attractive technique in view of the present availability of powerful integrated circuits and minicomputers with adequate support. The viability of this method can be readily seen in this thesis. A block diagram of the system as implemented is shown in Fig. 4.1.

Three components of the data logging system which may be immediately identified are:

1) a minicomputer
2) an interface between a multitude of sensors and the minicomputer

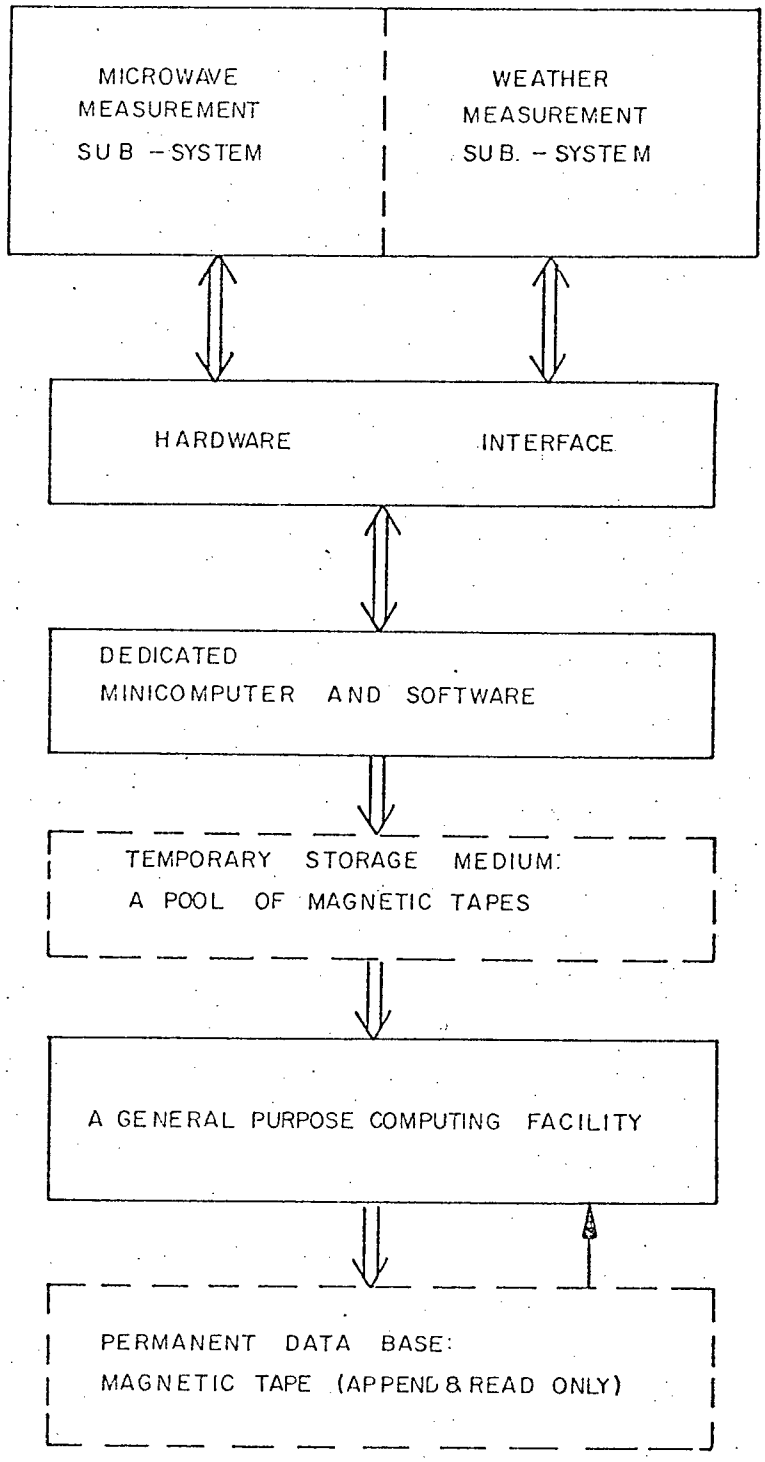

Fig. 4.1 Data acquisition system block diagram.

3) a storage medium on which to record data.

The interface must be compatible with the minicomputer family selected and must be able to handle the required data rates. Other than this, it may be designed with little knowledge of the rest of the system (as outlined in Section 4.2). On the other hand, selection of an intermediate storage medium on which data are held before transfer to the analysis computer requires substantial knowledge of the data logging problem and depends on the strategy by which data is recorded.

4.1.1 Possible Recording Strategies

By the use of recording strategies of varying levels of sophistication, the same information may be stored at differing degrees of compactness. The four strategies considered here are given below, in order of increasing efficiency:

1) To record values for all variables at a single fixed rate
2) To record values for all variables at a special rate for each variable
3) To record by strategy (1) or (2) but only when the output meets some predetermined criteria of being "interesting"
4) To record the output of a sensor only when it has changed a predetermined amount form the previous recorded value.

Method (4) recognizes the fact that many of the sampled signals are usually slowly varying while providing adequate sampling when they do vary quickly. It is potentially the most efficient of the four strategies but offers no special advantage for continually fluctuating signals (such as wind speed). Method (1) is inefficient in its utilization of storage space since the output of each sensor is recorded at the rate appropriate to the fastest-varying one. However, it has the advantage of simplicity,

completeness and of requiring little advance knowledge of signal characteristics. Methods (2) and (3) are variations of (1) and, while more efficient, they are also more complex. Method (3) could lead to loss of important information due to uninformed definition of what is "interesting".

4.1.2 Storage Media

The storage media usually associated with minicomputers are:

1) paper tape
2) magnetic tape
3) disk

The decision as to which to use depends upon the instantaneous rate at which data is written, the medium's capacity and its reliability. Table 4.1 gives a comparison of the above media on these points.

Storage Medium	Maximum Output Rate [Bytes/sec]	Capacity [10^6 bytes]	Relative Reliability
Paper tape: ASR 33	10	0.13	Very Low
Paper tape: high speed punch	63.5	0.13	Low
Magnetic tape (800 BPI)	> 10,000	19.	High
Disk (single platter)	> 100,000	2.4	High

Table 4.1 A comparison of various intermediate bulk storage media.

Paper tape is immediately ruledout by its relatively poor reliability and small capacity; for this application, the capacity of a suitable medium should at least allow unattended operation overnight and preferably over a weekend. Magnetic tape is well-suited on all counts. (One 2400' magnetic tape will hold 80 hours recording at 64 bytes/second.) It is also a standard medium for intercomputer information exchange.

The application of disk storage is somewhat different. For a variety of reasons disk storage cannot be physically transported between computers. The usual mode of operation on disk would then be to store data on disk and periodically dump them to the analysis computer via a data link. Scheduled downtime on the IBM 370 is long enough that only daily transmissions are feasible (this limits the average recording rate to 11 bytes/second). With a suitable recording strategy this is certainly feasible and would offer, in theory, completely unattended operation. Disk storage is,however, not used in this system because the capacity of the available disk is rather small and because it would require, simultaneously, the correct operation of two computers. The increased complexity of such a system was thought to be undesirable at this time.

Magnetic tape appeared to be the storage medium most suited to this data logging application. The high capacity of magnetic tape allowed the use of recording strategy (1), one sample of each of 32 variables every second. Such a strategy was expedient in the development stages of this system as it required little advance knowledge of signal characteristics and afforded a maximum of flexibility.

The purpose of the data acquisition system is to log data on a real time and continuous basis and to enter this data, suitably edited and formatted, into a permanent data base at a more powerful computing facility for later analysis. It is intended that data base formation be routine and relatively automatic.

In the following sections, details of the flow of data into a permanent data base are given. Specifically the interface allowing minicomputer access to the microwave and weather sensors, the minicomputer-based data logging scheme and the post processing of data on an IBM 370 are described.

4.2 Minicomputer Interface

The local availability of minicomputing facilities indicated that an interface should be compatible with the Nova line of computers. Interfacing techniques are well known [59] and considerable experience with them exists within the department.

This interface allows computer interrogation of 5 measurement units: 2 digital amplitude displays, a phase display, a frequency meter and a rain gauge monitoring unit. It also permits reading of the time of day and the voltage levels on 16 analog inputs (meteorological sensors and receiver parameters).

Internal to the interface circuitry, three subsystems can be identified, each with its own device number. These are: a 16 channel A/D converter, an 8 channel x 16 line data selector and a real time clock. The remaining units: the display panel, 24 hour clock and I/O bus terminator are associated with the interface as a whole. A block diagram of these units and associated interconnections is given by Fig. 4.2.

The A/D converter subsystem is built around an Analogic MP6912 16-channel 12 bit Data Aquisition module. Over-voltage protection and selectable filtering of the 16 analog inputs are provided by a custom circuit board. Two other boards, the Device 56 interrupt card and the A/D control unit, allow minicomputer control of channel selection and the start of conversion processes. Interrupts on Device 56 have been disabled for software reasons; hence the end-of-conversion condition must be sensed by checking busy and done flags. The cycle time of this subsystem is about 15 μsec per channel.

The 5 measurements units listed above and the 24 hour clock are accessed by the minicomputer through a digital multiplexer controlled

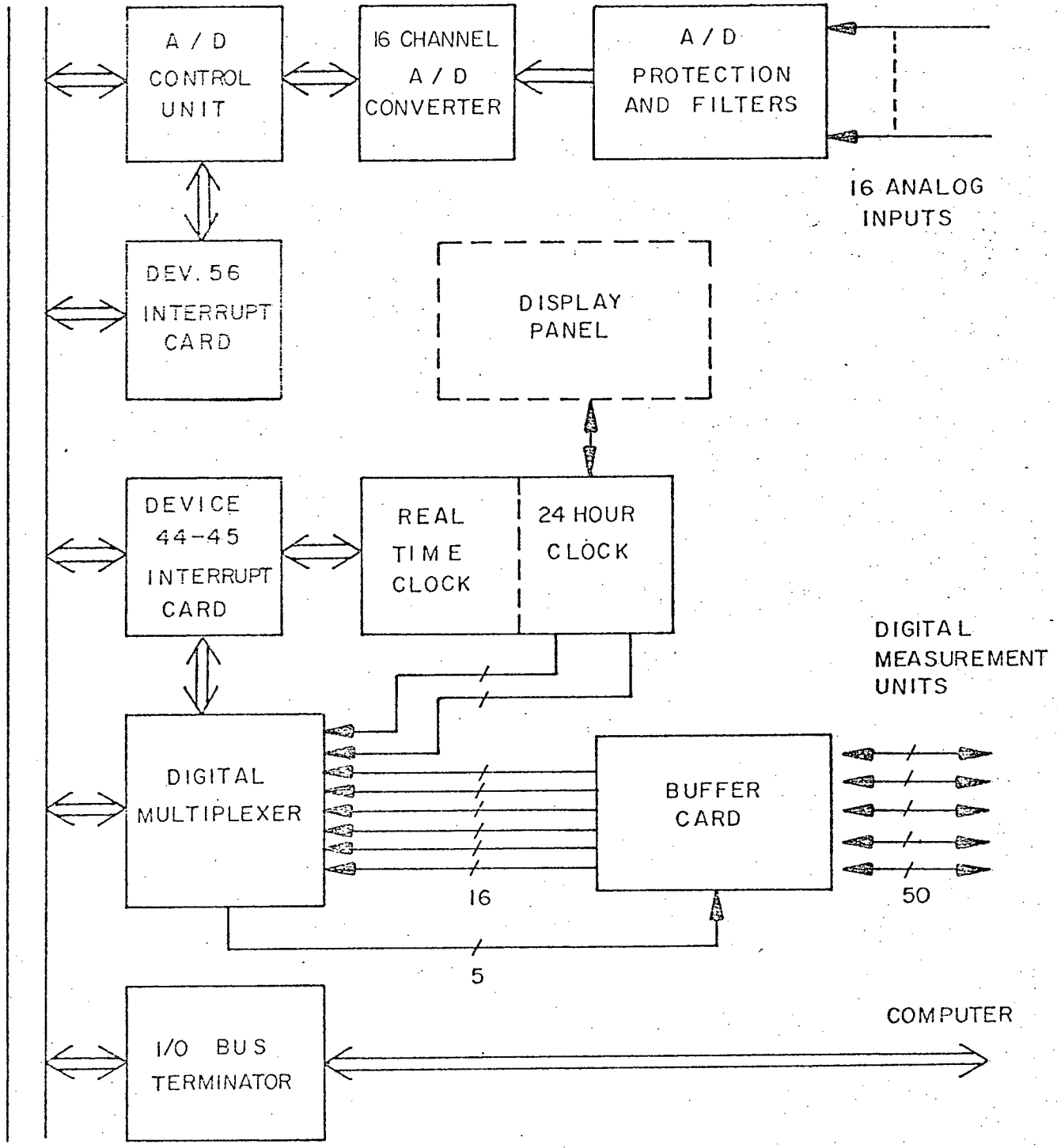

Fig. 4.2 Block diagram of the minicomputer interface.

by the device 45 interrupt card. The digital multiplexer selects one group of 16 lines out of 8 groups and places it on the data bus when strobed. Each of the measurement units and the clock are assigned one or two multiplexer channels as required; the hardware connections for this being made on the Digital Buffer card. By sampling a channel, a delayed pulse is generated which is used by most measurement units to restart conversion processes. These pulses keep measurements synchronous with the computer.

Device 44 controls the real time clock which, when started, interrupts the minicomputer on a regular basis. The interrupt rate is set by the minicomputer and may range from 0.0015 Hz to 200 KHz. In particular, exact values of 100 Hz, 10 Hz, 1 Hz, 0.1 Hz and 0.01 Hz are available. These values are "exact" with respect to the 24 hour clock as both the 24 hour clock and the real time clock are derived from the same source, a 2.4576 MHz crystal oscillator. The real time clock initiates sampling of various interface channels by the minicomputer software.

The particular instruction sequences for interface operation are given in Appendix D. Detailed circuit diagrams are also contained there.

To summarize, the interface described above allows reading of the microwave and weather sensors described in Chapters 2 and 3 by the minicomputer, via an 8 channel data selector and a 16 channel A/D converter.

4.3 Real Time Data Acquisition and Recording

4.3.1 The Computing Facility

The real time data acquisition system is designed to operate with the Nova line of minicomputers. The minimum hardware configuration under

which the software developed here will operate includes:

1) a Nova CPU with 16 K words of memory

2) a 9 track IBM compatible magnetic tape unit and controller

3) a teletype

(in addition, hardware multiply/divide is used although the software version is fast enough for this application).

This facility would be run under a core resident operating system; in this case with the Real Time Operating System (RTOS), a software package available from Data General Canada Corp.

At present, however, data acquisition is carried out at a more powerful Nova 840 minicomputer facility (32 K of core memory), with a disk operating system (RDOS - Rev. 5). While the software written for RTOS operation is fully compatible with the disk operating system, a version was written especially for RDOS Rev. 5. It makes program interruption simple and relatively foolproof; this is a necessary feature as the Nova 840 is shared by many users.

4.3.2 Multitask Programming

The software developed here uses a multitask program environment rather than the more conventional single task environment. A multitask environment is one in which more than one task competes for CPU control. Tasks operate asynchronously, and in real time, with control being allocated to the ready task of highest priority by a supervisory program, the Task Scheduler. Synchronization between tasks is maintained by transmission and reception of messages by tasks. This allows any task to go into suspension pending the arrival of fresh data.

A general task structure was adopted here. The task is divided into three parts: initiation, process loop and termination. The initi-

ation sets pointers and counters to initial values, allocates required system resources and then passes control to the process loop. One pass through the "process loop' occurs each time an unprocessed data record becomes available; any time no data are available, the task is in suspension. Upon occurence of an end condition, the termination routine is entered. This releases previously allocated system resources and then removes the task from the program environment. The above task structure reduces connection between tasks to data buffers and single word messages. Such modularization eases software modification and clarifies operation.

4.3.3 Program Operation

The data acquisition software operates with six core resident tasks in competition for CPU control. Tasks communicate with each other through five message addresses and operate on data held in two data structures, a circular queue and an output buffer.

Both data structures are two-dimensional arrays indexed by relative time (of data sampling) and by a variable number. Thus each data structure is composed of an integral number of records. A record, if it holds active data, contains all data acquired in an interval of time (one second). The assignment of variables to record elements is detailed in Table 4.2. The circular queue [60] is used to hold data records during various stages of processing. The definition of the pointers associated with the queue is given in Fig. 4.3. The output buffer is a linear array into which processed data records are assembled before being written onto magnetic tape.

Three tasks: INPUT, PROCESS, and OUTPUT are central to the data acquisition and recording, fulfilling functions analogous to their names. INPUT samples various channels under synchronization from the interface,

WORD (Octal)	DESIGNATION
0	Amplitude 1 [10^{-2} dB]
1	Amplitude 2 [10^{-2} dB]
2	Phase [10^{-1} degrees]
3	Frequency, upper four digits [10^{7} Hz]
4	Frequency, lower four digits [10^{3} Hz]
5	Rain gauge monitor output
6	24 hour clock, hours
7	24 hour clock, minutes and seconds
10 to 27	A/D channels 1 to 16 [5mv/bit]
30 to 37	Rain rates on gauges 1 to 8, [mm/hr] x 182.2

Table 4.2 The 32 word record structure used in the real time data acquisition system.

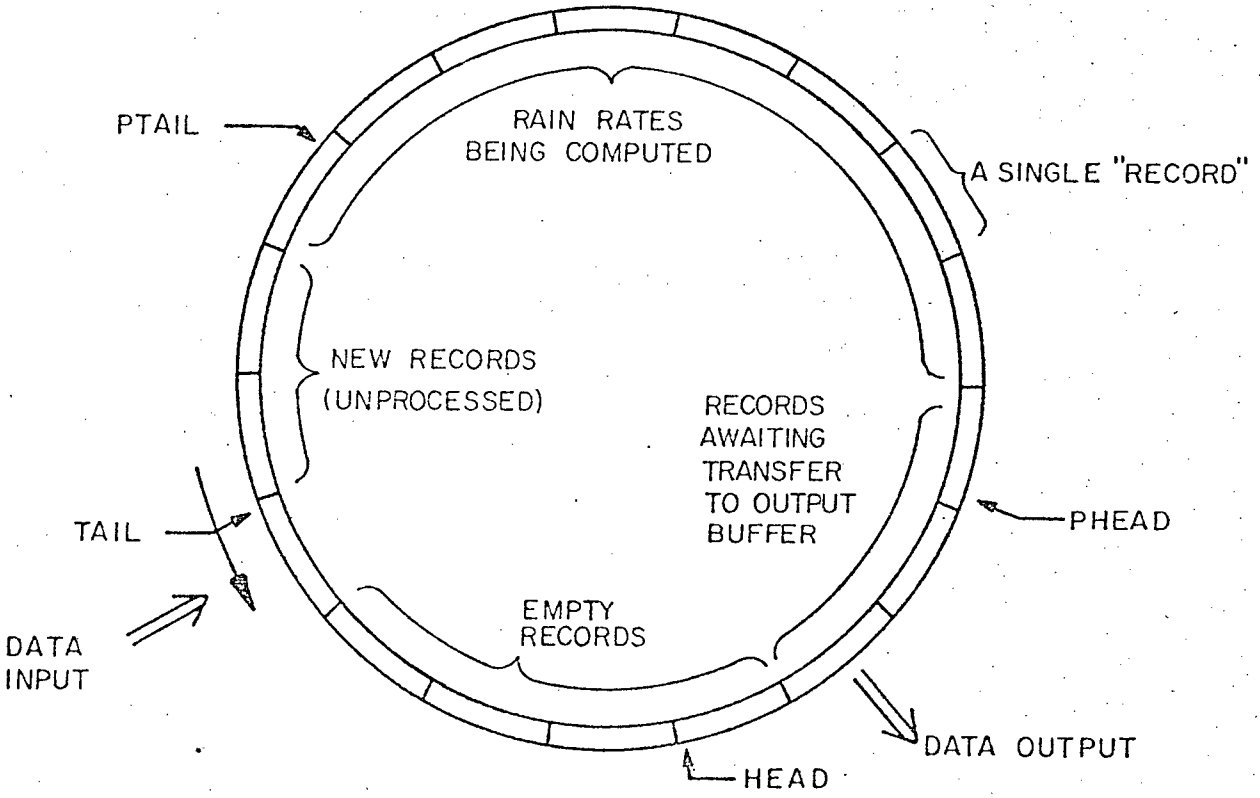

Fig. 4.3 The circular queue and associated pointers.

converts all inputs to 16 bit 2's complement format and places the result in the queue. PROCESS examines new records, computes rain rates, inserts results in the queue and releases records for output. OUTPUT assembles blocks of records in the output buffer and writes them on tape as required. It also divides the output into files and performs associated bookkeeping activities.

The remaining three tasks fill secondary roles. START initiates program operation in an ordered manner and terminates it in similar fashion when CONSOLE detects the end condition. MONITOR allows the operator to check the output buffer to ascertain program and hardware performance.

The above description of each task together with Fig. 4.4 provide some insight into how the software operates. The actual flow of CPU control is indeterminate and data dependent; in general, it does not follow directly the same path as message transmissions. All tasks were designed so they could operate considerably delayed with respect to tasks in front of them in the process chain. Being a real time system with finite buffer sizes, program failure will occur if delays become large enough. The software, however, contains enough flexibility that failure by this mechanism is rare. No such events have occurred at the output rate of 1 record/second.

A more detailed explanation of program operation together with software listings is given in Appendix E. Appendix E also deals with operation and backup of the software.

4.3.4 Rain Gauge Processing

A data word read from the rain gauge monitoring unit shows which rain gauges, if any, have tipped in the last clock cycle; it does not per se yield the point rain rate at each gauge. However, knowing the

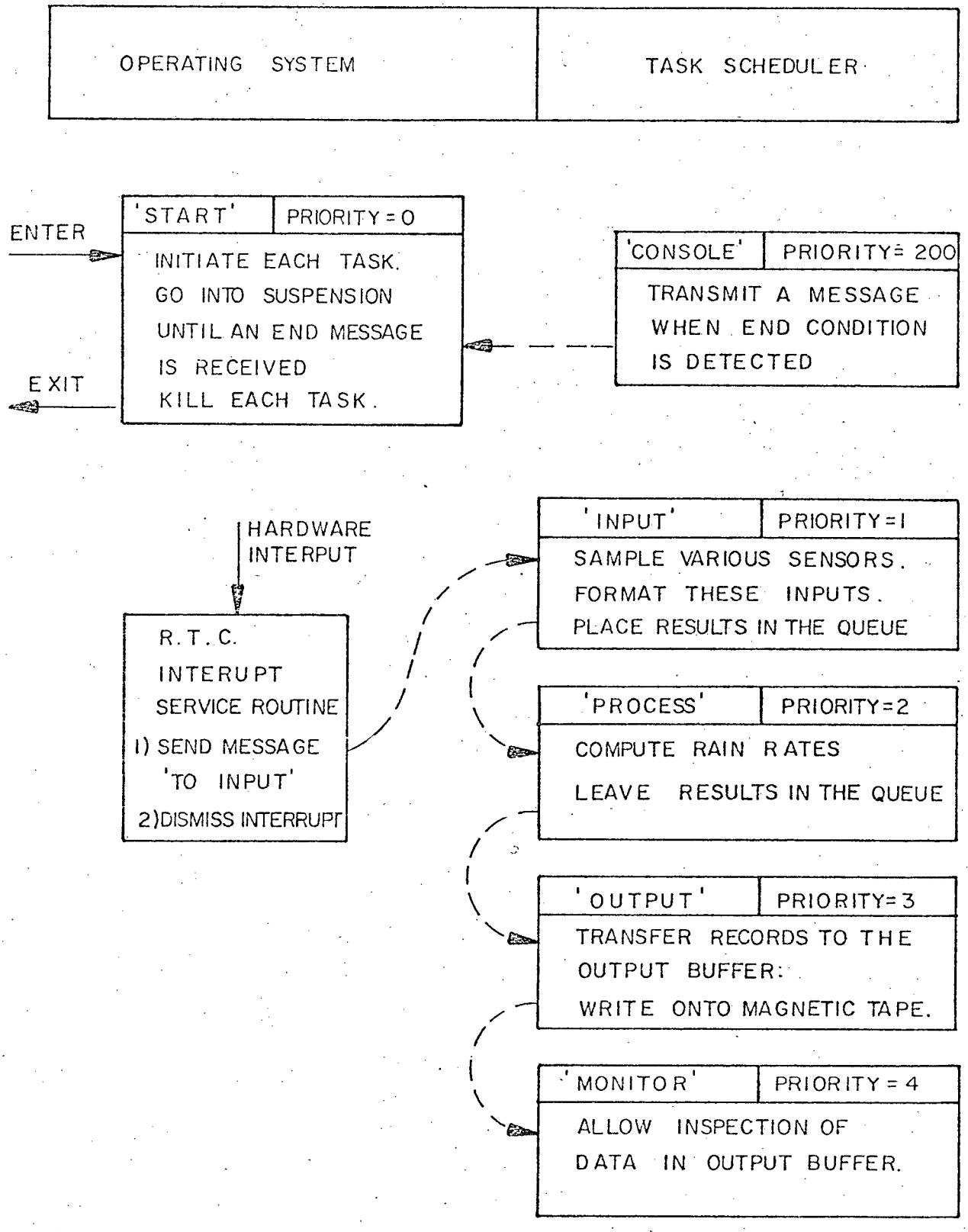

Fig. 4.4 A block diagram of the data acquisition software showing the messages which connect various tasks (Dashed lines represent message transfers).

interval between successive tips on a gauge the average rain rate in that interval may be computed; it is inversely proportional to the interval length. At high rain rates (50 mm/hr) time between tips is short (3.6 sec for 1/20 mm tip size) requiring that gauges be sampled sufficiently often to accurately quantize the interval between tips. A rate of 16 Hz was used giving 6 bits resolution at this rain rate.

At sufficiently low rain rates, tip interval will exceed the queue length (6.5 minutes) and inevitably distortion will occur because data must be written onto tape before sufficient information is available to complete the calculation. With the 1/20 mm tip size distortion only occurs for rates below 1/2 mm/hr, a rain rate of little interest in this propagation study.

4.3.5 Summary

A real time data logging system implemented on a Nova 840 minicomputer was described in this section. It allows unattended recording of microwave and weather sensor outputs on magnetic tape for 80 hour periods. All data are processed so that they appear as quantized discrete random variables.

4.4 Creation of a Data Base

4.4.1 Data Base

The data base to be created in the propagation study will be a collection of "interesting" propagation-related phenomena. Such phenomena would include signal level fluctuations by any atmospheric mechanism and rain itself even if no microwave signal were available. Short periods of the clear air propagation preceding and following storm activity would be included to avoid "out of context" events.

The data base is resident on labelled magnetic tape. It is com-

posed of unit length files (1/2 hour of original recording) each of which has a header describing its contents and a unique file name. By the use of labelled tape formats and headers, data files may be referenced with minimal knowledge of their physical characteristics. Roughly 250 files may be held on each tape.

An estimate of the size of above data base is of interest. An upper bound on its annual growth may be obtained from the yearly accumulated rainfall; 1070 mm in Vancouver [61]. If data is saved during rain rates exceeding 2 mm/hr, it is apparent that such events cannot occur more than 540 hours per annum; an annual growth of five tapes or less. This data base for a 5 year study would be 25 magnetic tapes, a reasonable size.

4.4.2 Data Base Formation

After recording on the Nova 840, the data tapes are taken to the IBM 370 facility. There, data are read from these tapes, formatted to the proper labelled tape file structure (this includes scaling of data), edited to eliminate uninteresting data and the balance appended to the permanent data base. This action is initiated through the submission of various batch-processing jobs.

Although it is possible to do the above in a single step, this is not done at present because unfamiliarity with the data has inhibited definition of formal criteria for data selection. Currently, a multi-step process is used, with decisions being made by a human observer. The software employed provides various printed and plotted summaries to aid in the decision process.

The software is written in FORTRAN IV and uses Michigan Terminal Systems (MTS) input/output and plotting routines. Programs are of two

types: those which transfer the data from one to another and those which provide the user summaries of the data. Specifically they are:

Transfer

1. Scaling/Conversion: Input data are from an unlabelled tape written on the Nova system at a density of 800 BPI (bits per inch) in half-word integer format. Inputs are scaled to proper units and selected variables are written to the output tape (labelled) at 1600 BPI, in floating point, and in files not longer than 1/2 hour (< 64,000 values). A statistical summary of the variables in each file is printed. After this step, input tapes may be returned to the Nova system to be written with new data.
2. Transfer to Data Base: Selected files from the tapes written by program 1 are appended to the permanent data base tapes. After this step, input tapes may be emptied and reused in program 1.

Summary Information

3. Calcomp Plotting: A collection of programs written using the Calcomp plotter allows plotting of several variables together as a function of time. Combinations include attenuation with path-average rain rate and individual point rain rates with path-average rain rate.
4. Tape Listing: This program gives a highly condensed summary of contents of each file stored on a particular tape. It is useful in data editing.

The data acquisition system involves the use of three magnetic tape pools:

1. Intermediate storage between Nova 840 and IBM 370
2. Temporary storage of Program 1 results pending transfer to the permanent data base

3. Permanent data base.

Tapes in pools 1 and 2 are cycled continually while those in pool 3 are read - only.

4.4.3 Processing Costs

Because of the high volume of data to be processed, care was exercised during program development to keep computing costs to reasonable levels. The approximate cost in "computing center dollars" per 1000 hours of original recording with jobs run on low priority is:

1.	Scaling/Conversion	350.
2.	Plotting (all types at 1/2 hour/inch)	1000.
3.	Transfer to Data Base	200.
4.	Tape Listing	240.

Only programs 1 and 4 are run on all recordings made. Plotting is usually carried out on 20% of recordings and less than 10% are entered in the final data base. Based on continuous-recording by the data-logging system, the cost of processing data to create the data base would not exceed 7100 "computing center dollars" per year. The real dollar cost to the user would be a fraction of this amount.

CHAPTER V

PRELIMINARY RESULTS

5.1 Post Processing

As outlined in Section 4.4, data recorded on magnetic tape by the data acquisition system is passed through several stages of processing and is entered into the permanent data base. Samples of the data at the various stages are included below.

Fig. 5.1 is a summary sheet of data file 'RAIN102884' showing the mean, standard deviation, minimum and maximum of each of 23 variables which were retained out of those recorded on the Nova 840. The length of the file, date of recording, and certain comments are also included. The overall contents of a tape may more easily be assessed with a summary of the type given in Fig. 5.2.

A sample of rain activity in plotted form is included in Fig. 5.3 (a, b, c). The salient points are:

- the duration of the rain is 9:00 a.m. to 10:30 a.m.
- the rain occurs in identifiable bursts.
- both attenuation and rain rate can vary by a factor of two in less than one minute. However, attenuation can still be considered smoothly varying.
- the receiver was out of lock for 15 minutes at 10:30 a.m. The signal during that period is the system noise level.
- both crystal current and frequency were stable; hence baselining the signal level should be reliable.
- rain gauges 1, 2, and 3 functioned normally. Number 4 was not installed and number 5 was malfunctioning.

Other samples of data are included in Figs. 5.4 (a, b, c, d).

```
***THIS FILE IS CONTINUOUS IN TIME FROM THE PREVIOUS FILE
DSN=RAIN102884        LENGTH= 1800SECONDS        STORED ON AAAAAAAA
DATA AQUISITION:  3: 4:77 ON MTO:  2    8AAAA


GLOBAL COMMENT: RAIN GAUGES: 1=F.F.,2=CHEM.ENG.,3=WESBROOK,5=GAGE TOWERS
                ANO1=HORIZ. WIND, ANO2=SLANT WIND, ANO3=WIND DIR'N.
                ANO5,ANO6 ARE TEMPERATURES.
                ANO7,ANO8: CAPACITATIVE RAIN GAUGES.
                ANO4=XTAL CURRENT IN MA.


PARTICULAR COMMENT:
                AAAAAAAAAAAAAAAAAAAAAAAAAAAAAAAAAAAAAAAAAAAAAAAAAAAAAAAAAAAAAAAA
                AAAAAAAAAAAAAAAAAAAAAAAAAAAAAAAAAAAAAAAAAAAAAAAAAAAAAAAAAAAAAAAA
                AAAAAAAAAAAAAAAAAAAAAAAAAAAAAAAAAAAAAAAAAAAAAAAAAAAAAAAAAAAAAAAA
                AAAAAAAAAAAAAAAAAAAAAAAAAAAAAAAAAAAAAAAAAAAAAAAAAAAAAAAAAAAAAAAA
```

	MEAN	STD DEV	MINIMUM	MAXIMUM
AMP1(DB)	-8.24	0.96	-11.10	-6.60
AMP2(DB)	-327.68	0.00	-327.68	-327.68
PHAS(DEG)	1638.30	0.00	1638.30	1638.30
FREQ(KHZ)	3624651.81	2.52	3624645.00	3624661.00
TIME(H:M:S)	150487.83	2039.18	145545.00	152544.00
ANO1(VOLTS)	-0.36	0.19	-1.11	0.17
ANO2(VOLTS)	-0.18	0.13	-0.63	0.15
ANO3(VOLTS)	1.01	0.34	-0.08	3.53
ANO4(VOLTS)	-2.07	0.01	-2.08	-2.05
ANO5(VOLTS)	0.46	0.01	0.43	0.49
ANO6(VOLTS)	0.44	0.01	0.41	0.47
ANO7(VOLTS)	-0.01	0.00	-0.01	0.01
ANO8(VOLTS)	-0.01	0.00	-0.01	0.01
ANO9(VOLTS)	-0.04	0.00	-0.05	-0.03
AN10(VOLTS)	-0.01	0.00	-0.02	0.00
RGN1(MM/HR)	2.72	1.70	1.03	12.86
RGN2(MM/HR)	2.24	1.67	1.30	9.72
RGN3(MM/HR)	2.59	1.58	1.19	14.31
RGN4(MM/HR)	2.42	1.70	1.09	15.14
RGN5(MM/HR)	1.64	0.92	0.87	7.09
RGN6(MM/HR)	0.0	0.0	0.0	0.0
RGN7(MM/HR)	0.0	0.0	0.0	0.0
RGN8(MM/HR)	71.61	2.11	69.33	73.78

```
DSN=RAIN102885
         14
```

Fig. 5.1 A typical summary sheet for a data file generated in the first processing step.

TAPE SERIAL # : P05614

	DATA SET NAME	LENGTH (SEC)	DATE	TIME	AMPLITUDE (DB) MEAN	STD DEV	MIN.	MAX.	RAIN RATES (MM/HR) 1	2	3	4	5
1	RAIN102623	1800	2/22/77	6:48:57	-5.01	0.12	-5.30	-4.70	0.0	0.0	0.0	0.0	0.0
2	RAIN102624	0											
3	RAIN102625	1800	2/22/77	7:18:57	-5.19	0.14	-5.70	-4.90	0.0	0.0	0.0	0.0	0.0
4	RAIN102627	1900	2/22/77	8:19:57	-5.33	0.29	-6.50	-5.20	0.60	0.35	0.44	0.20	0.24
5	RAIN102628	1600	2/22/77	8:48:57	-4.60	0.22	-5.40	-4.20	0.0	0.0	0.0	0.0	0.08
6	RAIN102629	0											
7	RAIN102630	1800	2/22/77	9:18:57	-5.30	1.31	-9.00	-4.20	0.20	0.40	0.70	0.60	0.50
8	RAIN102631	1800	2/22/77	9:49:57	-4.51	0.11	-5.10	-4.20	0.0	0.10	0.0	0.0	0.0
9	RAIN102632	60	2/22/77	10:18:57	-4.43	0.05	-4.50	-4.30	0.0	0.0	0.0	0.0	0.0
10	RAIN102709	1800	2/26/77	17:52:32	-5.90	0.87	-8.40	-4.90	0.0	0.10	0.20	0.09	0.06
11	RAIN102710	1260	2/26/77	18:22:32	-6.57	0.43	-7.90	-5.50	0.29	0.0	0.14	0.02	0.05
12	RAIN102711	1800	2/26/77	19:29:20	-6.95	0.65	-8.90	-5.90	0.74	0.50	0.50	0.36	0.34
13	RAIN102712	960	2/26/77	19:59:20	-6.02	0.22	-6.80	-5.40	0.27	0.19	0.37	0.25	0.26
14	RAIN102713	1800	2/26/77	22:53:36	-7.82	0.56	-9.20	-6.40	1.71	1.42	1.62	1.36	1.17
15	RAIN102714	1800	2/26/77	23:23:36	-6.30	0.79	-9.40	-5.40	0.69	0.57	0.67	0.71	0.56
16	RAIN102715	1800	2/26/77	0: 0: 0	-5.85	0.40	-7.40	-5.30	0.40	0.27	0.22	0.22	0.19
17	RAIN102716	1800	2/27/77	0:23:36	-5.82	0.50	-7.50	-5.40	0.29	0.15	0.12	0.13	0.08
18	RAIN102717	0											
19	RAIN102718	1800	2/27/77	0:53:36	-5.65	0.67	-7.70	-4.90	0.31	0.17	0.16	0.17	0.0
20	RAIN102719	1600	2/27/77	1:23:36	-5.13	0.12	-5.60	-4.80	0.0	0.0	0.0	0.0	0.0
21	RAIN102720	1600	2/27/77	1:55:36	-5.05	0.08	-5.40	-4.70	0.0	0.0	0.0	0.0	0.0
22	RAIN102721	1800	2/27/77	2:23:36	-5.14	0.09	-5.40	-4.90	0.0	0.0	0.0	0.0	0.0
23	RAIN102746	1800	2/28/77	0:35:26	-7.89	0.71	-9.60	-5.90	2.05	1.86	1.95	1.47	1.52
24	RAIN102747	1800	2/28/77	1: 5:26	-7.42	0.82	-9.10	-5.70	1.53	1.33	1.44	1.28	1.47
25	RAIN102748	1800	2/28/77	1:35:26	-5.59	0.31	-6.80	-5.00	0.0	0.03	0.0	0.04	0.10
26	RAIN102749	1800	2/28/77	2: 5:26	-5.85	0.55	-7.70	-5.00	0.40	0.42	0.42	0.40	0.28
27	RAIN102750	0											
28	RAIN102751	1800	2/28/77	2:35:26	-6.54	0.57	-8.40	-5.70	0.78	0.64	0.65	0.67	0.56
29	RAIN102882	540	3/ 4/77	12:27:27	-4.78	0.10	-5.00	-4.50	0.0	0.0	0.23	0.0	0.0
30	RAIN102883	1800	3/ 4/77	14:25:45	-26.08	17.27	-47.00	-1.00	1.08	0.97	1.16	1.01	0.89
31	RAIN102884	1800	3/ 4/77	14:55:45	-8.24	0.96	-11.10	-6.60	2.72	2.24	2.59	2.42	1.64
32	RAIN102885	1800	3/ 4/77	15:25:45	-21.68	18.75	-44.90	-4.70	0.48	0.49	0.47	0.45	0.29
33	RAIN102886	1800	3/ 4/77	15:55:45	-21.04	18.60	-45.40	-4.60	0.74	0.67	0.74	0.71	0.53
34	RAIN102887	0											
35	RAIN102888	300	3/ 4/77	16:25:45	-5.16	0.07	-5.30	-5.00	0.92	0.56	0.66	0.58	0.28
36	RAIN102926	1800	3/ 5/77	20:57:56	-4.77	0.38	-5.50	-3.80	0.46	0.38	0.38	0.52	0.35
37	RAIN102927	1800	3/ 5/77	21:27:56	-6.42	0.57	-8.00	-5.10	1.64	1.62	1.59	2.13	1.24
38	RAIN102928	1800	3/ 5/77	21:57:56	-4.52	0.54	-6.20	-3.90	0.09	0.10	0.13	0.14	0.10
39	RAIN102929	0											
40	RAIN102930	1800	3/ 5/77	22:27:56	-7.81	11.57	-45.30	-3.90	0.0	0.0	0.0	0.0	0.0
41	RAIN102931	1800	3/ 5/77	22:57:56	-4.26	0.26	-5.00	-3.80	0.16	0.10	0.0	0.10	0.05
42	RAIN102932	1800	3/ 5/77	23:27:56	-7.58	10.54	-44.80	-4.10	0.24	0.10	0.20	0.10	0.08
43	RAIN102933	1800	3/ 5/77	0: 0: 0	-3.91	0.08	-4.20	-3.70	0.0	0.10	0.0	0.0	0.07
44	RAIN102961	1800	3/ 6/77	10:57:56	-5.65	0.25	-6.20	-4.90	0.90	0.77	0.70	0.95	0.64
45	RAIN102962	1800	3/ 6/77	11:27:56	-6.23	0.43	-7.80	-5.60	0.97	0.77	0.69	0.90	0.64
46	RAIN102979	1800	3/ 6/77	22:15:58	-3.74	0.30	-4.80	-3.30	0.0	0.0	0.0	0.08	0.10
47	RAIN102980	1800	3/ 6/77	0: 0: 0	-4.71	0.49	-6.10	-3.70	0.65	0.60	0.56	0.74	0.30
48	RAIN102981	1800	3/ 7/77	0:15:58	-4.18	0.43	-5.20	-3.40	0.35	0.20	0.24	0.28	0.10
49	RAIN102982	0											
50	RAIN102983	1800	3/ 7/77	0:45:58	-4.43	0.89	-6.20	-3.50	0.40	0.40	0.30	0.40	0.30
51	RAIN102984	1800	3/ 7/77	1:15:58	-4.31	0.54	-5.80	-3.70	0.13	0.20	0.20	0.10	0.10

Fig. 5.2 A compact summary of the data in each file stored on a particular magnetic tape.

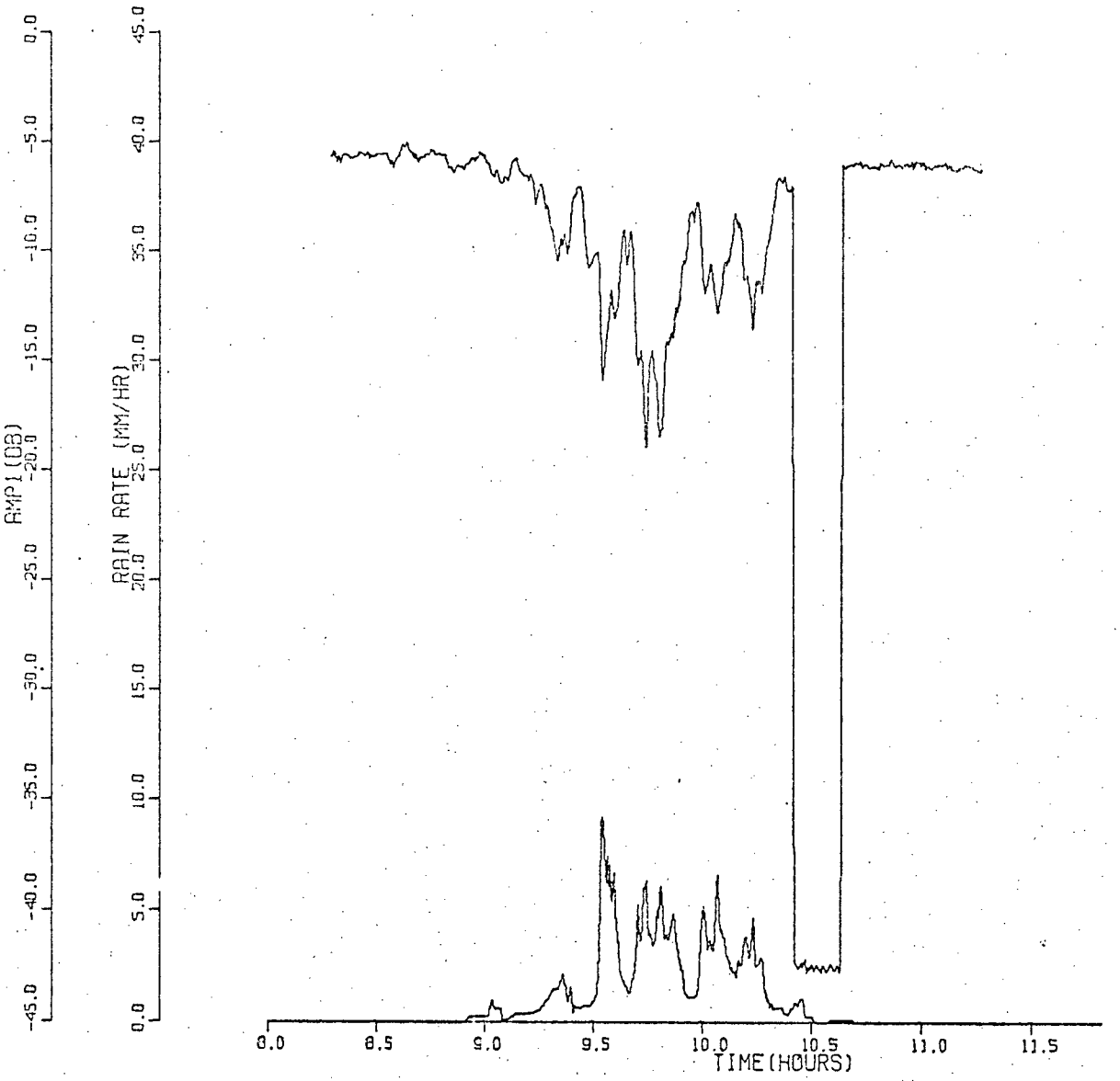

Fig. 5.3 (a) A plot of received signal level and path-average rain rate for the period 0813 to 1113, February 12, 1977.

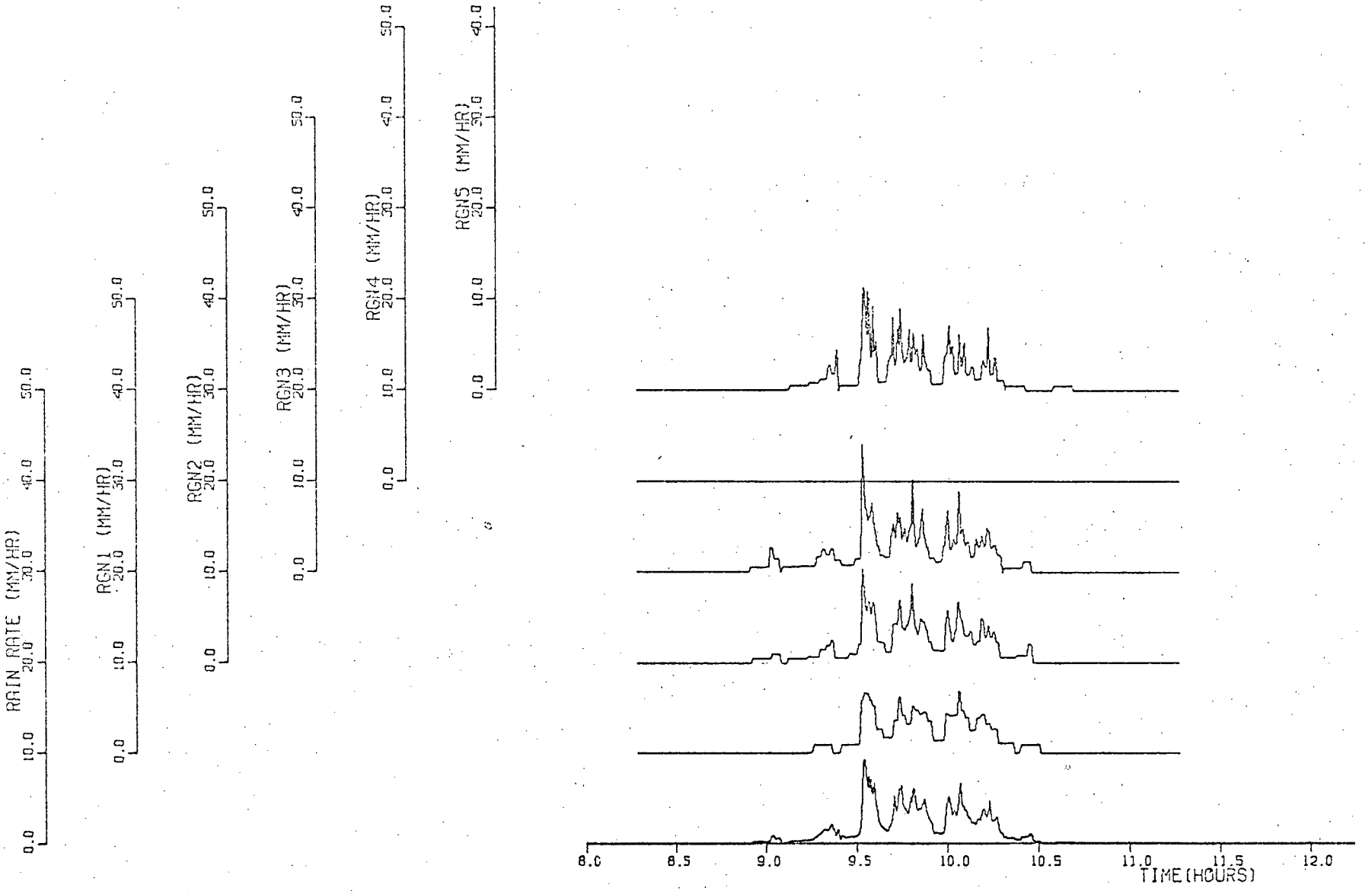

Fig. 5.3 (b) Path-average rain rate and 4 point rain rates for 0813 to 1113, February 12, 1977.

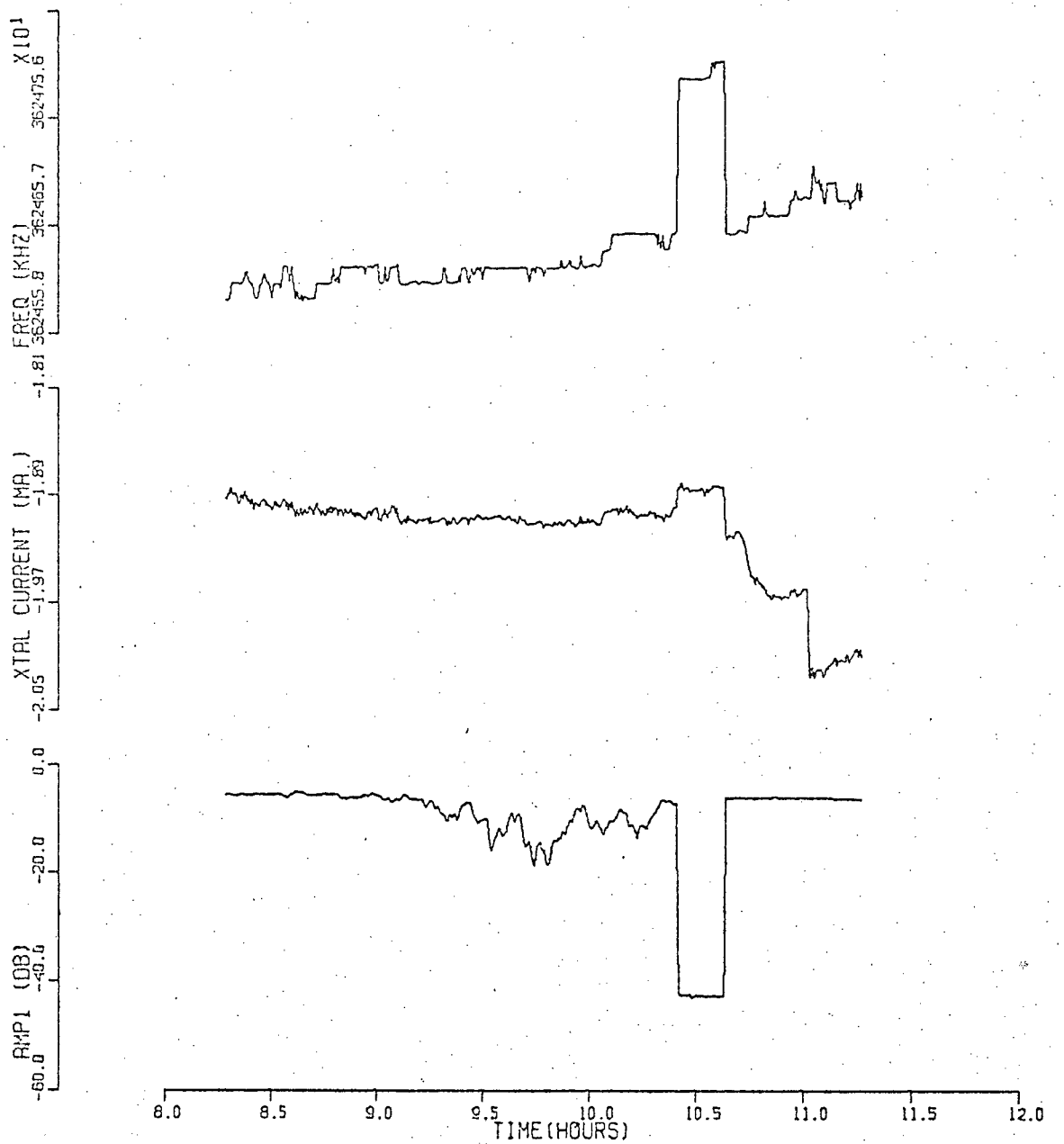

Fig. 5.3 (c) Local oscillator frequency, crystal current and signal level for the period 0813 to 1113, February 12, 1977.

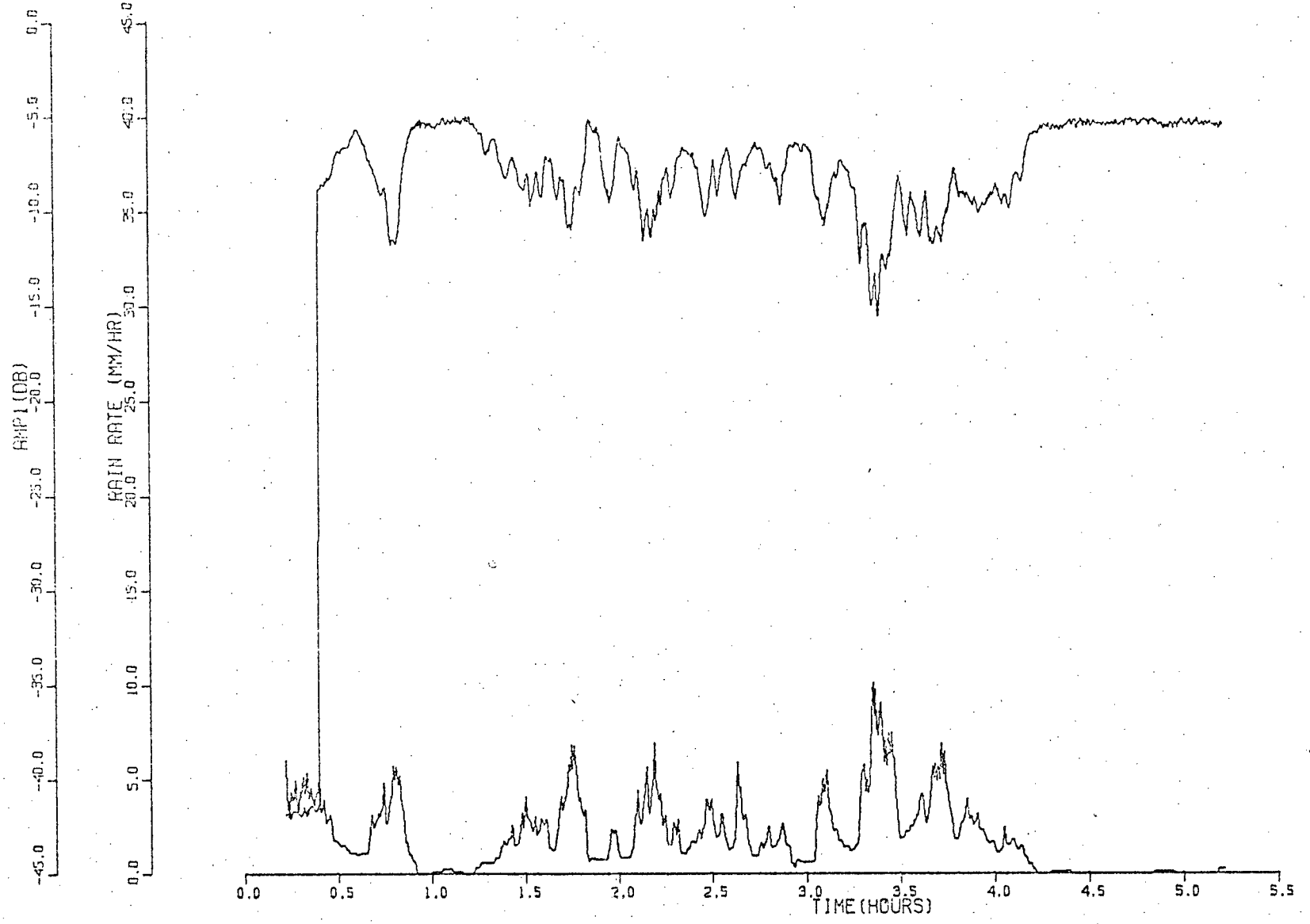

Fig. 5.4 (a) Received signal level and path-average rain rate for the period 0013 to 0513, February 12, 1977.

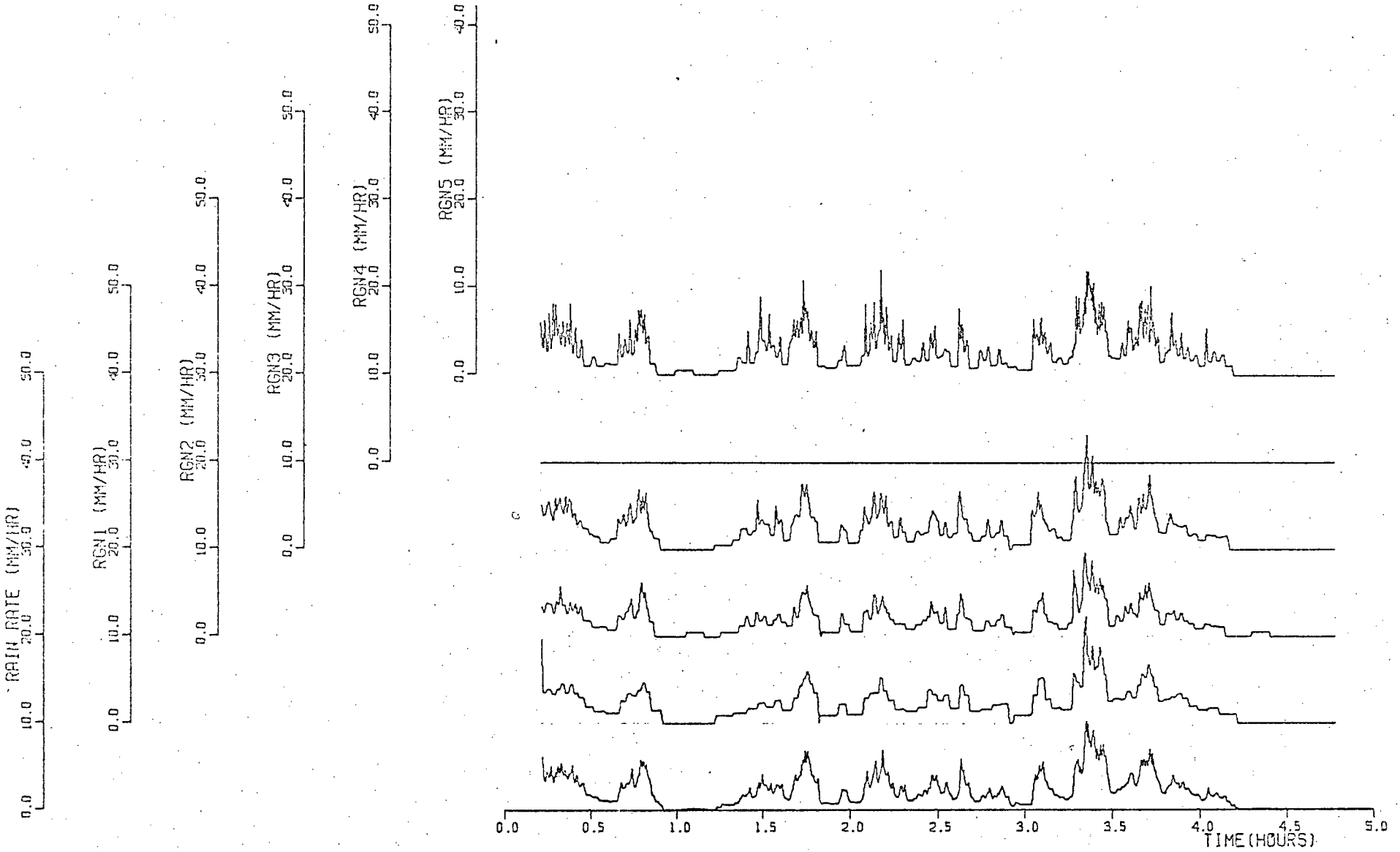

Fig. 5.4 (b) Path-average rain rate and 4 point rain rates for the period 0013 to 0442, February 12, 1977.

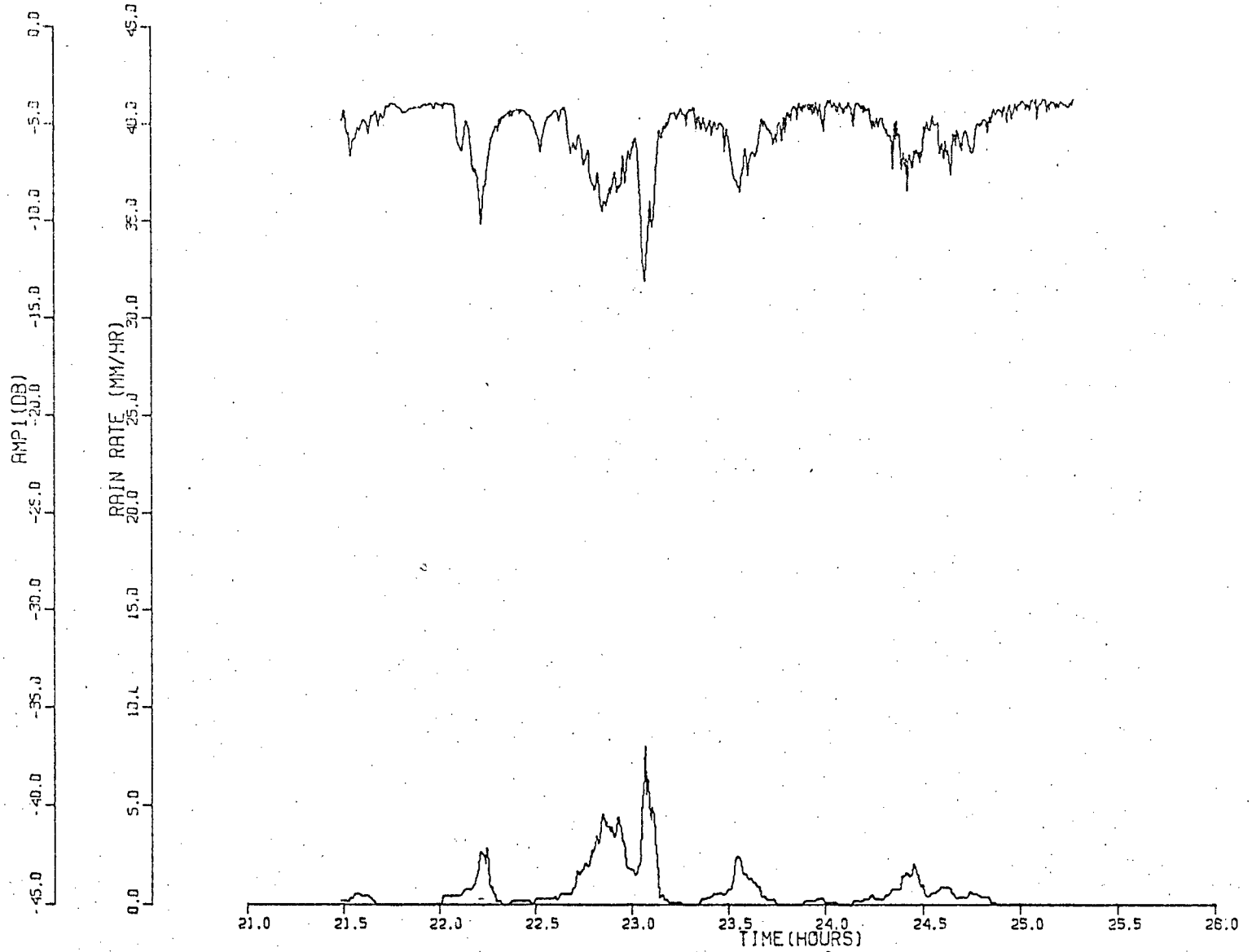

Fig. 5.4 (c) Received signal level and path-average rain rate for the period 2128, March 7, 1977 to 0116, March 8, 1977.

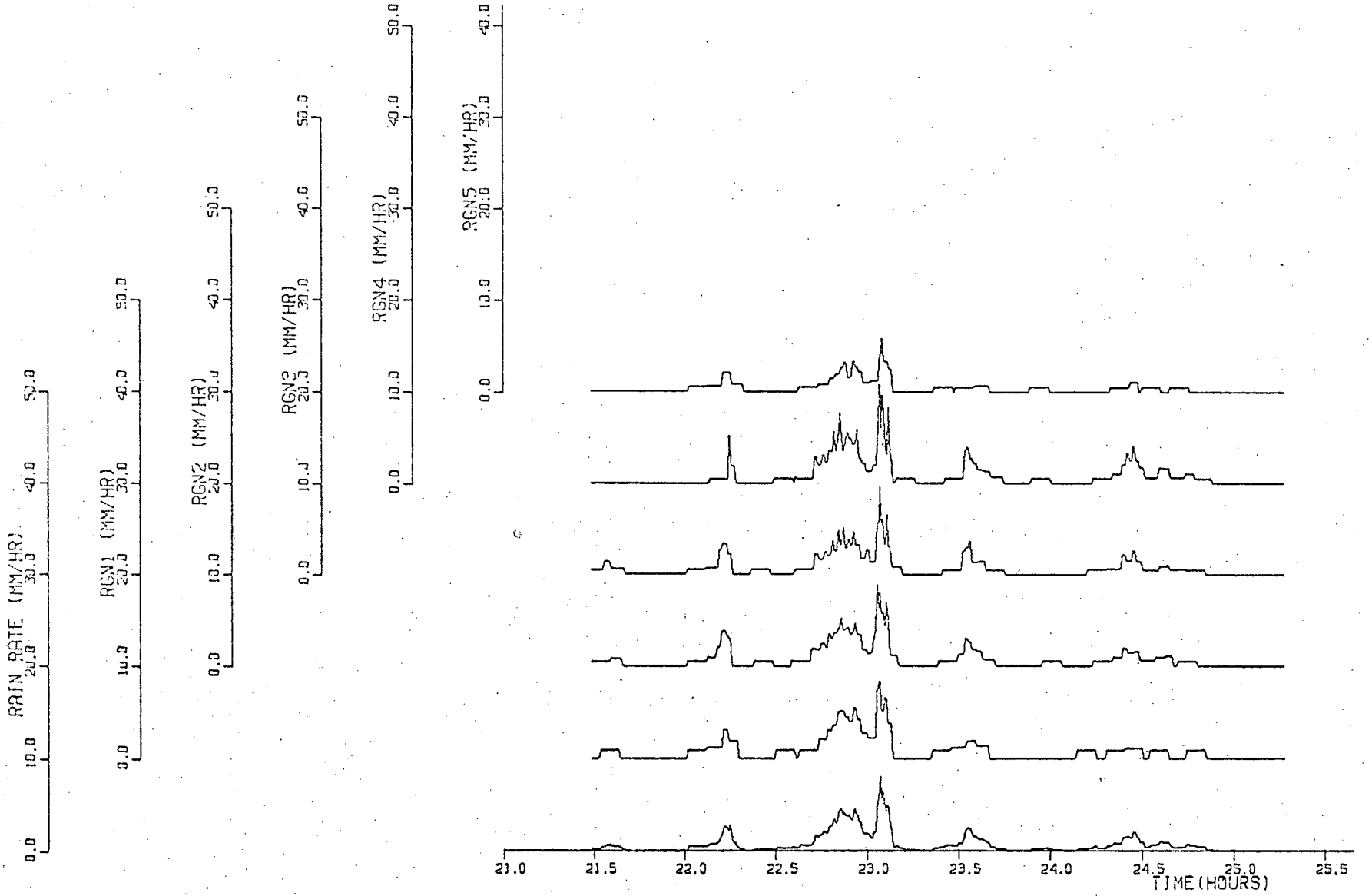

Fig. 5.4 (d) Path-average rain rate and 4 point rain rates for the period 2128, March 7, 1977 to 0116, March 8, 1977.

It is evident from the above examples that data must be manually scrutinized to some extent to eliminate spurious results caused by equipment failures.

5.2 Statistical Treatment of the Data Base

A collection of programs, described in Appendix F, allows an abbreviated version of selected data files to be placed in disk storage for analysis. The data used are 10 second averages of path-average rain rate and signal level. It is felt that no substantial distortion was caused by the use of 10 second averages in view of the low rain rates involved. A statistical summary of the form shown in Fig. 5.5 is appended to each file. This gives the amplitude statistics of data within 0.5 mm/hr rain rate classes.

To obtain specific attenuation (dB/km) vs rain rate, the baseline clear air propagation signal level must be defined. This baseline is determined subjectively for each file by inspection of signal levels during zero or light rain near that file in time. In cases where it was suspected that substantial drifts occurred within a file, the data was not used for analysis. It is felt that baselining data by this method was accurate to ±0.3 dB/km.

Plots and tables of attenuation vs. rain rate may be produced for individual files or groups of files. A sample is given in Fig. 5.6.

5.3 Comparison with Theory

Out of the data base available at the present time, files were selected for statistical analysis if they met the following criteria:

1. both amplitude and rain rate were available
2. the signal baseline was certain
3. they contained periods of rain > 1 mm/hr.

FILENAME: RAIN102299 DATA ACQUISITION 2/12/77 3:12:42 CONTAINS 180 RECORDS OF LENGTH 10 SECONDS

NO. OF SAMPLES (SECONDS)	RAIN RATE (MM/HR)	AMPLITUDE (DB) MEAN	STD DEV	MIN.	MAX.
170	1.27	-8.06	0.44	-8.73	-7.54
170	1.81	-8.60	0.31	-9.12	-7.93
110	2.24	-10.26	0.63	-11.30	-9.19
170	2.68	-9.58	0.58	-11.11	-8.86
140	3.13	-9.72	0.54	-10.82	-8.85
80	3.79	-10.49	0.55	-11.20	-9.76
150	4.24	-10.82	0.30	-11.42	-10.34
120	4.74	-10.97	0.33	-11.65	-10.63
120	5.19	-11.65	0.68	-12.78	-10.57
120	5.82	-11.96	0.66	-12.80	-10.89
110	6.27	-11.92	0.66	-12.93	-10.84
60	6.80	-12.59	0.92	-13.81	-11.14
60	7.27	-12.45	0.96	-13.96	-10.96
70	7.69	-13.10	0.50	-13.78	-12.15
50	8.32	-14.54	0.77	-15.31	-13.27
40	8.83	-14.96	0.73	-15.62	-14.03
20	9.31	-14.71	0.26	-14.90	-14.53
10	9.93	-15.36	0.0	-15.36	-15.36
20	10.14	-14.64	0.40	-14.92	-14.36
10	10.79	-14.86	0.0	-14.86	-14.86

END OF DATA DECK HIT: NORMAL EXIT
EXECUTION TERMINATED

Fig. 5.5 The statistics of attenuation and rain rate for data file 'RAIN102299' using 10 second averages.

NO. OF SAMPLES (SECONDS)	RAIN RATE (MM/HR)	ATTENUATION (DB/KM) MEAN	STD DEV	MIN.	MAX.
4960	0.06	0.00	0.09	-0.25	0.68
1780	0.72	0.63	0.33	-0.17	1.78
1590	1.28	1.26	0.25	0.53	2.25
1950	1.70	1.55	0.30	0.72	2.56
1240	2.26	1.95	0.35	0.98	3.41
1150	2.73	2.01	0.29	1.15	3.30
1010	3.20	2.17	0.33	1.31	3.14
510	3.76	2.42	0.36	1.59	3.35
530	4.23	2.65	0.38	1.62	3.48
380	4.72	2.98	0.40	2.01	3.64
310	5.19	3.29	0.34	2.16	4.25
310	5.75	3.32	0.41	2.08	4.26
180	6.24	3.45	0.30	1.99	4.34
90	6.81	3.83	0.43	3.10	4.84
80	7.22	3.83	0.47	3.06	4.92
80	7.68	4.30	0.26	3.38	4.82
50	8.32	5.25	0.44	4.53	5.69
40	8.83	5.49	0.41	4.96	5.86
20	9.31	5.35	0.15	5.24	5.45
10	9.93	5.72	0.0	5.72	5.72
20	10.14	5.31	0.22	5.15	5.47
10	10.79	5.43	0.0	5.43	5.43

1	RAIN102293	-05.3
2	RAIN102294	-05.3
3	RAIN102295	-5.3
4	RAIN102297	-5.3
5	RAIN102298	-5.3
6	RAIN102299	-5.3
7	RAIN102300	-5.3
8	RAIN102302	-5.3
9	RAIN102303	-5.2

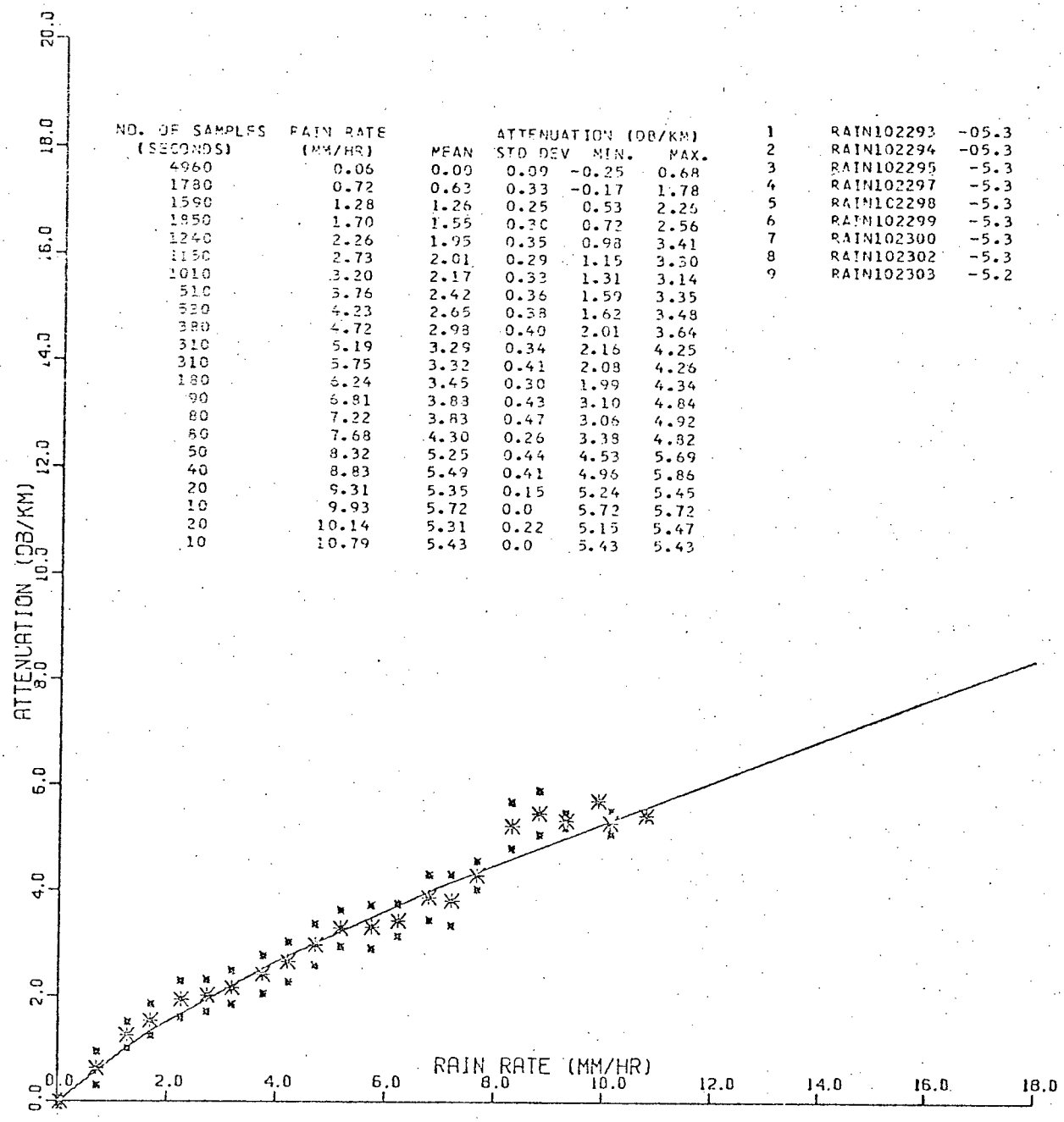

Fig. 5.6 Mean specific attenuation vs. path-average rain rate for the period 0042, February 12, 1977 to 0512, February 12, 1977. Large *'s mark the means; small *'s one standard deviation about the mean.

The selected files composed some 80,000 data records (or 25 hours of data).

A plot of the mean attenuation and one standard deviation on either side vs. rain rate together with the theoretical relation (Ryde) is given in Fig. 5.7 for the totality of selected data. It is observed that the number of data points above 7 mm/hr is small and caution should be exercised in interpreting these points. The plot and table of Fig. 5.7 indicate that at a particular rain rate:

1. The mean attenuation corresponds closely to the Ryde result.
2. The minimum attenuation is rarely more than 1.5 dB/km below the mean.
3. The maximum attenuation is up to 4 dB/km above the mean.

The data indicate that deviations of attenuation from the theoretical value do occur and that they are not distributed randomly, but rather, occur in bursts. For example, examine Figs. 5.4 (a, b) and 5.6 which include rain from February 12, 1977, 0030 to 0410, and Fig. 5.3 (a, b) and Fig. 5.8 which include rain of later the same morning. The data of 0030 to 0410 conform closely to the theoretical results and have standard deviations less than 0.5 dB/km. In contrast, the data of 0900 to 1030 have standard deviations up to 1.5 dB/km and mean values of attenuation substantially above the theoretical. Examination of Fig. 3a shows that rain bursts at 0935 and 1005 cause "normal" attenuations while that at 0945 corresponds to an attenuation substantially above the theoretical value. This effect is responsible for the results in Fig. 8. This could possibly be due to variations in the drop size distribution with time.

In summary, mean attenuation has been found to agree closely

NO. OF SAMPLES (SECONDS)	RAIN RATE (MM/HR)	ATTENUATION (DB/KM) MEAN	STD DEV	MIN.	MAX.
33740	0.08	0.09	0.20	-0.40	1.77
13550	0.78	0.84	0.37	-0.43	2.50
12230	1.25	1.35	0.30	0.15	2.59
8970	1.72	1.60	0.36	0.44	3.36
6000	2.25	1.96	0.30	0.91	3.91
5400	2.76	2.24	0.28	0.66	3.32
4150	3.22	2.32	0.32	1.31	3.65
2420	3.70	2.54	0.41	1.39	3.81
1410	4.22	2.79	0.35	1.62	3.81
1160	4.70	3.04	0.33	1.81	5.86
890	5.20	3.34	0.55	1.97	8.79
660	5.79	3.57	0.44	2.08	8.44
400	6.25	3.60	0.31	1.99	9.24
200	6.78	3.48	0.41	2.70	4.84
130	7.20	4.15	0.40	3.06	9.09
140	7.69	4.23	0.20	2.41	7.52
70	8.31	6.37	0.41	4.53	9.41
50	8.82	6.26	0.37	4.96	9.43
20	9.31	5.35	0.15	5.24	5.45
20	9.81	6.37	0.0	5.72	7.03
20	10.14	5.31	0.22	5.15	5.47
10	10.79	5.43	0.0	5.43	5.43

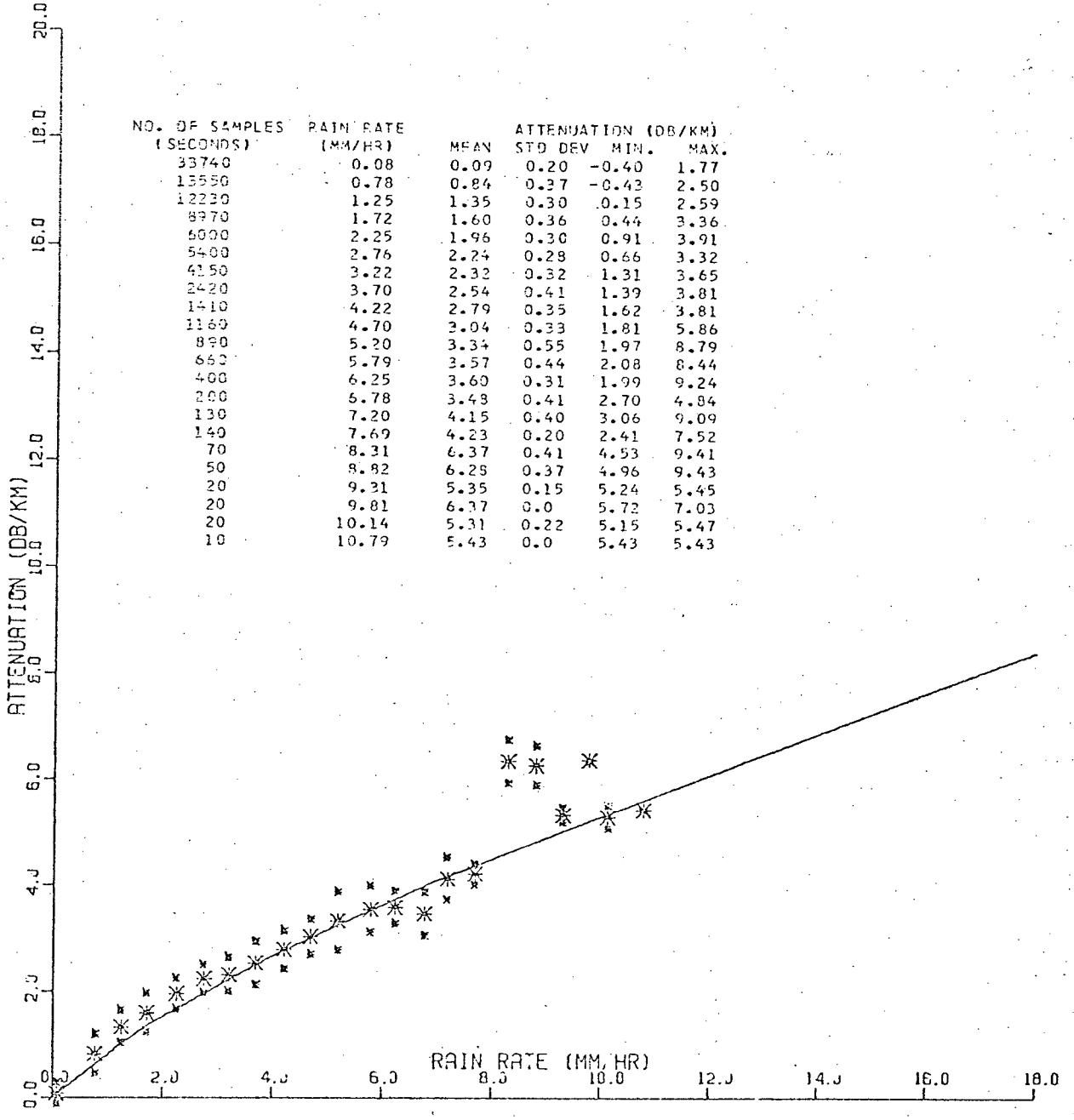

Fig. 5.7 Mean specific attenuation vs. path-average rain rate for the totality of selected data.

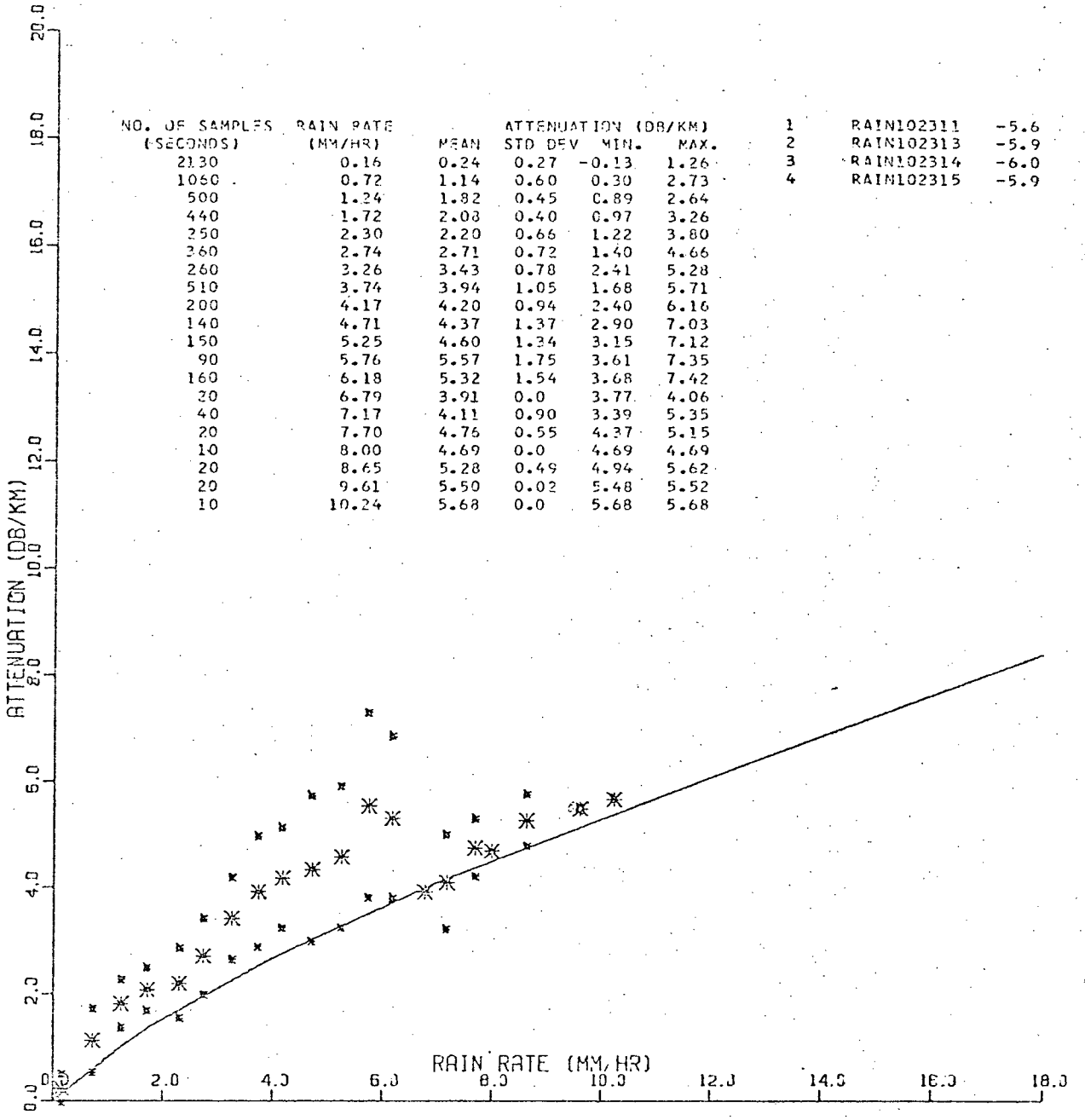

Fig. 5.8 Mean specific attenuation vs. path-average rain rate for the period 0846 to 1046, February 12, 1977.

with Ryde theory for the limited range of rain rates available (0 to 10 mm/hr). Values of attenuation substantially above the mean have been shown to occur. The above results, however, are based on a very small data set and must be treated as such.

CHAPTER VI

CONCLUSIONS AND DISCUSSION

6.1 Conclusions

The objectives of this thesis have been met; in particular:

1. A mm-wave link has been installed which allows the automatic measurement of excess path attenuation.
2. A network of rain gauges has been positioned along the path. It permits the accurate measurement of path-average rain rate. Other meteorological equipment has also been installed.
3. A real time data acquisition system has been implemented. It allows the automatic recording, in a form suitable for later analysis, of data from the microwave and weather sensors.
4. Software to edit data and enter it into a data base has been developed.

In addition, some 1400 hours of data have been recorded and passed through the various post-processing steps. Due to unusually dry weather and occasional equipment malfunctions only 25 hours of data were sufficiently complete and interesting to warrant analysis. Preliminary analysis of the latter data indicates that the mean specific attenuation at a given rain rate agrees closely with that predicted by the Ryde and Ryde theory. It has also been shown that substantial deviations from the mean occur at certain times.

6.2 Discussion

6.2.1 Suggestions for Improvements to the Present System

While the system developed in this work functions well, it can be improved by modifying sub-systems in the following ways:

1. Microwave system:

   (a) The receiver is not attended 24 hours a day and valuable data has been lost due to the loss of phase lock. The implementation of a more reliable receiver would be advantageous.

   (b) The present mixer could advantageously be replaced with a more efficient downconverter.

   (c) Similarly, the klystron and waveguiding could be replaced with an antenna-mounted solid state source. This would reduce operating costs and potentially improve long term stability.

2. Meteorological system:

   (a) The attenuation corresponding to a given rain rate is dependent upon the drop size distribution. An appropriate measurement system for drop size distribution is necessary to allow accurate comparison of theory and experiment.

   (b) At present, the anemometer is mounted too close to the outside wall of a building to permit reliable measurements. It should be moved to a more suitable location.

3. Interface:

   To reduce down time due to component failures, wire-wrapped circuit cards should be replaced with printed circuit boards.

4. Data Acquisition system:

   There have been some reliability problems associated with the data acquisition system when run under the disk operating system (RDOS Rev. 5). As disk storage is not necessary in this application, it may improve reliability to use the core-resident operating system (RTOS).

6.2.2 Related Work

To draw conclusions from this work the data base should be expanded considerably. The collection of data over several years would seem appropriate because of the short-term deviations of weather patterns from what might be considered normal. It is hoped that from this expanded data base, one would be able to:

1) Determine the validity of current theoretical relations of attenuation to rain rate.
2) Determine the statistics of deviations in attenuation from the mean attenuation at a given rain rate. Demonstrate the extent to which such deviations increase outage times above those calculated from the mean attenuation vs. rain rate relation.
3) Generate a rain rate distribution for this area.
4) Determine the average drop size distribution relation for this area and also show the extent of deviations from this average relation.
5) If possible, compute the joint probabilities of point rain rates at separated locations.
6) Determine the reliability of mm-wave links in this area.

6.2.3 Other Directions for Research

In the longer term, several aspects of practical importance to mm-wave transmission system design should be investigated. These are:

1) Cross Polarization:

   In microwave relays, signals may be transmitted using orthogonal polarizations. The extent to which power is coupled between orthogonal polarizations by rain is of interest in practical transmission systems.

2) Long Paths:

Radio transmission systems with outage times of 500 minutes/year or more are adequate for some applications. A long mm-wave link (5 to 10 km) should be established to measure the properties of such transmission systems.

APPENDIX A

Mixer Evaluation

As mentioned in Section 2.3.5, mixers were tested to determine which of the varieties available was most sensitive. The sensitivity vs local oscillator power relation for two mixers, the Scientific Atlanta Model 13A-50 and the S/A Model 17-50, was measured and is given in Fig. A-1. Since the available local oscillator drive at the receiving antenna is only + 8 dBm, the S/A Model 13A-50 mixer is clearly superior.

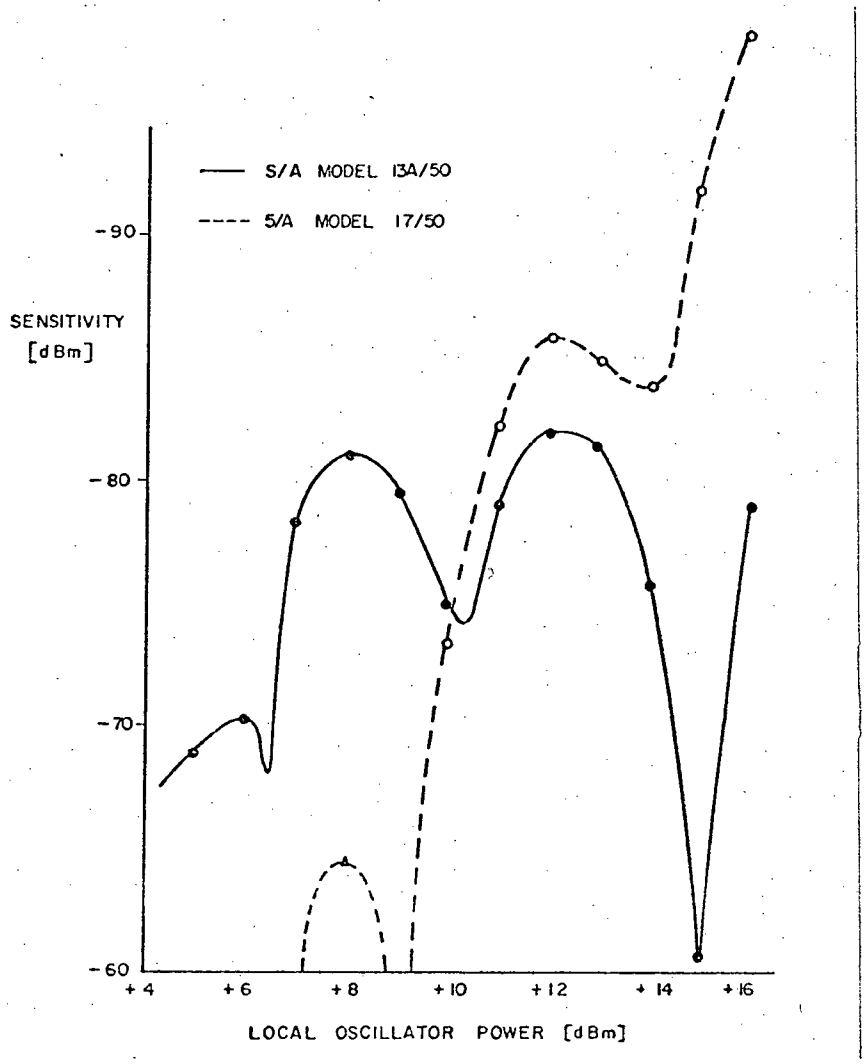

Fig. A-1 The sensitivity of two mixers as a function of local oscillator power.

APPENDIX B

Rain Gauge Monitor

The rain gauge monitor is a self contained unit which detects the state of tipping-bucket rain guages and generates a machine-readable output indicating which gauges have tipped during the last clock cycle. The unit has eight channels; to each, a rain gauge may be connected by a twisted pair (in this case, a dedicated telephone line). The circuit diagram is given in Fig. B-1.

A floating 78 volt bias is applied to each line through optical couplers IC 1 to 8. This provides 1500 volt isolation against lightning surges. Schmitt triggers, IC 13 to 16, detect the loop current giving a "high" output if the loop resistance sensed is less than 100 K Ω. IC's 9 to 12 are wired as 2 bit shift registers and are strobed each time the output of this unit is read. The output of each channel is the exclusive OR of the two bits in the shift register, that is, the previous two states of the rain gauge. The output then is a "high" if the bucket had tipped in the previous clock cycle. The state of each rain gauge is displayed on LD 1 to 8, the outputs on LD 9 to 16, and an indication of clock activity on LD 17.

Because digital circuitry is used throughout this unit, it may be clocked at any reasonable rate without hardware changes.

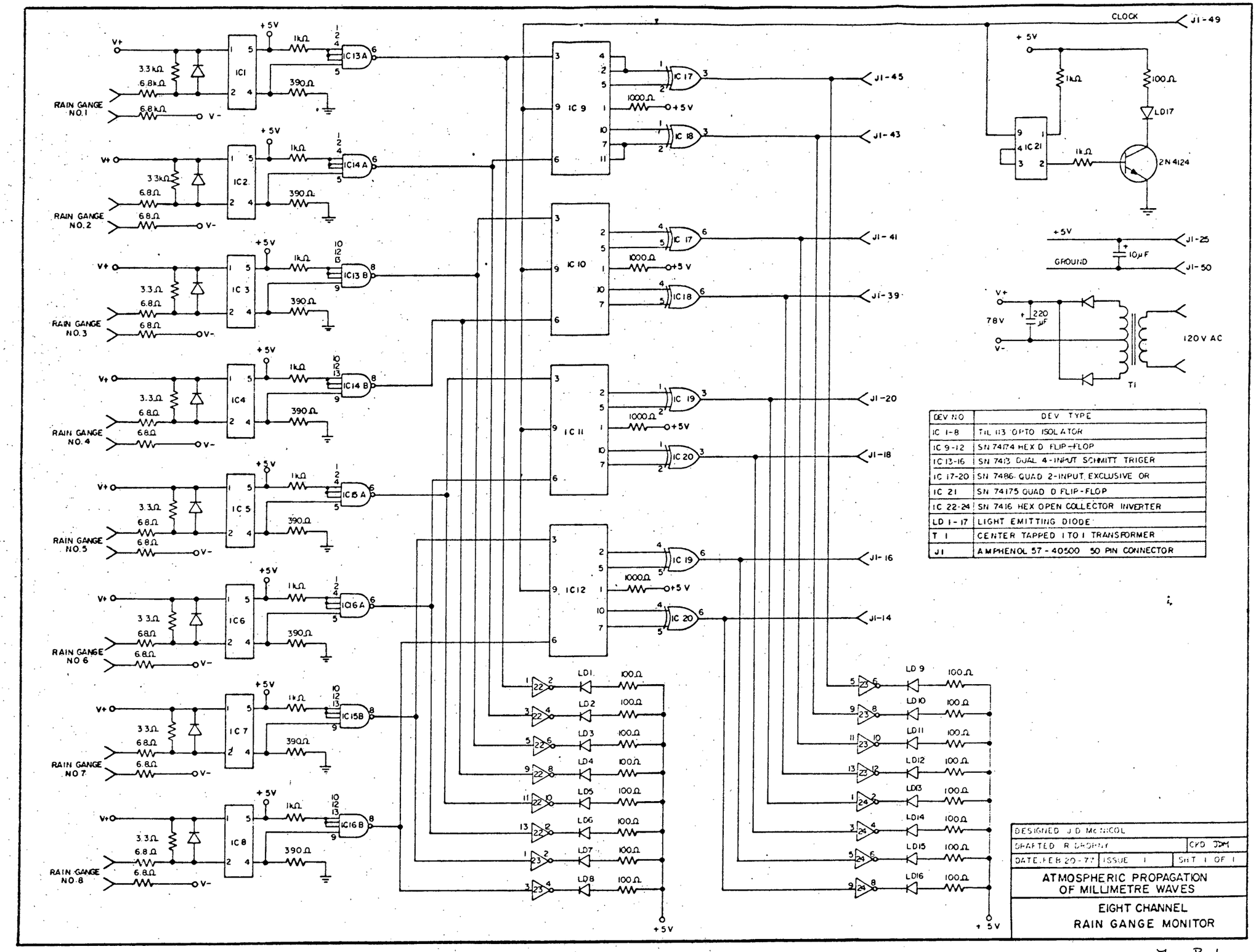

DEV NO	DEV TYPE
IC 1-8	TIL 113 OPTO ISOLATOR
IC 9-12	SN 74174 HEX D FLIP-FLOP
IC 13-16	SN 7413 DUAL 4-INPUT SCHMITT TRIGER
IC 17-20	SN 7486 QUAD 2-INPUT EXCLUSIVE OR
IC 21	SN 74175 QUAD D FLIP-FLOP
IC 22-24	SN 7416 HEX OPEN COLLECTOR INVERTER
LD 1-17	LIGHT EMITTING DIODE
T 1	CENTER TAPPED 1 TO 1 TRANSFORMER
J1	AMPHENOL 57-40500 50 PIN CONNECTOR

DESIGNED J D McNICOL		
DRAFTED R BROWN	CKD JDM	
DATE FEB 20-77	ISSUE 1	SHT 1 OF 1

ATMOSPHERIC PROPAGATION OF MILLIMETRE WAVES

EIGHT CHANNEL RAIN GANGE MONITOR

Fig B-1

APPENDIX C

Anemometer

The anemometer designed for this work allows the measurement of horizontal and vertical wind speed and wind direction. A photograph of it may be seen in Fig. 2.4.

The speed transducers are propellor driven dc generators. They were calibrated in a wind tunnel to over 30 meters/second and found to give a linear output of 0.26 volt/m sec^{-1}.

The platform to which the transducers are mounted is free to face into the wind, allowing the direction to be sensed with a synchro geared to the platform. A block diagram of the direction sensing apparatus is given in Fig. C-1.

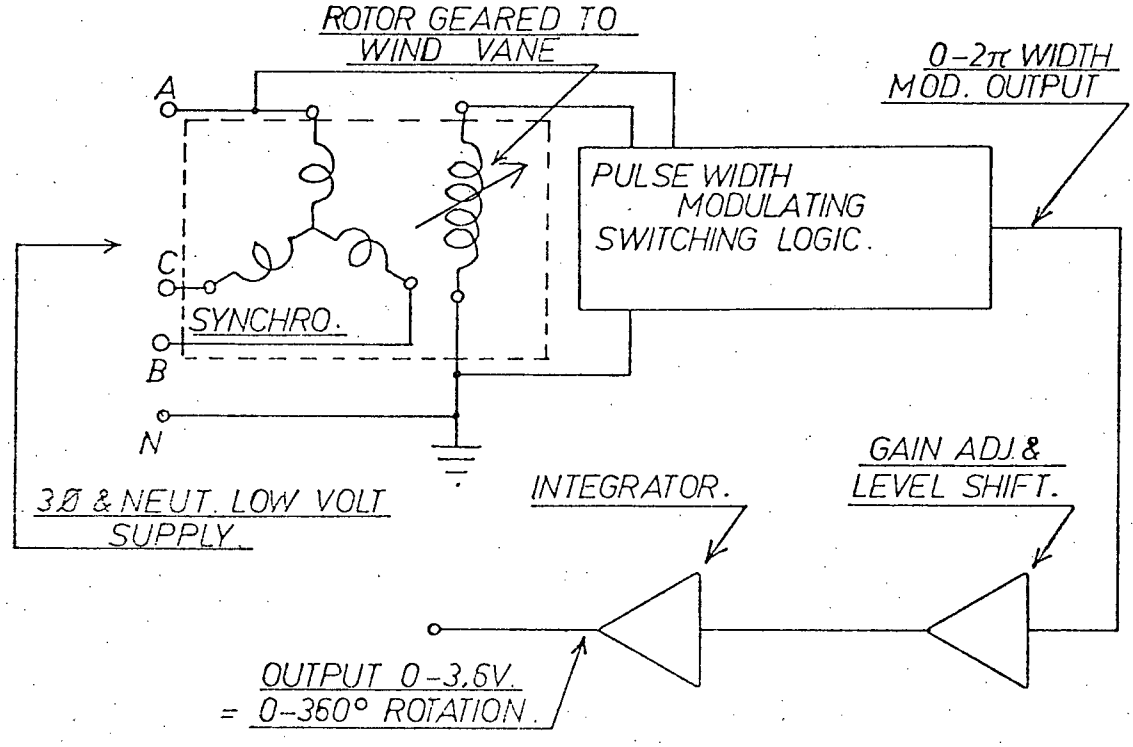

Fig. C-1 Block diagram of wind direction sensing apparatus.

APPENDIX D

Interface

D-1 Physical Construction

The interface comprises three assembiles: a 16 position wire-wrapped backplane with 8 circuit cards, a display panel and a connector panel. The panels are connected into the backplane through an additional 4 circuit cards. For repair purposes all three assemblies are easily separated and individual circuit cards can be pulled from the backplane.

Cabling to the digital measurement units is via 50 pin Amphenol connectors, to analog inputs on coaxial cable and to the minicomputer on a 50 pair cable. A diagram of these inputs and the major components of the interface is given in Fig. D-1.

Most of the circuit cards in the interface are presently of wire-wrapped construction. This was done to save on construction time and to achieve high packing densities. There have not, however, been any reliability problems as a result of this construction technique.

D-2 Operation

The instructions by which data are read via the digital multiplexer and A/D converter are given in Table D-1. The data formats are also given there. The instructions for setting the interrupt rate on the real time clock are contained in Table D-2.

D-3 Circuit Diagrams

The circuit diagrams for a large part of the interface are included in Figs. D-2 - D-10. The remaining information, which is not included here, pertains to the A/D filter board, the I/O bus terminator and the backplane wiring diagram.

Output Number	Name	Code Format	Access Instructions
ϕ	Amplitude #1	Bit ϕ: 1 = 10^{-1} multiplier ϕ = 10^{-2} multiplier Bit 1: 1 = over range Bit 2: 1 = positive sign Bits 3 to 15: 3¼ digits BCD	DOA x,45 followed by DIA y,45 Result in ACy.
1	Amplitude #2	as above	DOA x,45 + DIB y,45
2	Phase	Bit ϕ: Data Lamp Bit 1: 1 = + sign Bits 2 to 15: 3½ digits BCD	DOA x,45 + DIC y,45 Result in ACy
3	Frequency (10's of MHz)	Bits ϕ to 15: 4 digits BCD	DOB x,45 + DIA y,45 Result in ACy
4	Frequency (KHz)	Bits ϕ to 15: 4 digits BCD	DOB x,45 + DIB y,45 Result in ACy
5	Rain gauges (8 in total)	Bit ϕ: Rain gauge 1 to Bit 7: Rain gauge 8	DOB x,45 + DIC y,45 Result in ACy
6	Hours	Bits ϕ to 7: 2 digits BCD	DOC x,45 + DIA y,45
7	Minutes & Seconds	Bits ϕ to 7: 2 digits BCD Bits 8 to 15: 2 digits BCD	DOC x,45 + DIB y,45 Result in ACy
8-23	A/D #1 to A/D #16	Bits ϕ to 3: extended sign Bits 4 to 15: 2's complement	NIOC 56: clear mux address NIOP 56: increment address NIOS 56: start conversion DIA y,56: result in ACy

Table D-1 Access commands and output formats associated with the minicomputer interface.

Bit Position	Function	Operational Instructions
ϕ	not used	Divisor in AC x.
1 to 3	ϕ: 0 Hz 1: 100 Hz 2: 10 Hz 3: 1 Hz 4: 0.1 Hz 5: 0.01 Hz 6: 0.00244 Hz 7: 0 Hz	DOA x,44: set rate NIOS 44: start clock NIOC 44: clear clock
4 to 15	divisor in binary (1 to 4095)	

Interrupt rates with divisor bits 4-15 = 2048 and bits 1 to 3 as shown.

Table D-2 Setting the interrupt rate of the real time clock.

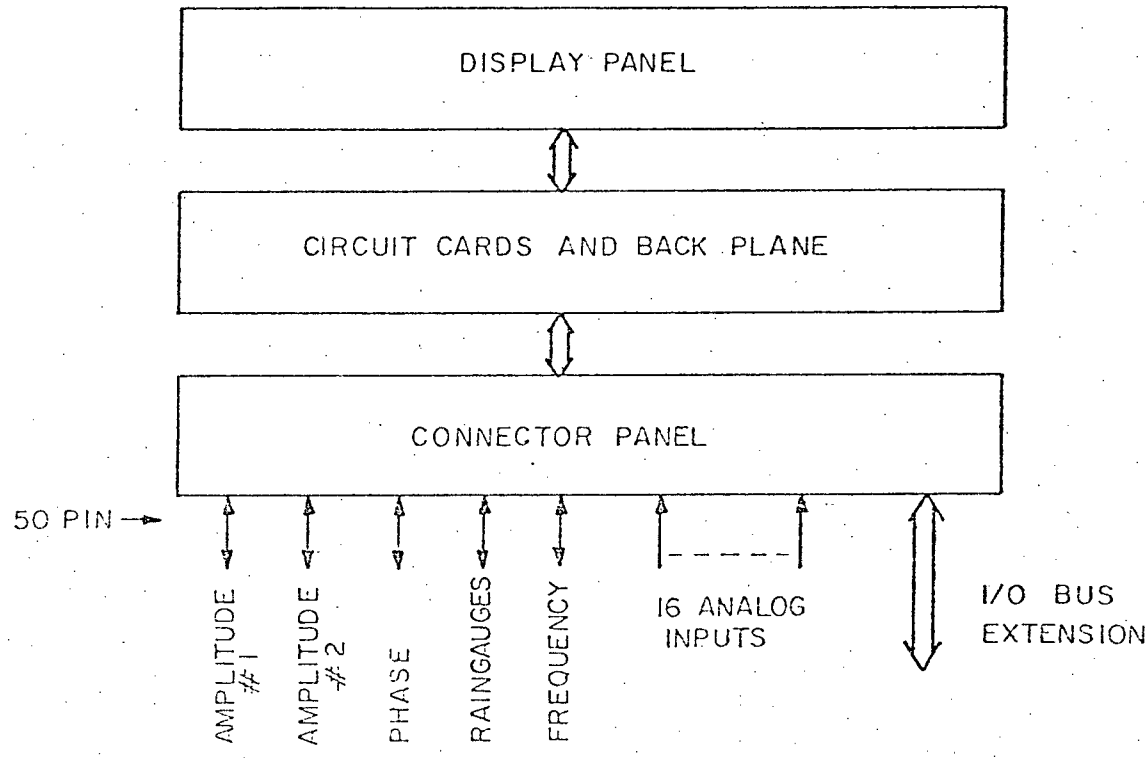

Fig. D-1 Physical configuration of the minicomputer interface.

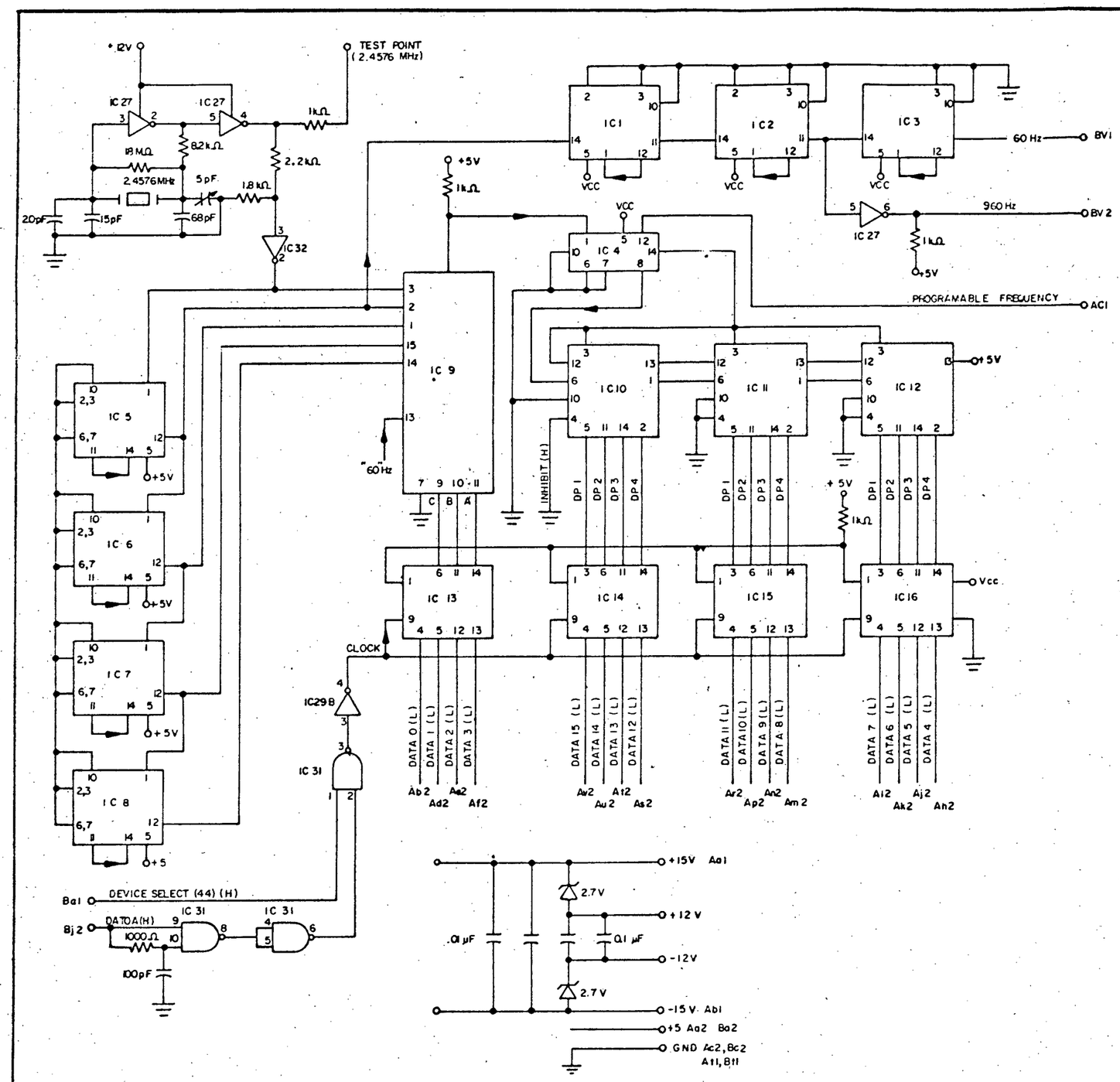

DEV NO	TYPE	DESCRIPTION
IC1 - 3	SN 7493	4 BIT BINARY COUNTER ÷ 16
IC 4	SN 7492	DIVIDE BY 2 AND 6
IC 5 - 8	SN 7490	DECADE COUNTER
IC 9	SN 74151	1OF8 MULTIPLEXER
IC 10-12	MC 14526	PROGRAMMABLE DIVIDER
IC-13-22	SN 74175	QUAD D FLIPFLOP
IC 23	MM 5375AE	DIGITAL CLOCK
IC 24	INTEL 3601	PROM 7 SEGMENT TO BCD
IC 26	MC 14050	HEX CMOS BUFFER
IC 25, 27, 28	MC 14049	HEX CMOS INVERTER BUFFER
IC 29-30	SN 7406	HEX INVERTER, OPEN COLLECTOR
IC 31	SN 7400	QUAD 2-INPUT NAND
IC 32	MC 14049	HEX CMOS INVERTER BUFFER
IC 33	SN 7408	QUAD 2-INPUT AND
A, B		16 PIN DIP SOCKET CONNECTOR
		2.4576 MHz CRYSTAL

DESIGNED J D McNICOL		
DRAFTED R DROBNY		CKD JDM
DATE FEB 15-77	ISSUE 1	SHT 1 OF 2

ATMOSPHERIC PROPAGATION OF MILLIMETRE WAVES

NOVA COMPUTER INTERFACE – DIGITAL CLOCK CARD

Fig D-2

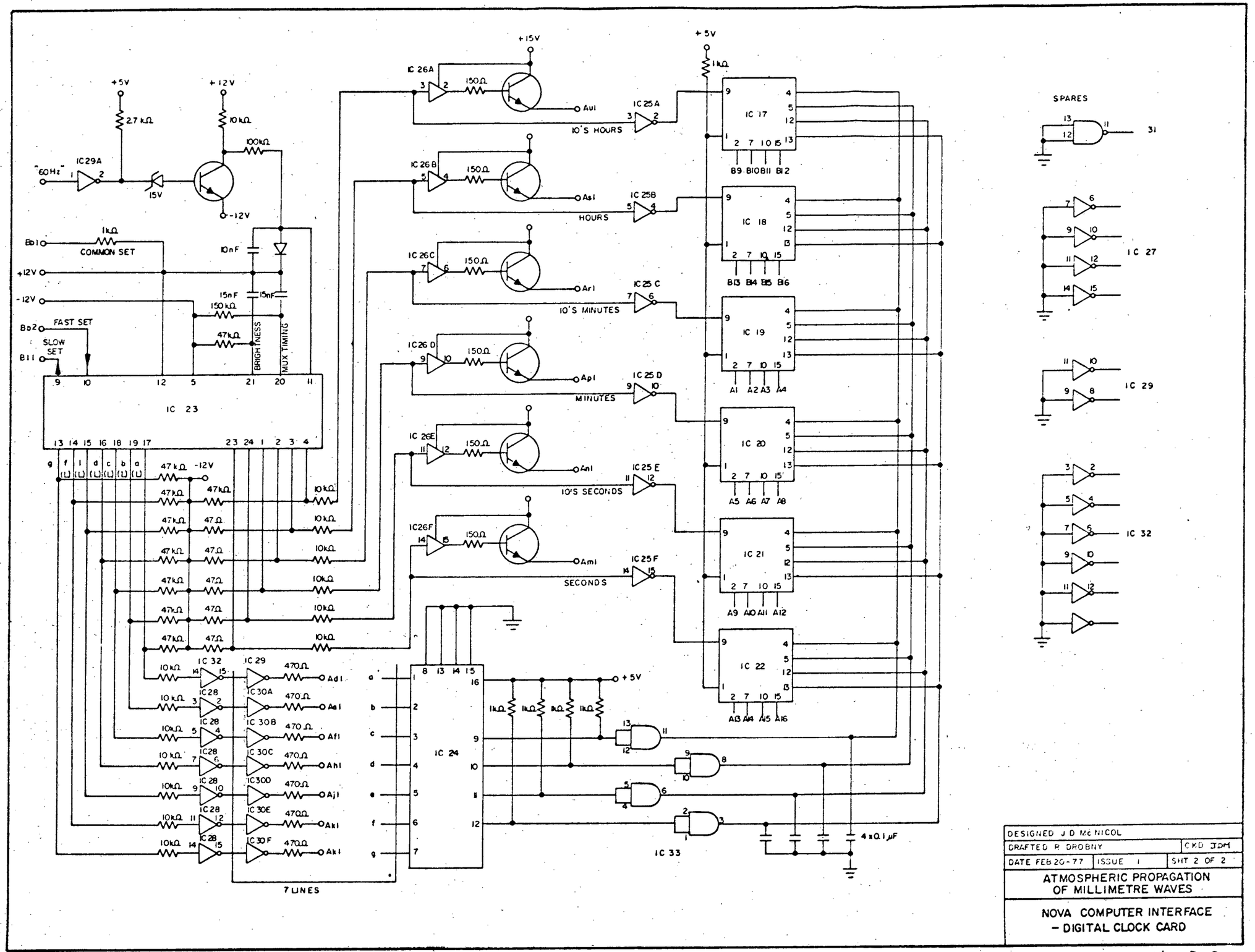

DESIGNED J D McNICOL		
DRAFTED R DROBNY		CKD JDM
DATE FEB 20-77	ISSUE 1	SHT 2 OF 2

ATMOSPHERIC PROPAGATION OF MILLIMETRE WAVES

NOVA COMPUTER INTERFACE – DIGITAL CLOCK CARD

Fig D-3

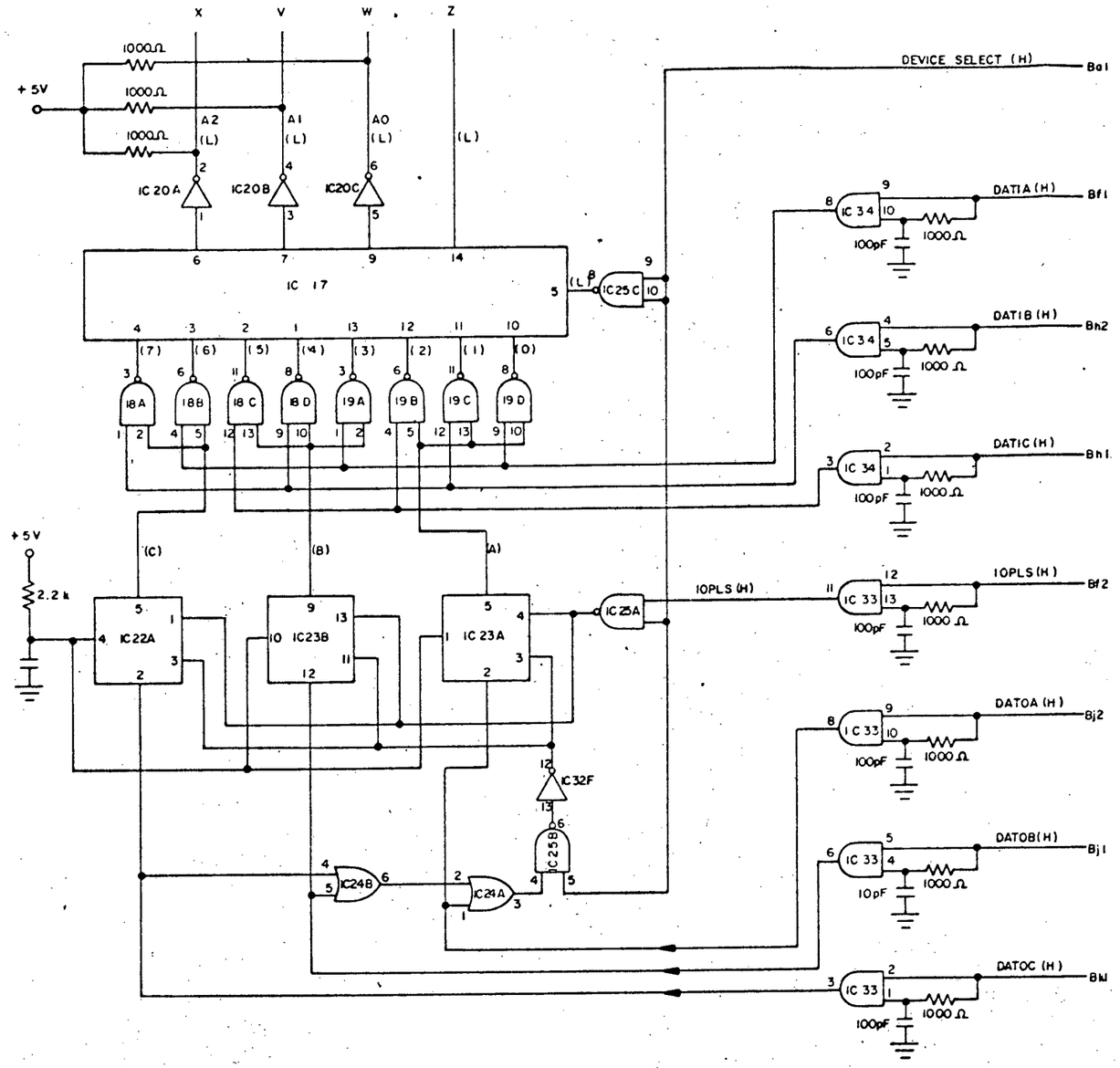

DEV NO	TYPE	DESCRIPTION
IC1-16	SN 74251	8 TO 1 MULTIPLEXER OPEN COLLECTOR
IC 17	SN 74148	8 LINE PRIORITY ENCODER
IC 18-19	SN 7400	QUAD 2 INPUT NAND
IC 20-21	SN 7406	HEX INVERTER BUFFER OPEN COLLECTOR
IC 22-23	SN 7474	DUAL D FLOP
IC 24	SN 7432	QUAD 2 INPUT OR
IC 25	SN 7400	QUAD. 2 INPUT NAND
IC 26-27	SN 74123	DUAL RETRIG MONOSTABLE MULTIVIBRATOR
IC 28		
IC 29-30	SN 74279	QUAD $\overline{S}$-$\overline{R}$ FLIP FLOP
IC 31	F 9301	1 LINE TO 10 LINE DEMULTIPLEXER
IC 32	SN 7416	HEX INVERTER BUFFER
IC 33-34	MC 3001	QUAD AND GATE

DESIGNED J D McNICOL		
DRAFTED R DROBNY		CK'D JDM
DATE FEB 15-77	ISSUE 1	SHT 1 OF 2

ATMOSPHERIC PROPAGATION OF MILLIMETRE WAVES

INTERFACE-DIGITAL MULTIPLEXER

Fig D-4

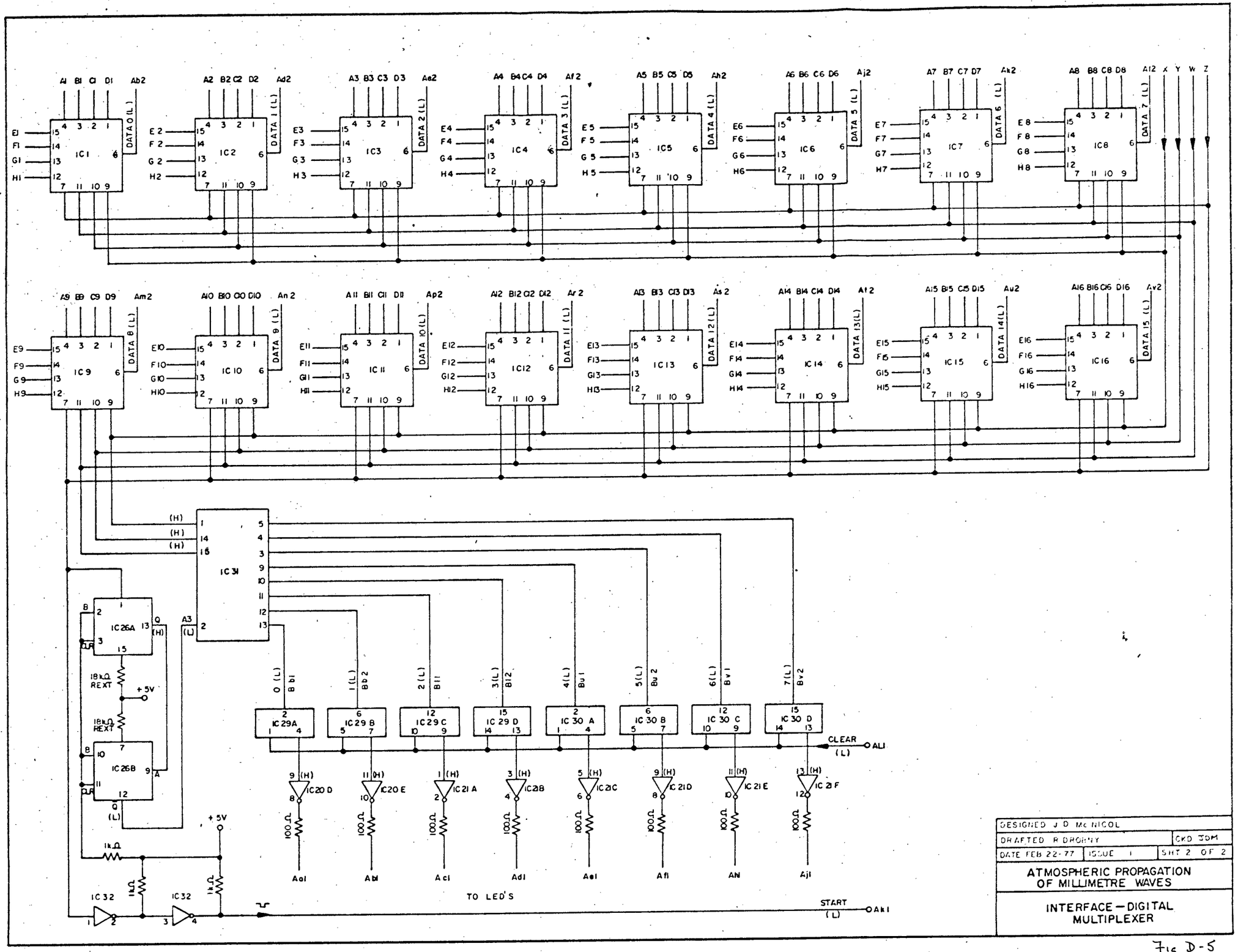
IC1
IC2
IC3
IC4
IC5
IC6
IC7
IC8
IC9
IC10
IC11
IC12
IC13
IC14
IC15
IC16
IC31
IC26A
IC26B
IC32
IC29A
IC29B
IC29C
IC29D
IC30A
IC30B
IC30C
IC30D
IC20D
IC20E
IC21A
IC21B
IC21C
IC21D
IC21E
IC21F
DATA 0 (L)
DATA 1 (L)
DATA 2 (L)
DATA 3 (L)
DATA 4 (L)
DATA 5 (L)
DATA 6 (L)
DATA 7 (L)
DATA 8 (L)
DATA 9 (L)
DATA 10 (L)
DATA 11 (L)
DATA 12 (L)
DATA 13 (L)
DATA 14 (L)
DATA 15 (L)
18kΩ REXT
+5V
1kΩ
100Ω
CLEAR (L)
START (L)
TO LED'S
DESIGNED J D McNICOL
DRAFTED R DROPPY
CKD JDM
DATE FEB 22-77
ISSUE 1
SHT 2 OF 2
ATMOSPHERIC PROPAGATION OF MILLIMETRE WAVES
INTERFACE – DIGITAL MULTIPLEXER

Fig D-5

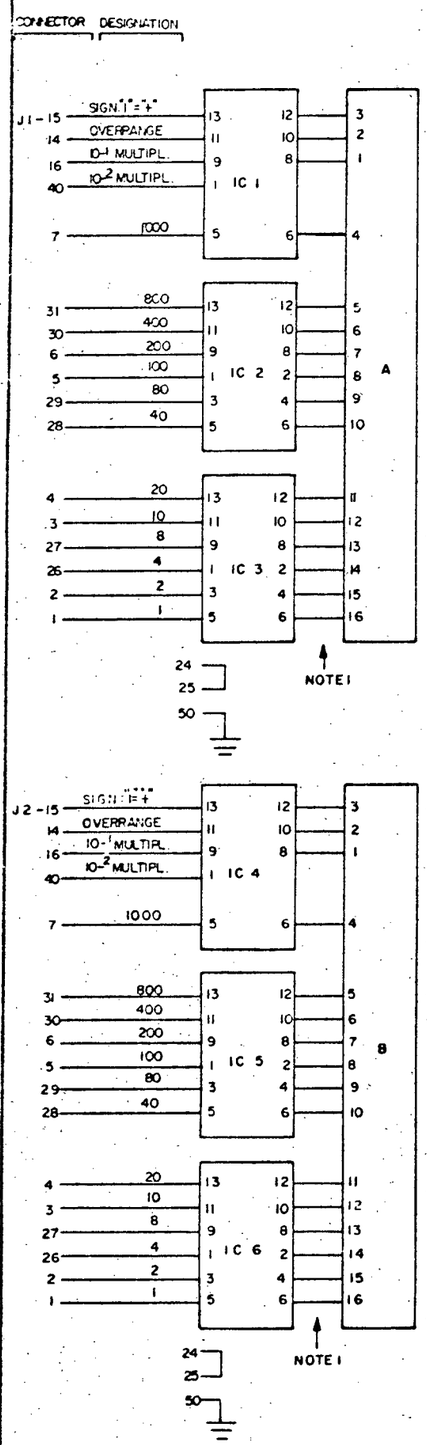

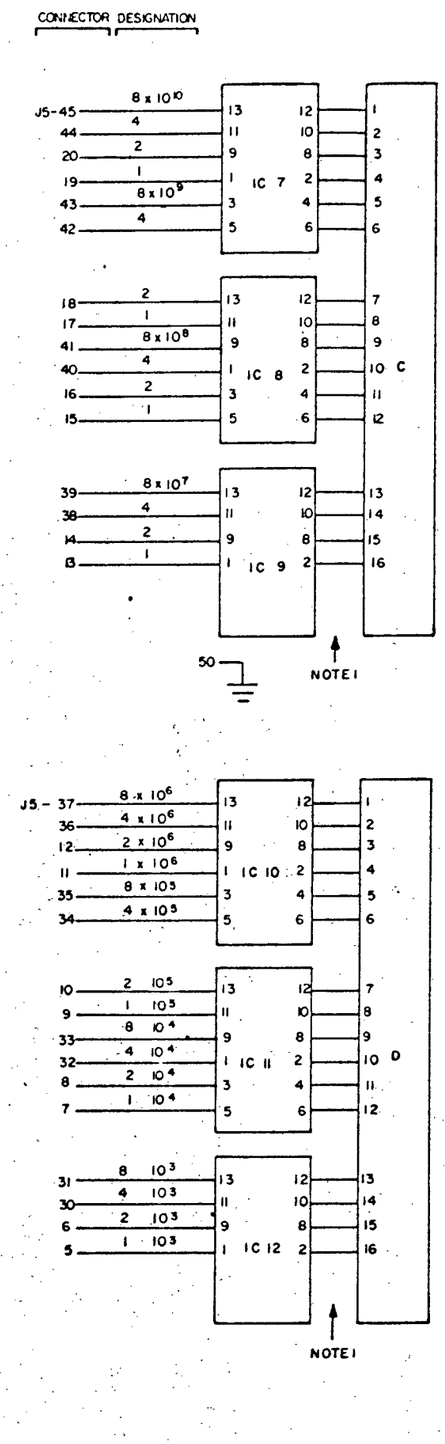

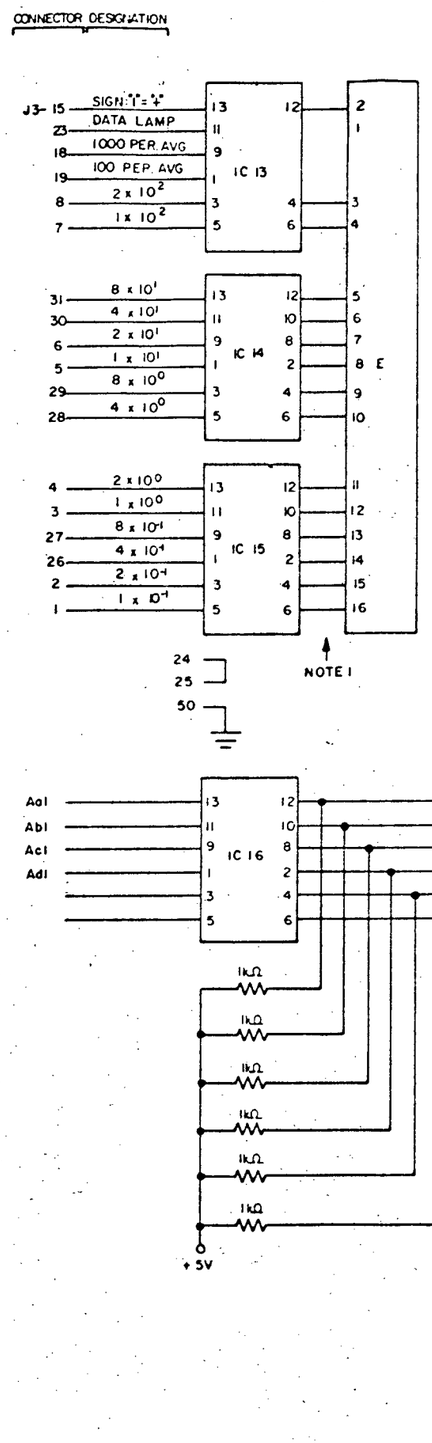

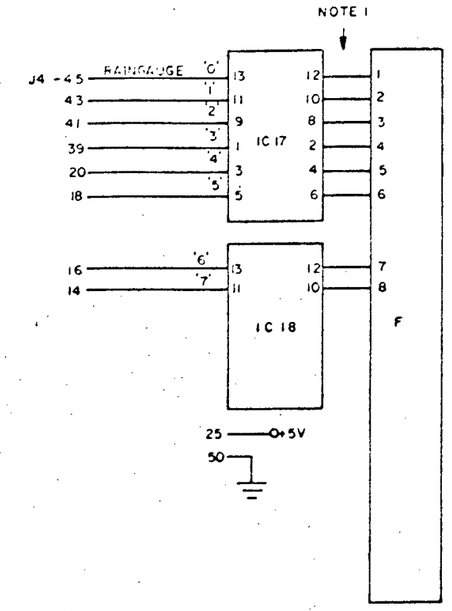

NOTES

1. 1000 Ω, 1/8 WATT PULL UP RESISTORS TO EACH CONNECTOR PIN.

DEV NO	DEV TYPE
IC 1 - 18	SN 7417 HEX BUFFER - OPEN COLLECTOR

DESIGNED J D Mc NICOL		
DRAFTED R DROBNY		CKD JDM
DATE FEB 20-77	ISSUE 1	SHT 1 OF 1

ATMOSPHERIC PROPAGATION OF MILLIMETRE WAVES

INTERFACE - BUFFER

Fig D-6

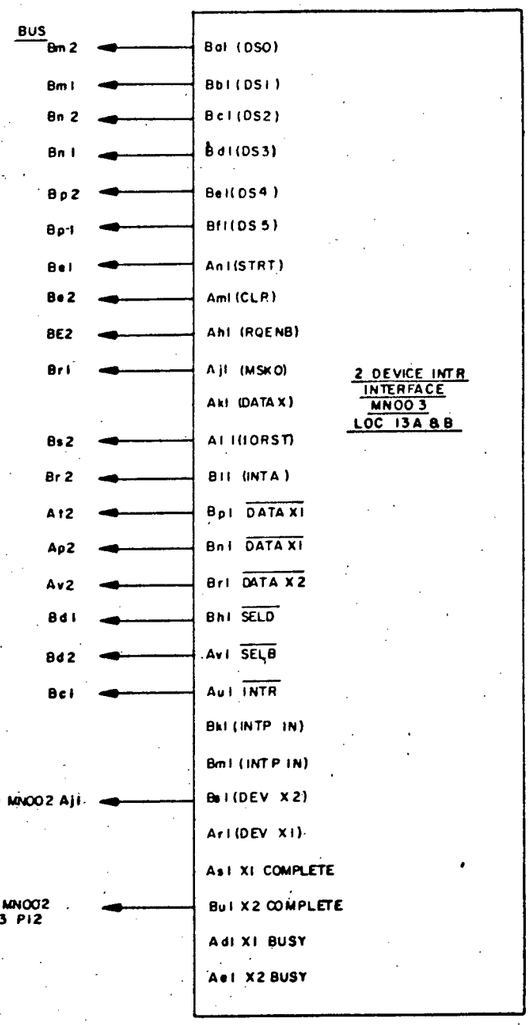

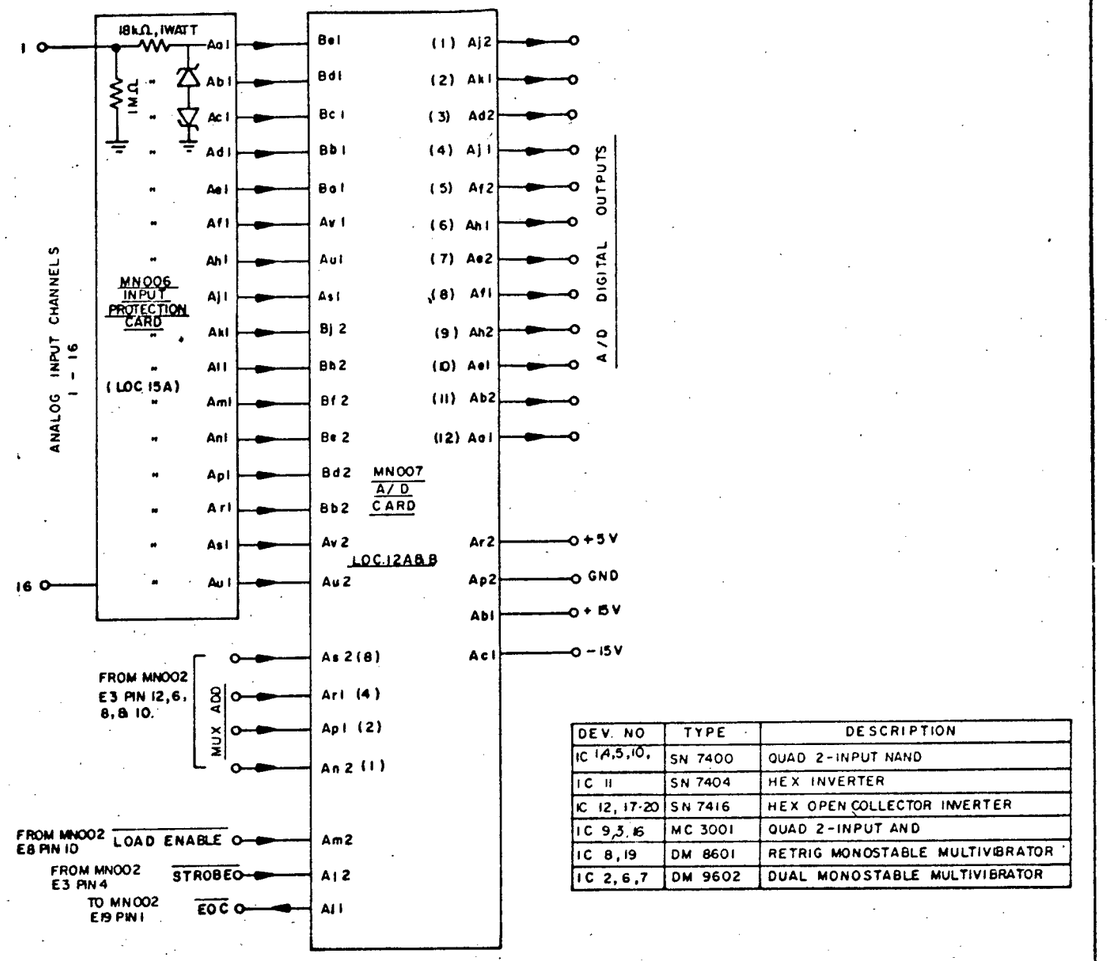

DEV. NO	TYPE	DESCRIPTION
IC 1,4,5,10,	SN 7400	QUAD 2-INPUT NAND
IC 11	SN 7404	HEX INVERTER
IC 12, 17-20	SN 7416	HEX OPEN COLLECTOR INVERTER
IC 9,3,16	MC 3001	QUAD 2-INPUT AND
IC 8, 19	DM 8601	RETRIG MONOSTABLE MULTIVIBRATOR
IC 2, 6, 7	DM 9602	DUAL MONOSTABLE MULTIVIBRATOR

DESIGNED D HOLMES		
DRAFTED R DROBNY		CKD JDM
DATE FEB 21 - 77	ISSUE 1	SHT 1 OF 2

ATMOSPHERIC PROPAGATION OF MILLIMETRE WAVES

INTERFACE: A/D CONTROL UNIT

Fig D-7

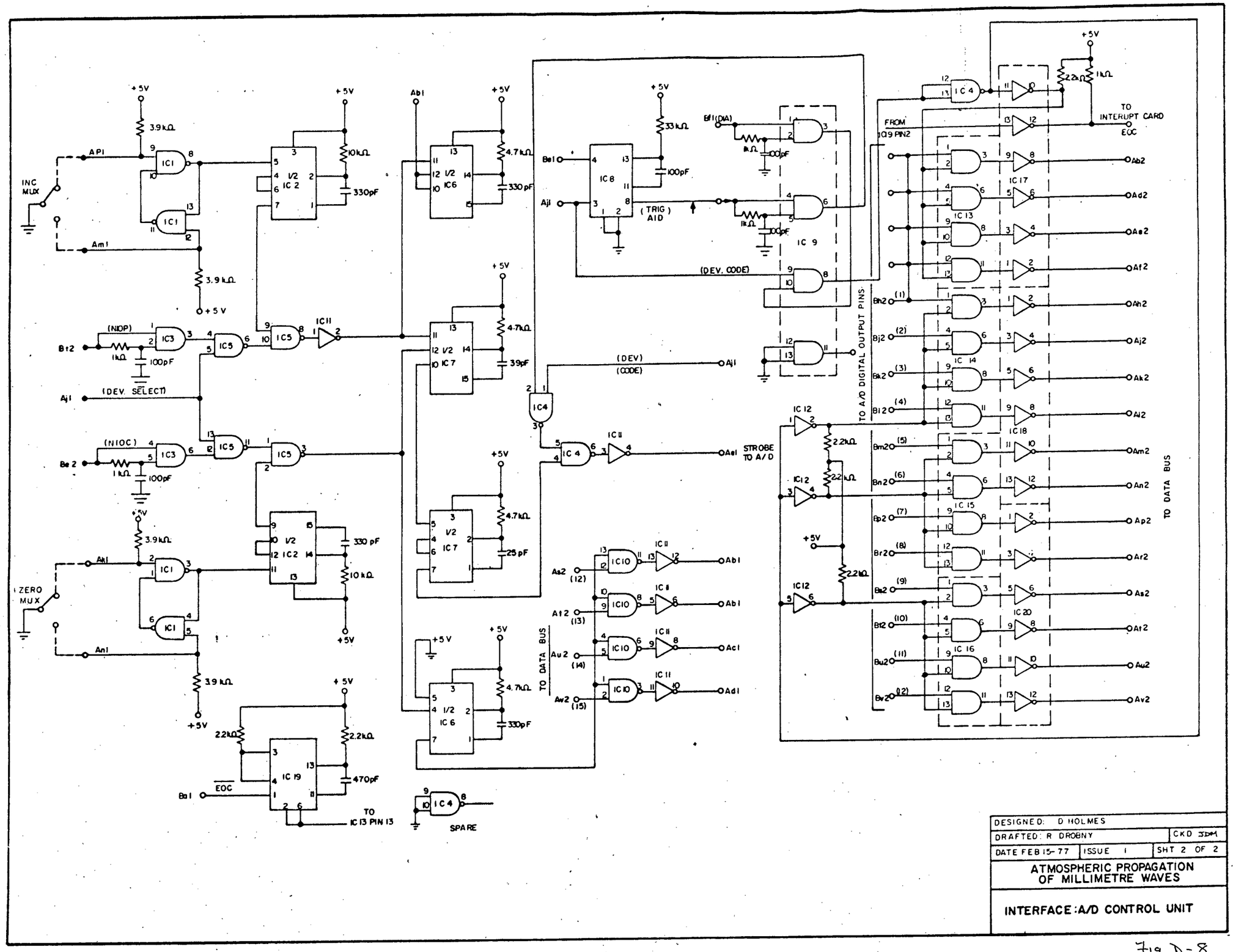
+5V
3.9kΩ
API
INC MUX
IC1
IC1
Am1
3.9 kΩ
+5V
10kΩ
330pF
V2 IC 2
Ab1
4.7kΩ
330pF
IC6
Be1
Aj1
IC8
33kΩ
100pF
(TRIG) AID
Bf1(DIA)
1kΩ
100pF
IC 9
(DEV. CODE)
FROM 1019 PIN2
TO INTERUPT CARD EOC
IC 4
2.2kΩ
1kΩ
TO A/D DIGITAL OUTPUT PINS
(NIOP)
IC3
IC5
IC11
Bf2
1kΩ
100pF
(DEV. SELECT)
Aj1
4.7kΩ
39pF
IC7
(DEV) (CODE)
Aj1
IC4
IC11
Ae1
STROBE TO A/D
IC 12
2.2kΩ
(NIOC)
Be2
1kΩ
100pF
IC5
IC5
IC5
4.7kΩ
25pF
IC7
Ak1
3.9kΩ
ZERO MUX
IC1
IC1
An1
3.9 kΩ
+5V
330 pF
10 kΩ
V2 IC2
+5V
4.7kΩ
330pF
IC6
As2 (12)
A12 (13)
Au2 (14)
Av2 (15)
IC10
IC8
IC11
Ab1
Ab1
Ac1
Ad1
TO DATA BUS
IC 17
IC 13
IC 14
IC 18
IC 15
IC 20
IC 16
Ab2
Ad2
Ae2
Af2
Ah2
Aj2
Ak2
Al2
Am2
An2
Ap2
Ar2
As2
At2
Au2
Av2
Bh2 (1)
Bj2 (2)
Bk2 (3)
Bl2 (4)
Bm2 (5)
Bn2 (6)
Bp2 (7)
Br2 (8)
Bs2 (9)
Bt2 (10)
Bu2 (11)
Bv2 (12)
TO DATA BUS
+5V
2.2kΩ
IC12
2.2kΩ
IC12
2.2kΩ
+5V
2.2kΩ
IC 19
470pF
EOC
Ba1
TO IC 13 PIN 13
IC4
SPARE
DESIGNED: D HOLMES
DRAFTED: R DROBNY
CKD JDM
DATE FEB 15-77
ISSUE 1
SHT 2 OF 2
ATMOSPHERIC PROPAGATION OF MILLIMETRE WAVES
INTERFACE: A/D CONTROL UNIT

Fig D-8

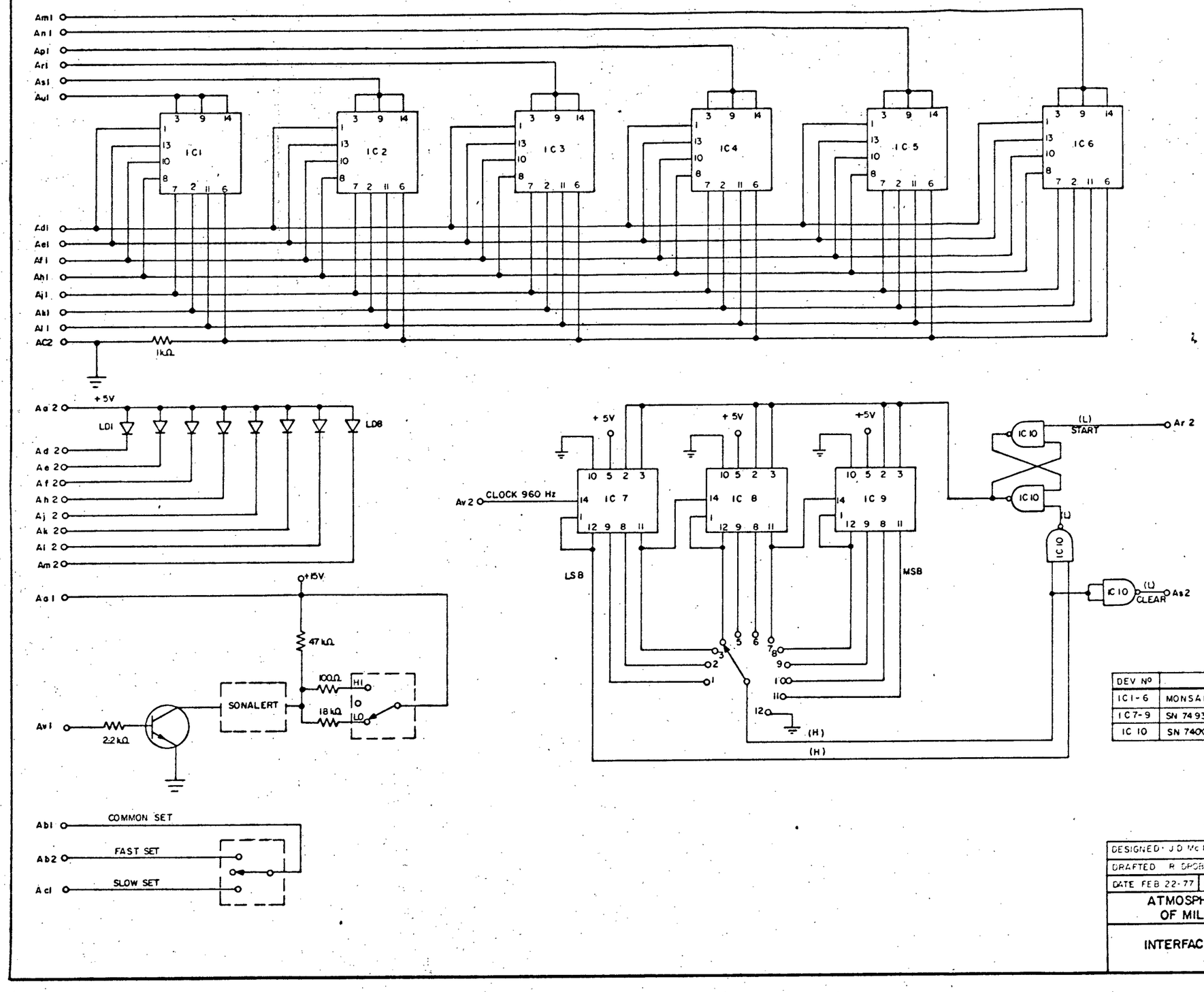

DEV Nº	DEV TYPE
IC1-6	MONSANTO MAN1 DIGIT DISPLAY
IC7-9	SN 7493 4 BIT BINARY COUNTER
IC 10	SN 7400 QUAD 2-INPUT NAND

DESIGNED: J D McNICOL		
DRAFTED R SPOBNY		CKD JDM
DATE FEB 22-77	ISSUE 1	SHT 1 OF 1

ATMOSPHERIC PROPAGATION OF MILLIMETRE WAVES

INTERFACE-DISPLAY PANEL

Fig D-9

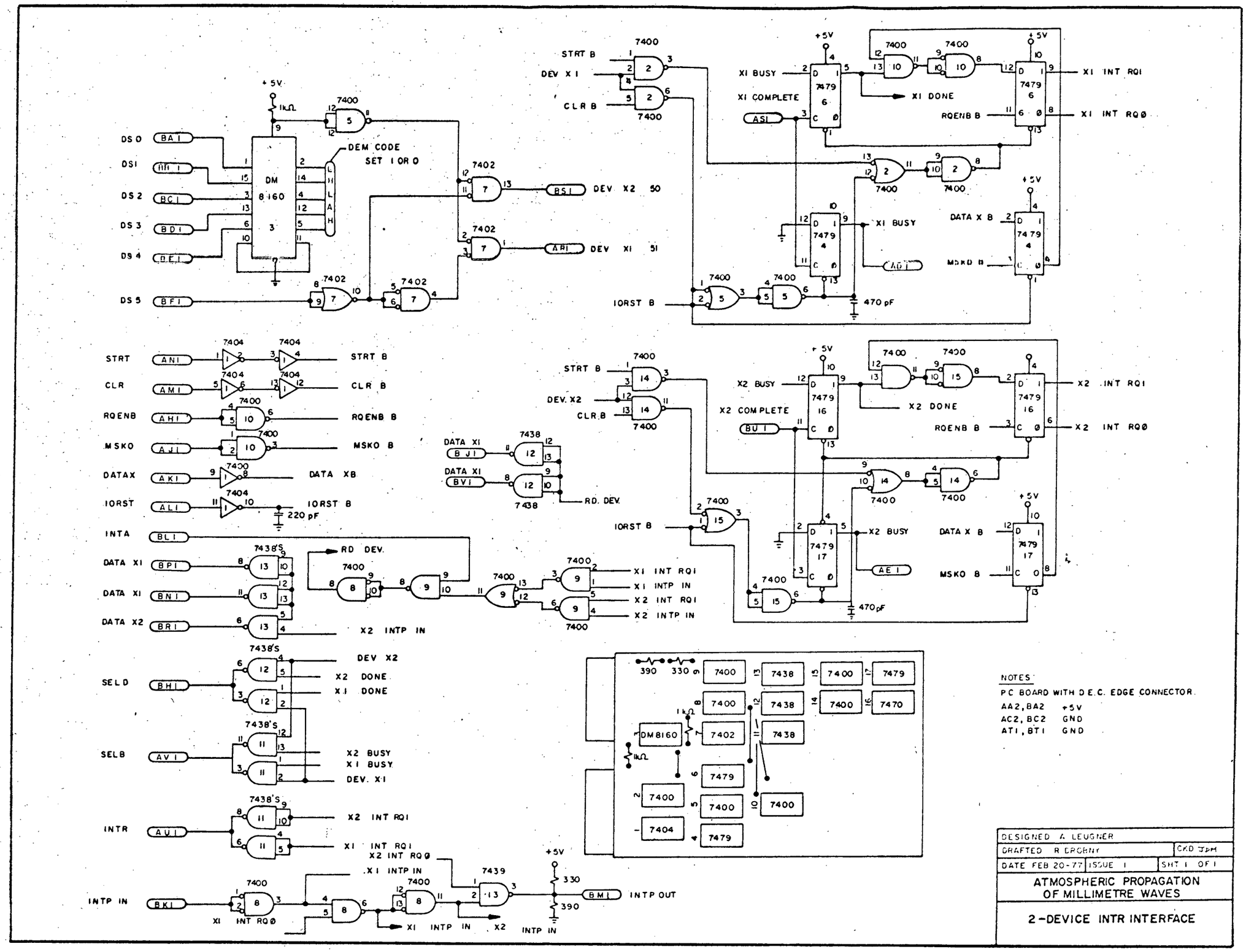
+5V
1kΩ
7400
DS 0
DS 1
DS 2
DS 3
DS 4
DS 5
BA I
BC I
BD I
BE I
BF I
DM 8160
DEM CODE SET 1 OR 0
7402
BS I
DEV X2 50
AR I
DEV X1 51
STRT B
DEV X1
CLR B
X1 BUSY
XI COMPLETE
ASI
X1 DONE
RQENB B
X1 INT RQ1
X1 INT RQ0
7479 6
7479 4
DATA X B
MSKO B
AD I
IORST B
470 pF
STRT
CLR
RQENB
MSKO
DATAX
IORST
INTA
AN I
AM I
AH I
AJ I
AK I
AL I
BL I
220 pF
STRT B
CLR B
RQENB B
MSKO B
DATA XB
IORST B
DATA X1
BJ I
BV I
7438
RD. DEV.
DEV. X2
CLR.B
X2 BUSY
X2 COMPLETE
BU I
X2 DONE
X2 INT RQ1
X2 INT RQ0
7479 16
7479 17
AE I
DATA X1
DATA X2
BP I
BN I
BR I
7438'S
X2 INTP IN
X1 INT RQ1
X1 INTP IN
X2 INT RQ1
X2 INTP IN
SEL D
SEL B
INTR
BH I
AV I
AU I
DEV X2
X2 DONE
X1 DONE
X2 BUSY
X1 BUSY
DEV. X1
X2 INT RQ1
X1 INT RQ1
X2 INT RQ0
.X1 INTP IN
INTP IN
BK I
X1 INT RQ0
X1 INTP IN
X2
INTP IN
7439
330
390
BM I
INTP OUT
390 330 Ω
DM8160
1kΩ
7438
7479
7470
7404
NOTES
PC BOARD WITH D.E.C. EDGE CONNECTOR.
AA2, BA2 +5V
AC2, BC2 GND
AT1, BT1 GND
DESIGNED A. LEUGNER
DRAFTED R. DROHNY
CKD JDM
DATE FEB 20-77
ISSUE 1
SHT 1 OF 1
ATMOSPHERIC PROPAGATION OF MILLIMETRE WAVES
2-DEVICE INTR INTERFACE

Fig D-10

APPENDIX E

Data Acquisition Software

E-1 Operation

As the Nova 840 minicomputer facility was shared by many users it was necessary to allow easy interruption of this program. A single sheet of operating instructions, given in Fig. E-1, supplied the essential information. For users with some familiarity with the computer, few problems were encountered in correctly stopping and restarting the program.

A magnetic tape becomes full after about 80 hours of recording. At that time the operator should stop the program, load a blank tape and, while restarting, notify the program as to the rack number of the new tape and the file number (presumably '00'). This action modifies the contents of the bookkeeping file 'PARAM', which holds the current tape rack number and the next file to be opened. A sample of the dialogue is contained in Fig. E-2.

The data acquisition program maintains a record of program activity in a line file named 'LOGFILE'; in particular, it indicates starting and stopping times and which files were written. A sample of a typical log entry is given in Fig. E-3. The operator will note that it is advisable to delete old entries occasionally to prevent the length becoming excessive.

E-2 Software Backup and Restoration

Through either hardware or software errors, the disk-resident operating system or user programs may be overwritten. To minimize downtime due to this, two disks are maintained in working order. Restoration of disks is performed on the minicomputer from a magnetic tape backup.

The prodecure is as follows:

1. Perform a full initialization per DGC manual 093-000188-00
2. LOAD/V/R MTO:3

   LOAD/V/R MTO:6

   LOAD/V/R MTO:7
3. CDIR JOHN

   DIR JOHN

   @DPO:LINK.CM@
4. LOAD/V/R MTO:XX
5. @ASSEMBLE@
6. @LOADER.B@

In the above, file XX contains the latest backup of the data acquisition software. If changes are made to the software, a new back-up may be written by loading the above tape and entering '@BACKUP.MY@'. (Care must be taken to modify this source file so as to write to the next free tape file and not overwrite the previous backup.)

E-3 Magnetic Tape Data Format

The output is composed of an integral number of records, each 32 words long and of the format given in Table 4.2. On the tape, each file contains not greater than 120 blocks of exactly 60 records (3840 bytes) each.

E-4 Software Modification

Most minor adjustments to the data acquisition software may be made by modifying the task 'START' alone. Table E-1 lists 6 parameters which control the output data format, the queue length, the interrupt rate and the sampling sequence. They may be changed within certain limits.

The sequence in which tasks are initiated and the priorities which they are assigned are contained in a table in 'START'. When adding new tasks to the system, it is normal to place their name and priority in this table. Care must be taken that program start-up and operation are not hampered by the new task.

Name	Present Value	Definition
LRELR	32	Number of words per record
NRECB	60	Number of records per tape block
NBLKF	120	Maximum number of blocks per file
NRECQ	400	Number of records in the queue
IRATE	$(30200)_8$	Interrupt rate control word [16 Hz]
NSAMS	16	Number of interrupts per data record

Table E-1 Certain data acquisition program parameters.

WEATHER DATA AQUISITION SYSTEM

FROM: John McNicol, Rm. 448

Starting and Stopping Procedures

TO STOP:

1. Momentarily, flick switch register bit Ø to Zero (downward).
2. Press "Return".
3. Remove the disk pack and tape.

TO START:

1. Correctly load the magnetic tape (with "REMOTE" on).
2. Connect the I/O bus with switch 2 up.
3. Perform the usual sign on procedures.
4. Type @ GO @.
5. Respond with a carriage return to the next statement.
6. That's all. [The magnetic tape should now be spacing forward, or the lights under the computer flashing].

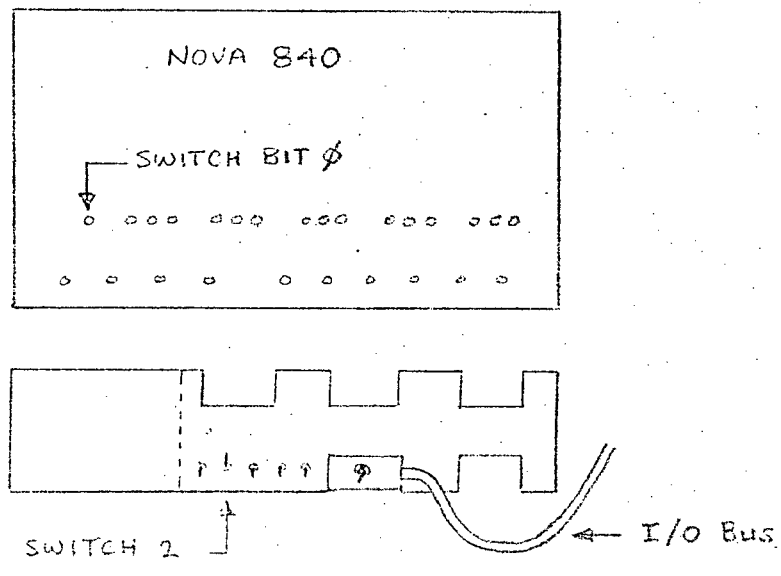

Fig. E-1 Instruction sheet for the data acquisition system.

```
START
CURRENT TAPE ID IS RB0889
NEXT TAPE FILE TO BE WRITTEN IS MT0:31
IF OK,RETURN. OTHERWISE ENTER 'NO' AND RETURN.
NO
ENTER TAPE RACK NUMBER: RB0891
ENTER TWO DIGIT FILE NUMBER: 00
CURRENT TAPE ID IS RB0891
NEXT TAPE FILE TO BE WRITTEN IS MT0:00
IF OK,RETURN. OTHERWISE ENTER 'NO' AND RETURN.

LOAD MAGNETIC TAPE, STRIKE ANY KEY
?24
DATA AQUISITION TERMINATED
R
```

Fig. E-2 Dialogue while changing tapes

```
+++++DATA AQUISITION PROGRAM ENTRY+++++RB0889
03/15/77  23:12:25
MT0:24
03/16/77  01:20:49
MT0:25
03/16/77  03:20:49
MT0:26
03/16/77  05:20:49
MT0:27
03/16/77  07:20:49
MT0:28
03/16/77  09:20:49
MT0:29
03/16/77  10:05:06
MT0:30
NORMAL TERMINATION AT 03/16/77  10:05:12
```

Fig. E-3 A typical 'LOGFILE' entry. It indicates that data was written on files 24 to 29 between 2312 March 15 and 1005 March 16.

APPENDIX F

Post-Processing And Analysis Programs

F-1 Post-Processing

A general description of the programs which facilitate data base formation is given in Section 4.4.2. The names of the particular programs and the required device assignments are given here. Certain device assignments are common to all programs; they are:

0 = input magnetic tape

5 = control cards (usually give tape positioning data)

12 = a "scratch pad" line file.

The individual programs are:

1. Scaling/Conversion

   name = HASH2

   1 = output tape

   10 = a line file containing variable names etc.

2. Transfer to Data Base

   name = COPY

   1 = output tape

3. Calcomp Plotting

   name = PLOT1B, PLOT2B, PLOT3B, PLOT4B

4. Tape Lisiting (unit 5 not used)

   name = DATASNIFF

The format of the data on labelled tape is given by Table F-1.

F-2 Analysis Programs

To facilitate the analysis of data a collection of programs were written to place an abreviated version of data base files in disk storage and to produce various statistical summaries of the data. All

of these programs require a scratch pad line file assigned to unit 12 and accept a list of data files and baseline signal levels on unit 5. A short description of each is given below:

'Z3' Transfers a filtered version of the amplitude and path-average rain rate to a sequential file with the same name as the tape file. Unit 0 is assigned to the source magnetic tape.

'Z4' Computes and appends the statistics to selected files.

'Z5' Prints the individual statistics of each file.

'Z6' Prints the group statistics of the files specified by unit 5.

'Z7' Accepts the baseline signal level with each file and prints group statistics of attenuation vs rain rate.

'Z8' As Z7, but in addition plots the statistics.

The format of the sequential file used here is given in Fig. F-2.

RECORD	WORD ASSIGNMENT
1	A(2) = MONTH, A(3) = DAY, A(4) = YEAR A(5) = N number of channels; A(7, 8, 9) = file name
2 to 6	Five 64-character comments
7 to 9	The title and units associated with the i^{th} channel are contained in the i^{th} word of records 7, 8 and 9.
10 to 14	Five 64-character comments
15 to end	The floating point values of the i^{th} channel at successive points in time are given by the i^{th} word in successive records.

Table F-1 Format of data base files

RECORD NUMBER	LENGTH (WORDS)	CONTENTS
1	11	A(1) = Number of words in record 2 and 3 = N A(2) = Averaging time A(3), A(4), A(5) = Source file name A(6), A(7), A(8) = MONTH/DAY/YEAR A(9), A(10), A(11) = HOURS/MIN/SEC
2	N	Path-average rain rate at successive points in time
3	N	Amplitude at corresponding points in time
4	100	Number of sample points in 100 classes of rain rate
5	500	To be read as a 5 x 100 matrix A(1,J) = mean path-average rain rate A(2,J) = mean amplitude of points in J^{th} rain rate class A(3,J) = standard deviation of amplitude A(4,J) = minimum amplitude in the class A(5,J) = maximum amplitude in the class

Table F-2 Format of disk-resident statistical summaries.

REFERENCES

1. D. Silverthorn and R. Tetarenko, "Microwave Radio Spreads TV", Telesis, Vol. 5, pp. 209-213, 1976.

2. Special issue on "LD-4: High capacity digital cable system", Telesis, Vol. 3, pp. 281-312, 1974.

3. W.D. Warters, "Millimeter Waveguide Scores High in Field Test", Bell Laboratories RECORD, Vol. 53, pp. 400-408, 1975.

4. I. Jacobs, "Lightwave Communications Passes its First Test", Bell Laboratories RECORD, Vol. 54, pp. 290-297, 1976.

5. P. Hervieux, "RD-3: an 8 GHz digital radio system for Canada", Telesis, Vol. 4, pp. 53-59, 1975.

6. G.H. Swan, "Microwave Interference: Keeping It Under Control", Bell Laboratiries RECORD, Vol. 52, p. 103, 1974.

7. L.C. Tillotson, "Use of Frequencies Above 10 GHz for Common Carrier Applications", Bell System Technical Journal, Vol. 48, pp. 1563-1576, 1969.

8. R.K. Crane, "Propagation Phenomena Affecting Satellite Communication Systems Operating in the Centimeter and Millimeter Wavelength Bands", Proc. IEEE, Vol. 59, pp. 173-188, 1971.

9. L.J. Ippolito, "Millimeter wave propagation measurements from the Applications Technology Satellite (ATS-V)", IEEE Trans. Antennas Propagat., Vol. AP-18, pp. 535-552, July 1970.

10. C.L. Ruthroff and L.C. Tillotson, "Interference in a Dense Radio Network", Bell System Technical Journal, Vol. 58, pp. 1727-1743, 1969.

11. H.J. Wintroub and L.A. Hoffman, "Space Communications Systems Considerations at 94 GHz", NATO-AGARD Conference Proceedings No. 107, 1972.

12. C.L. Ruthroff, T.L. Osborne and W.F. Bodtmann, "Short Hop Radio Experiment", Bell System Technical Journal, Vol. 48, pp. 1577-1604, 1969.

13. F. Fedi, "Atmospheric effects on electromagnetic-wave free propagation at frequencies above 10 GHz", European Microwave Conference, Brussels, Belgium, September 4-7, 1973.

14. W.W. Snell and M.V. Schneider, "Millimeter-Wave Thin Film Downconverter", IEEE Trans. Microwave Theory and Techniques, Vol. MTT-24, pp. 804-806, 1976.

15. T.F. McMaster, M.V. Schneider and W.W. Snell, "Millimeter-Wave Receivers with Subharmonic Pump", IEEE Trans. on Microwave Theory and Techniques, Vol. MTT-24, pp. 948-952, 1976.

16. T.H. Oxley, "MIC's Using Hybrid Techniques for Application at mm Wavelengths", Microwave Journal, Vol. 19, No. 12, pp. 46-47, 1976.

17. "New Digital Radio Transmission System", Bell Laboratories Record, Vol. 52, p. 362, 1974.

18. J.W. Meyer, "Radar Astronomy at Millimeter and Submillimeter Wavelengths", Proc. IEEE, Vol. 54, pp. 484-492, 1966.

19. D.V. Rogers and R.L. Olsen, "Calculation of Radiowave Attenuation due to Rain at Frequencies up to 1000 GHz", Communications Research Center (Canada) Report No. 1299, 1976.

20. T.L. Osborne, "Rain Outage Performance of Tandem and Path Diversity 18 GHz Short Hop Radio Systems", Bell System Technical Journal, Vol. 50, pp. 59-79, 1971.

21. A.B. Crawford and R.H. Turrin, "A Packaged Antenna for Short Hop Microwave Radio Systems", Bell System Technical Journal, Vol. 48, pp. 1605-1622, 1969.

22. J.A. Arnaud and J.T. Rusico, "Guidance of 100 GHz beams by cylindrical mirrors", IEEE Trans. on Microwave Theory and Techniques, Vol. MTT-23, No. 4, pp. 377-379, 1975.

23. J.W. Ryde, "The attenuation and radar echoes produced at centimetre wave-lengths by various meteorological phenomena", Report of the Physics Society, London and the Royal Meteorological Society "Meteorological Factors in Radio-Wave Propagation".

24. R.G. Medhurst, "Rainfall Attenuation of Centimeter Waves: Comparison of Theory and Experiment", IEEE Trans. Antennas and Prop., Vol. Ap-13, pp. 550-564, 1965.

25. J.C. Lin, and A. Ishimaru (1971), Propagation of Millimeter Waves in Rain, Technical Report 144, Department of Electrical Engineering, University of Washington, Seattle, Washington.

26. A.M. Zavody and B.N. Harden, "Attenuation/Rain-Rate Relationships at 36 and 110 GHz", Electronics Letters, Vol. 12, pp. 422-423, 1976.

27. J. Joss, J.C. Thams, and A. Waldvogel (1968), The Variation of Raindrop Size Distributions at Locarno, in Proceedings of the International Conference on Cloud Physics, Toronto, Canada, 369-373.

28. A.E. Freeny, and J.D. Gabbe (1969), A Statistical Description of Intense Rainfall, B.S.T.J., 48, 1789-1851.

29. D.C. Hogg, "Path Diversity in Propagation of Millimetric Waves through Rain", IEEE Trans. on Antennas and Propagation, Vol. AP-13, pp. 410-415, 1967.

30. M.J. Saunders, "Cross Polarization at 18 and 30 GHz due to Rain", IEEE Trans. on Antennas and Propagation, Vol. AP-19, pp. 273-277, 1971.

31. R.A. Semplak, "Effect of Oblate Raindrops on Attenuation at 30.9 GHz", Radio Science, Vol. 5, pp. 559-564, 1970.

32. H.E. Bussey, Microwave attenuation statistics estimated from rainfall and water vapor statistics, Proc. IRE, Vol. 38, July 1950, pp. 781-785.

33. G.E. Weibel and H.O. Dressel, "Propagation studies in millimeter-wave link systems", Proc. IEEE, Vol. 55, pp. 497-513, April 1967.

34. T. Oguchi,"Attenuation of electro-magnetic wave due to rain with distorted raindrops", J. Radio Research Labs. (Tokyo), Vol. 7, Sept. 1960, pp. 467-485.

35. T. Oguchi, "Attenuation of electromagnetic wave due to rain with distorted raindrops (pt. II)", J. Radio Res. Lab. Jap., Vol. 11, pp. 19-44, 1964.

36. D.C. Hogg, "Depolarization of Microwaves in Transmission Through Rain", NATO-AGARD Conference Proceedings, No. 107, 1972.

37. B.C. Blevis, R.M. Dohoo, and K.S. McCormick, "Measurements of rainfall attenuation at 8 and 15 GHz", IEEE Trans. Antennas Propagat., Vol. AP-15, pp. 394-403, May 1967.

38. S.D. Robertson and A.P. King, "The Effect of Rain on Propagation of Waves in the 1- and 3-cm Regions", Proc. IRE, Vol. 34, pp. 178p-180p, 1946.

39. R.E. Skerjanec and C.A. Samson, "Rain Attenuation Measurements in Mississippi at 10 and 14.3 GHz", IEEE Trans. on Antennas and Propagation, Vol. 19, pp. 575-578, 1971.

40. A.V. Vorst and E. Gaudissart, "Effects due to Precipitation on Horizontal Links at 12 and 35 GHz", NATO-AGARD Conference Proceedings No. 107, 1972.

41. A.W. Straiton, C.R. Bailey, and W. Vogel, "Amplitude variations of 15-GHz radio waves transmitted through clear air and through rain", Radio Sci., Vol. 5, March 1970, pp. 551-557.

42. R.A. Semplak and R.H. Turrin, "Some measurements of attenuation by rainfall at 18.5 GHz", Bell System Tech. J., Vol. 48, pp. 1767-1787, 1969.

43. R.A. Semplak, "The influence of heavy rainfall on attenuation at 18.5 and 30.9 GHz", IEEE Trans. Antennas Propagat., Vol. AP-18, pp. 507-511, July 1970.

44. L.J. Anderson, J.P. Day, C.H. Freres, and A.P.D. Stokes, "Attenuation of 1.25-centimeter radiation through rain", Proc. IRE, Vol. 35, pp. 351-354, 1947.

45. T.W. Harrold, "Attenuation of 8.6 mm-wavelength radiation in rain", Proc. Inst. Elec. Eng., Vol. 114, pp. 201-203, 1967.

46. J.F. Roche, H. Lake, D.T. Worthington, C.K.H. Tsao and J.T. deBettencourt, "Radio propagation 27-40 GHz", IEEE Trans. Antennas Propagat., Vol. AP-18, pp. 452-462, July 1970.

47. J.R. Norbury and W.J.K. White, "Microwave Attenuation at 35.8 GHz due to Rainfall", Electronics Letters, Vol. 8, pp. 91-92, 1972.

48. G.E. Muller,"Propagation of 6-millimeter waves", Proc. IRE, Vol. 34, April 1946, pp. 181P-183P.

49. L.A. Hoffman, H.J. Wintroub, and W.A. Garber, "Propagation Observations at 3.2 Millimeters", Proc. IEEE, Vol. 54, pp. 449-454, 1966.

50. J.A. Lane, A.C. Gordon-Smith, and A.M. Zavody, "Absorption and scintillation effects at 3mm wavelength on a short line-of-sight radio link", Electron. Lett., Vol. 3, pp. 185-186, 1967.

51. D.T. Llewelly-Jones and A.M. Zavody, "The Influence of Rainfall on Line-of-Sight Propagation at 110 GHz in S.E. England", NATO-AGARD Conference Proceedings, No. 107, 1972.

52. D.T. Llewellyn-Jones and A.M. Zavody, "Microwave Attenuation due to

Rain at 110 GHz in S.E. England", Electronics Letters, Vol. 8, pp. 97-98, 1972.

53. W.F. Bodtmann and C.L. Ruthoff, "Rain Attenuation on Short Radio Paths: Theory, Experiment and Design", Bell System Technical Journal, Vol. 53, pp. 1329-1349, 1974.

54. D.C. Hogg, "Statictics on attenuation of microwaves by intense rain", Bell Syst. Tech. J., Vol. 48, pp. 2949-2962, 1969.

55. C.L. Ruthroff, "Multiple-Path Fading on Line-of-Sight Microwave Radio Systems as a Function of Path Length and Frequency", Bell System Technical Journal, Vol. 50, pp. 2375-2398, 1971.

56. J.O. Laws and D.A. Parsons, "The Relation of Raindrop Size to Intensity", Amer. Geophys. Union Trans., Vol. 24, pp. 452-460, 1943.

57. H.E. Elder and V.J. Glinski, "Detector and Mixer Diodes and Circuits", Microwave Semiconductor Devices and Their Circuit Applications, pp. 370-395, McGraw-Hill Book Company, 1969.

58. H. Jasik, "Antenna Engineering Handbook", McGraw-Hill, 1961.

59. "How to Use Nova Computers", Data General Corporation, April 1971.

60. H.S. Stone, Introduction to Computer Organization and Data Structures, McGraw-Hill Book Company, 1972.

61. Annual Meteorological Summary for 1976: Vancouver Airport, Atmospheric Environment Service, Environment Canada.